Kinetic Studies of Hydrogen Oxidation by Cobaloximes

and

Synthesis, Spectroscopy and Boronation of a New Heteroleptic Ruthenium Cyanide Complex

Thesis by

Sarah Anne Del Ciello

In Partial Fulfillment of the Requirements for
the degree of
Doctor of Philosophy

Division of Chemistry and Chemical Engineering

CALIFORNIA INSTITUTE OF TECHNOLOGY
Pasadena, California

2020
(Defended November 22, 2019)

Dedicated to Emmy the cat and Opal the cat,

and Dan and Jess and Wojtus and all my friends and family;

without your support, this thesis would not exist.

Sarah Anne Del Ciello
ORCID: 0000-0002-7571-8944

ACKNOWLEDGEMENTS

My path to this degree and this thesis has wound through many valleys and over a few peaks; it is easily the most difficult thing I have accomplished to date. I could not have made it to this point alone, and I am humbled and grateful for those who helped me get here.

Thanks are first and foremost owed to my husband, Dan, who after four years of loving and supporting me from down the dorm room hall, took a leap of faith with me and endeavored to make PhDs, long-distance dating, and later marriage work all at the same time. Without his support, cheerleading, and occasional supplying of cake and beer to soothe my bruised ego, I might have quit years ago.

I'd also like to thank Dr. Steve Baldwin and the late great Prof. Greg Hillhouse, whose mentorship during my undergraduate research led me to the decision that not only did I want a PhD, but a Caltech PhD. Steve taught me most of the lab skills I still use today, and working in the Hillhouse lab ensured that I fell in love with all things colorful and terribly air-sensitive. If there is a Heaven, and I know Greg believed there was, I'm sure he's there reading this thesis and thinking up some interesting reaction I should have done with one of his favorite small molecules.

I consider myself incredibly fortunate to have been among the final few students to work with Prof. Harry Gray. Harry took me into his group at a time when rumors had it he was done taking students, and I was in a tough position, and for that I'm continually thankful. He has few peers when it comes to kindness toward students and enthusiasm for their work, and I was often relieved to work under someone who was unfazed that I'd rather be in Santa Barbara visiting my fiancé than in the lab on weekends.

Thanks also to those members of the Gray and Peters groups who directly helped me learn the skills I needed throughout my time at Caltech: Wes and Aaron Sattler, who taught me how to use my Schlenk line (and actually appreciated my no-strikeout summer of softball); David Lacy and Nik Thompson, who taught me to use the hi-vac line; Bryan Hunter, who taught me that in situ spectroscopy only looks easy when he's at the helm; Wes Kramer, whose work on group VI polypyridyl complexes laid the groundwork for my certainty that ^{CF3}bpy *will not coordinate to those metals*; Jay Winkler and Javier Fajardo for their help with the laser spectroscopy; and especially Danh Ngo and Brendon McNicholas, who rescued me from the death of that group VI project with their considerable expertise synthesizing and boronating metal cyanides. My work with Danh and Brendon was the difference between this thesis being worth a Master's and a doctorate, and so they have my eternal gratitude.

I lived for five-ish years with Jess Sampson, and am grateful to her for being so incredibly accepting of our "third roommate" during the long-distance relationship period, for supplying our household with such a thorough complement of cookware, and for adopting such a sweet and loving cat in Opal, who hung out with me during countless emotional breakdowns.

Speaking of cats, I'd be remiss to forget to thank Emmy, who will count this thesis as the fifth she has helped her human companions write. She was adopted as a stray by Dan and his three grad school roommates, all theoretical physicists, who named her for Emmy Noether. Despite her advanced age at adoption, she has been with us for three years and is a constant comfort.

Finally, I should thank my family, without whom I would (literally) not be here, and my non-grad school friends, who have been such a relief to talk to when my world was consumed with frustrating science. Mom, Rachel, John, Wojtus, and all of my supportive in-laws have my gratitude for their love and support.

ABSTRACT

Cobaloximes are macrocyclic complexes well-studied as homogeneous catalysts for hydrogen evolution, but they are also competent at the microscopic reverse reaction, hydrogen oxidation. Kinetic studies of $Co(dmgBF_2)_2L_2$ reacting with hydrogen and base reveal a rate law that is second-order in cobalt and first-order in H_2, indicating that the mechanism of H-H bond breaking is homolytic.

The reduction potentials of metal cyanide complexes can be tuned by appending boranes to the N-terminus. By boronating ruthenium cyanide complexes containing diimine ligands, the $Ru^{II/III}$ couple can be tuned without drastic modification of the $diimine^{0/-}$ couple. A new member of the $[Ru(dimmine)(CN)_4]^{2-}$ family is synthesized with the ligand 4,4'-bis(trifluoromethyl)-2,2'-bipyridine (^{CF3}bpy) and boronated, resulting in a molecule with two reversible redox events separated by 3.2 V.

PUBLISHED CONTENT AND CONTRIBUTIONS

Ngo, Danh; Del Ciello, Sarah A., et al. “Cyano-Ambivalence: Spectroscopy and Photophysics of $[Ru(diimine)(CN\text{-}BR_3)_4]^{2-}$ Complexes.” *Polyhedron,* **submitted.**

All authors participated in the conception and writing of the paper. S.A.D. synthesized the ^{CF3}bpy-containing molecules and took the UV-Vis spectroscopic data and participated in the collection of the luminescence data of those molecules. S.A.D. also created all plots of the aforementioned data.

Del Ciello, Sarah. A. et al. “Synthesis, Spectroscopy, and Boronation of a Fluorinated $[Ru(bpy)(CN)_4]^{2-}$ Derivative” Manuscript in preparation for submission to *Inorganic Chemistry.*

All authors participated in the conception and writing of the paper. S.A.D. synthesized the ^{CF3}bpy-containing molecules, grew the crystals, took the NMR data, and participated in the collection of the electrochemical and IR data of those molecules. S.A.D. also created all plots of the aforementioned data except those of the electrochemistry.

TABLE OF CONTENTS

NOMENCLATURE

2-MeTHF. 2-methyltetrahydrofuran.

BCF. Tris(pentafluorophenyl)borane.

bpy. 2,2'-bipyridine.

Bu. *N*-butyl.

^{CF3}**bpy**. 4,4'-bis(trifluoromethyl)-2,2'-bipyridine.

DCM. Dichloromethane.

DMF. Dimethylformamide.

dmg. Dianion of dimethylgyloxime.

dpg. Dianion of diphenylglyoxime.

Et_2O. Diethyl ether.

HER. The hydrogen evolution reaction, $2H^+ + 2e^- \rightarrow H_2$.

HOR. The hydrogen oxidation reaction, $H_2 \rightarrow 2H^+ + 2e^-$.

IR. Infrared.

LMCT. Ligand-to-metal charge transfer.

MeCN. Acetonitrile.

MeOH. Methanol.

MLCT. Metal-to-ligand charge transfer.

NMR. Nuclear magnetic resonance.

PEM. Proton-exchange membrane, a type of hydrogen fuel cell.

Ph. Phenyl.

phen. Phenanthroline.

ppm. Parts per million.

PPN. Bis(triphenylphosphine)iminium.

py. Pyridine.

SCE. Saturated calomel electrode, a reference electrode.

THF. Tetrahydrofuran.

TEMPO. (2,2,6,6,-Tetramethlpiperidin-1-yl)oxyl.

TFA. Trifluoroacetic acid.

CHAPTER 1

INTRODUCTION: RENEWABLE ENERGY STORAGE

Motivation: The Need for Storage

Progress in generation of carbon-neutral renewable energy has been rapid over the last decade and is projected to grow to meet nearly half of world electricity demand by 2050 (Figure 1).[1] As renewable energy becomes widespread and cost-competitive with fossil fuels, there will be increasing need for efficient, carbon-neutral storage technologies that can operate on a wide variety of time and power scales.

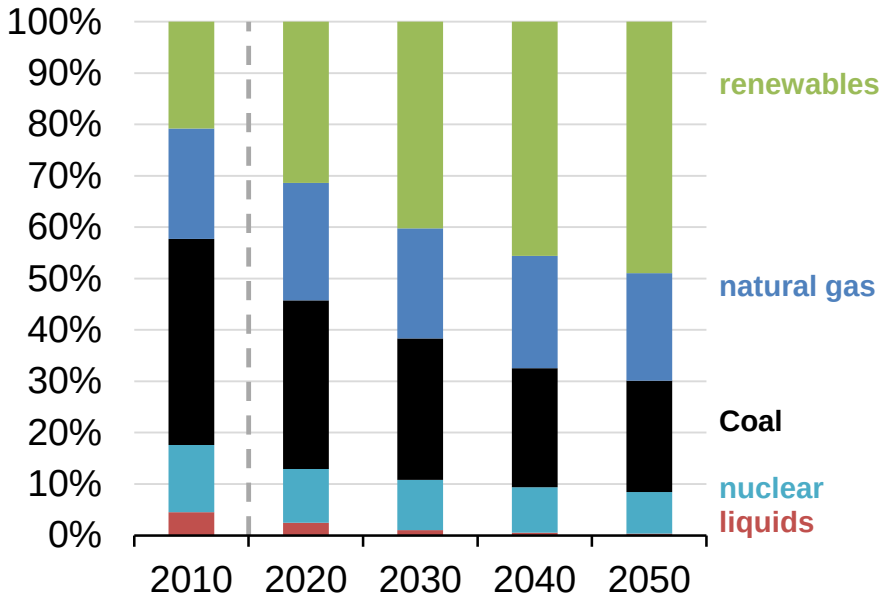

Figure 1: Share of net electricity generation, world. Source: US. Energy Information Administration International Energy Outlook, September 2019 (Public Domain).

The most abundant sources of renewable energy, sunlight and wind, are intermittent and need to be stored at peak production to be used most efficiently. In California, where solar photovoltaics have become ubiquitous, the high production of solar energy has created a problem known as the "duck curve" (Figure 2).[2] The peak of solar production occurs earlier in the day than peak electricity demand, resulting in a sharp rise in the net load on the grid as the sun sets, which requires generators to ramp up production very quickly. As solar gains even higher adoption rates, there will be an increasing number of sunny summer days where peak solar production outstrips demand and will need to be curtailed by grid operators, wasting energy. Wind power also varies on hourly, daily, and seasonal timescales that are uncoupled from demand, creating similar but even less predictable grid balancing and overgeneration problems.[3] The grid-level ability to store energy from these intermittent sources during periods of high production to be used during periods of low production and high demand is key to reducing strain on power plants and electrical grids, lowering the cost of renewable energy, and increasing the penetration of renewables.

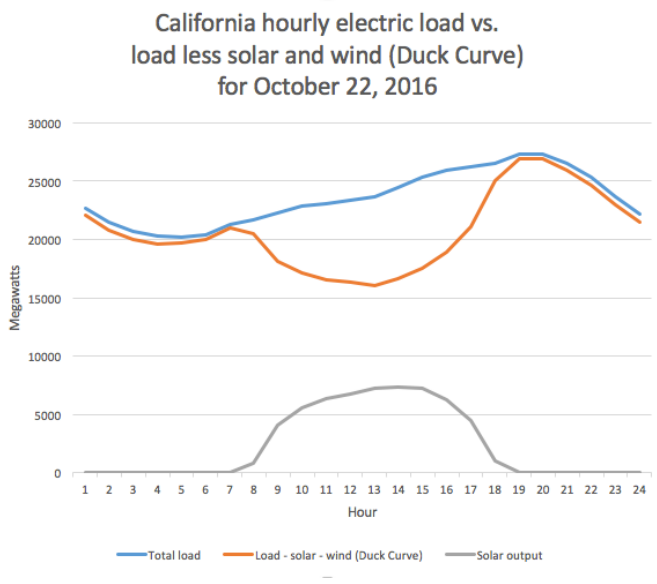

Figure 2: Illustration of the "duck curve". Created by Arnold Reinhold and reproduced under the Creative Commons Attribution-ShareAlike 4.0 International license.

A further challenge in the storage of renewable energy is applications such as long-range transportation and aviation which require energy sources that have a high energy density and fast refueling. These are the applications which are most difficult to transition from fossil fuels, which have high mass and volume energy densities (Figure 3).[4] While there are increasing adoption rates for light duty electric vehicles, especially in large, newly-industrialized countries such as China and India, the Li-ion batteries in those vehicles are too large and costly for heavy-duty applications such as freight transportation.[5]

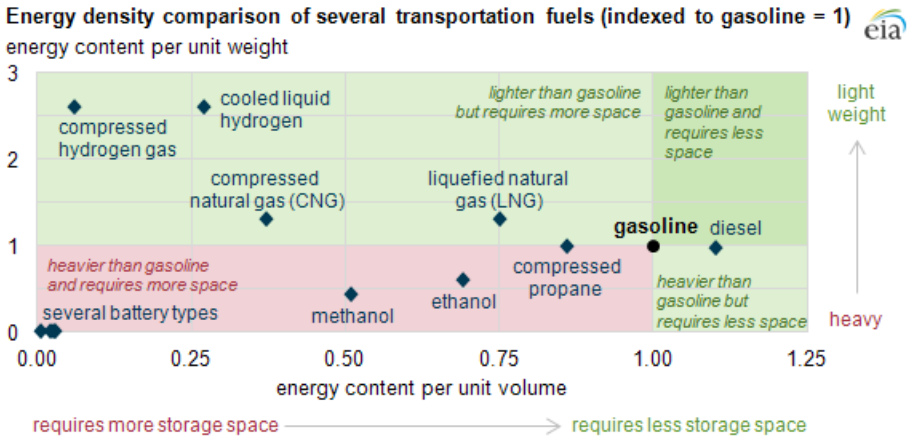

Figure 3: Energy density comparison of transportation fuels. Source: Energy Information Administration (Public Domain).

A wide variety of storage solutions will undoubtedly be needed for different sectors and different applications. Among the most efficient and flexible storage methods is electrochemical energy storage, wherein chemical oxidations and reductions store the energy – in short, batteries.[6] The work in this dissertation represents fundamental science with potential applicability to two types of electrochemical energy storage technologies: hydrogen fuel cells and redox flow batteries.

Hydrogen Evolution, Oxidation, and Fuel Cells

Hydrogen derived from water splitting has been recognized as a key target for energy storage and fuel applications since the oil embargo of the 1970s.[7,8] While the initial interest was in

developing alternatives to petroleum in order to secure energy independence from Middle Eastern oil producers, the climate crisis has renewed interest in hydrogen as a carbon-neutral energy source. Additionally, industrial feedstocks of hydrogen are currently primarily derived from steam reformation of hydrocarbons and the water-gas shift reaction, which are not only carbon intensive in their energy demands, but also produce CO_2 as a coproduct.[9] Development of renewable energy-fueled processes for producing hydrogen from water is therefore expected to be a key step toward the decarbonization of the global economy.

Electro- or photoelectrocatalysts for the hydrogen evolution reaction (HER) are frequently targeted for use in the cathode of water electrolyzers, and there has been rapid progress in the development of Earth-abundant catalysts.[10,11] However, a reversible catalyst which is also competent for the hydrogen oxidation reaction (HOR) has the advantage of being useful for water-based fuel cells, which are safer and more efficient than combustion at liberating energy from hydrogen. Hydrogen fuel cell cars additionally have several advantages over battery-powered electric vehicles, as they have longer driving ranges, faster refueling times, and are less disruptive to the electric grid.[5] State-of-the-art commercial electolyzers and fuel cells both currently use Pt or IrO_2 catalysts,[12,13] which are too rare and expensive to be a scalable and economical solution long-term and are a major contributor to the higher cost of hydrogen cars.[5] Thus, it is a critical area of research to identify Earth-abundant catalysts that are competent for HER and HOR to replace them.

Naturally occurring hydrogenases are a typical source of inspiration in this field, since they are reversible and contain only Earth-abundant Fe and Ni.[14] Indeed, a NiFe hydrogenase has been shown to catalyze HOR at a rate comparable to Pt.[15] HOR catalyst development has occurred primarily in the solid-state material realm, but despite success in reducing the Pt loading for proton-exchange membrane (PEM) fuel cells,[13] precious-metal-free catalysts are still unusual.[16] Even less well-studied are Earth-abundant small-molecule catalysts which are capable of reversibly catalyzing the interconversion of protons and electrons with hydrogen.

Redox Flow Batteries

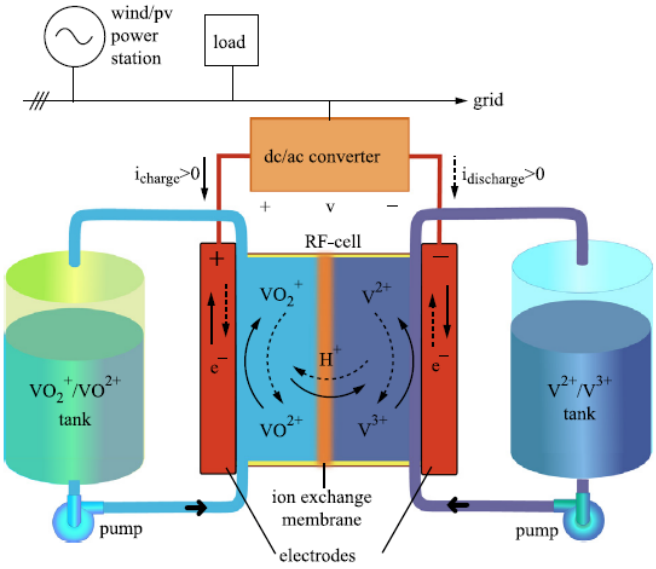

Figure 4: Diagram of a vanadium-based redox flow battery. Reproduced with permission from the copyright holder, Elsevier, from reference 6.

A redox flow battery (Figure 4) uses a solution-phase redox couple to store energy, as opposed to the solution-to-solid phase couples used by most conventional batteries. As the battery is charged, the charged electrolyte is pumped into a storage tank, and pumped back to the electrodes during discharge. Although it results in a low energy density, this design is advantageous for large, stationary applications such as grid balancing, since the capacity of the flow battery is as large as the storage tanks.[6,17] Additionally, unlike hydrogen fuel cells, redox flow batteries have no need for catalysts to assist the charge and discharge process, as the transfer electrons directly with the electrode.

A current limitation in redox flow battery technology is the reliance on water as the solvent. Water has an electrochemical stability window of only 1.23 V, limiting the cell voltage, and a high freezing point relative to outdoor temperatures during winter in much of the world. Non-aqueous redox flow battery electrolytes are desirable for applications where higher

voltages or lower working temperatures are needed, as there are many organic solvents which can overcome these limitations.[18]

In order to be a good candidate electrolyte for nonaqueous redox flow batteries, a molecule must have several properties. First, it must have a reversible electrochemical couple in the stability window of the desired solvent. Second, it must be stable in both the charged and discharged states over a long period of time and many charge/discharge cycles. Third, it should have high solubility in the solvent, which will improve the energy density of the battery.

The difference in voltage between the reduction potentials of the two couples employed sets the maximum cell voltage. If the same molecule has two suitable couples, it can be used to make a symmetric redox flow battery, which confers additional stability to the system in the event of membrane crossover over time.[19]

Summary of this Dissertation

Chapter Two of this dissertation focuses on one member of a series of macrocyclic Co catalysts that have been extensively studied for HER and its reaction with hydrogen. Further mechanistic information in this field is expected to aid the development of Earth-abundant catalysts for HER and HOR.

Chapter Three of this dissertation describes the synthesis and boronation of a new Ru bipyridine cyanide complex. This work aimed to improve on previous work toward developing symmetric nonaqueous redox flow battery electrolytes using similar molecules.

References

(1) EIA projects that renewables will provide nearly half of world electricity by 2050 - Today in Energy - U.S. Energy Information Administration (EIA) https://www.eia.gov/todayinenergy/detail.php?id=41533 (accessed Nov 6, 2019).

(2) Confronting the Duck Curve: How to Address Over-Generation of Solar Energy https://www.energy.gov/eere/articles/confronting-duck-curve-how-address-over-generation-solar-energy (accessed Nov 15, 2019).

(3) Holttinen, H.; Meibom, P.; Orths, A.; Lange, B.; O'Malley, M.; Tande, J. O.; Estanqueiro, A.; Gomez, E.; Söder, L.; Strbac, G.; et al. Impacts of Large Amounts of Wind Power on Design and Operation of Power Systems, Results of IEA Collaboration. *Wind Energy* **2011**, *14* (2), 179–192. https://doi.org/10.1002/we.410.

(4) Few transportation fuels surpass the energy densities of gasoline and diesel - Today in Energy - U.S. Energy Information Administration (EIA) https://www.eia.gov/todayinenergy/detail.php?id=9991 (accessed Nov 15, 2019).

(5) Cano, Z. P.; Banham, D.; Ye, S.; Hintennach, A.; Lu, J.; Fowler, M.; Chen, Z. Batteries and Fuel Cells for Emerging Electric Vehicle Markets. *Nat. Energy* **2018**, *3* (4), 279–289. https://doi.org/10.1038/s41560-018-0108-1.

(6) Alotto, P.; Guarnieri, M.; Moro, F. Redox Flow Batteries for the Storage of Renewable Energy: A Review. *Renew. Sustain. Energy Rev.* **2014**, *29*, 325–335. https://doi.org/10.1016/j.rser.2013.08.001.

(7) Gray, H. B. Powering the Planet with Solar Fuel. *Nat Chem* **2009**, *1* (1), 7–7. https://doi.org/10.1038/nchem.141.

(8) Holladay, J. D.; Hu, J.; King, D. L.; Wang, Y. An Overview of Hydrogen Production Technologies. *Catal. Today* **2009**, *139* (4), 244–260. https://doi.org/10.1016/j.cattod.2008.08.039.

(9) Shaner, M. R.; Atwater, H. A.; Lewis, N. S.; McFarland, E. W. A Comparative Technoeconomic Analysis of Renewable Hydrogen Production Using Solar Energy. *Energy Environ. Sci.* **2016**, *9* (7), 2354–2371. https://doi.org/10.1039/C5EE02573G.

(10) Zou, X.; Zhang, Y. Noble Metal-Free Hydrogen Evolution Catalysts for Water Splitting. *Chem. Soc. Rev.* **2015**, *44* (15), 5148–5180. https://doi.org/10.1039/C4CS00448E.

(11) McKone, J. R.; Marinescu, S. C.; Brunschwig, B. S.; Winkler, J. R.; Gray, H. B. Earth-Abundant Hydrogen Evolution Electrocatalysts. *Chem. Sci.* **2014**, *5* (3), 865–878. https://doi.org/10.1039/C3SC51711J.

(12) Carmo, M.; Fritz, D. L.; Mergel, J.; Stolten, D. A Comprehensive Review on PEM Water Electrolysis. *Int. J. Hydrog. Energy* **2013**, *38* (12), 4901–4934. https://doi.org/10.1016/j.ijhydene.2013.01.151.

(13) Wang, Y.; Chen, K. S.; Mishler, J.; Cho, S. C.; Adroher, X. C. A Review of Polymer Electrolyte Membrane Fuel Cells: Technology, Applications, and Needs on Fundamental Research. *Appl. Energy* **2011**, *88* (4), 981–1007. https://doi.org/10.1016/j.apenergy.2010.09.030.

(14) Lubitz, W.; Ogata, H.; Rüdiger, O.; Reijerse, E. Hydrogenases. *Chem. Rev.* **2014**, *114* (8), 4081–4148. https://doi.org/10.1021/cr4005814.

(15) Jones, A. K.; Sillery, E.; Albracht, S. P. J.; Armstrong, F. A. Direct Comparison of the Electrocatalytic Oxidation of Hydrogen by an Enzyme and a Platinum Catalyst. *Chem. Commun.* **2002**, No. 8, 866–867. https://doi.org/10.1039/B201337A.

(16) Tian, X.; Zhao, P.; Sheng, W. Hydrogen Evolution and Oxidation: Mechanistic Studies and Material Advances. *Adv. Mater.* **2019**, *31* (31), 1808066. https://doi.org/10.1002/adma.201808066.

(17) Weber, A. Z.; Mench, M. M.; Meyers, J. P.; Ross, P. N.; Gostick, J. T.; Liu, Q. Redox Flow Batteries: A Review. *J. Appl. Electrochem.* **2011**, *41* (10), 1137. https://doi.org/10.1007/s10800-011-0348-2.

(18) Gong, K.; Fang, Q.; Gu, S.; Li, S. F. Y.; Yan, Y. Nonaqueous Redox-Flow Batteries: Organic Solvents, Supporting Electrolytes, and Redox Pairs. *Energy Environ. Sci.* **2015**, *8* (12), 3515–3530. https://doi.org/10.1039/C5EE02341F.

(19) Potash, R. A.; McKone, J. R.; Conte, S.; Abruña, H. D. On the Benefits of a Symmetric Redox Flow Battery. *J. Electrochem. Soc.* **2016**, *163* (3), A338–A344. https://doi.org/10.1149/2.0971602jes.

CHAPTER 2

KINETIC STUDIES OF HYDROGEN OXIDATION BY COBALOXIMES

Introduction

Cobaloximes as HER Catalysts

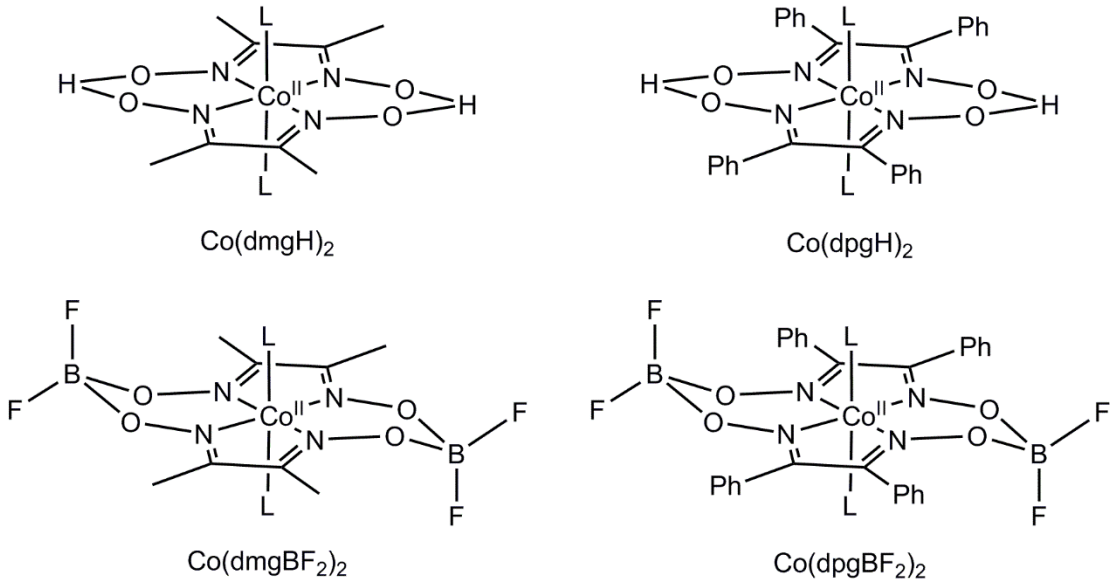

Chart 1: Cobaloxime complexes. L is typically solvent or pyridine.

In 1966, the first "cobaloximes" were synthesized by Schrauzer and Windgassen as models of the reduced form of vitamin B_{12}, and they coined the term for this family of molecules by analogy to "cobalamin".[1] The reaction of dimethylglyoxime (usually abbreviated $dmgH_2$) with cobaltous acetate resulted in the formation of a hydrogen-bonded macrocyclic complex, $Co(dmgH)_2L_2$, where the axial L sites are kinetically labile and usually occupied by solvent molecules. The remaining protons in the macrocycle can be replaced by BF_2 on reaction with

BF_3•Et_2O,[2] and the resulting complexes are generally much more stable, particularly in acid solution. Both reactions are quite general, and a number of similar complexes have been synthesized with varying substituents in the "backbone" of the diglyoxime macrocycle (Chart 1).[3]

Connolly and Espenson demonstrated in 1986 that trace amounts of $Co(dmgBF_2)_2L_2$ catalyzed the evolution of H_2 from acidic aqueous solutions of sufficiently reducing M(II) salts (M = Cr, Eu, V).[4] They reported that the reaction slowed considerably in the absence of halide ions, leading them to conclude that the rate limiting step was inner-sphere electron transfer in a halide-bridged intermediate. Without rate-limiting H-H bond formation, the authors were unable to interrogate the mechanism of that step, and so they proposed two possible routes proceeding from a Co(III) hydride intermediate formed by the protonation of the reduced Co(I) form of the catalyst (Scheme 1, red and blue arrows).

Scheme 1. Reproduced from reference 5 with permission from the copyright holder, American Chemical Society.

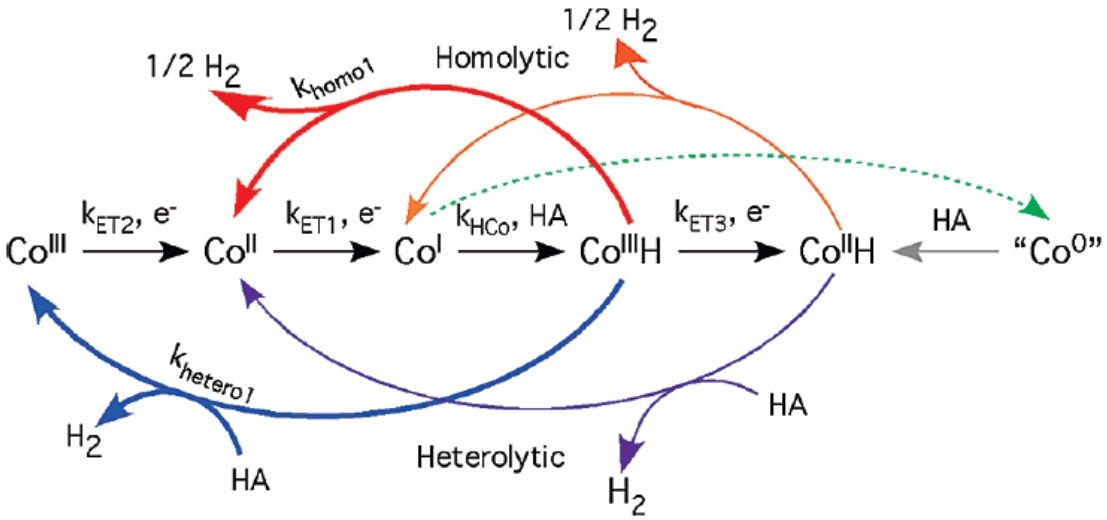

This result was not further investigated until 2005, when both the Artero[3] and Peters[6] groups reported nonaqueous electrocatalytic proton reduction using cobaloxime catalysts. Artero and coworkers found that $Co(dmgH)_2(py)Cl$ electrocatalyzes HER from triethylammonium

chloride in DMF (pK_a = 10.75) at the Co(II/I) couple (-0.98 V vs. Ag/AgCl). Notably, they report that substitution of BF_2 for the bridging protons or H or Ph for the backbone methyls shifted the Co(II/I) couple anodically by ca. 100 mV, but shut down catalysis, suggesting that the Co(I) species formed were no longer basic enough to be protonated by triethylammonium. The authors considered the same general scheme as Connolly and Espenson, and concluded based on simulations of the cyclic voltammagrams that the heterolytic mechanism (Scheme 1, blue arrow) predominated under their catalytic conditions.

In contrast, the Peters group found that the fluoroborated derivative $Co(dmgBF_2)_2(MeCN)_2$ was a competent electrocatalyst for HER from trifluoroacetic acid (TFA) in MeCN (pK_a = 12.7) at the Co(II/I) couple (-0.55 V vs. SCE). They also reported that the diphenylglyoxime congener $Co(dpgBF_2)_2(MeCN)_2$ was a competent HER catalyst, but that the positive shift in the Co(II/I) couple relative to the methyl variant requires use of a stronger acid (HBF_4•Et_2O, pK_a = 0.1) to maintain activity; neither complex showed activity when a weaker acid such as benzoic acid (pK_a = 20.7) or TFA, respectively. Similar to Artero et al., Peters et al. used simulations of the catalytic cyclic voltammagrams to examine the mechanism of HER, but they concluded that the hemolytic mechanism (Scheme 1, red arrow) predominated for $Co(dmgBF_2)_2(MeCN)_2$ and were unable to distinguish between the two mechanisms for $Co(dpgBF_2)_2(MeCN)_2$.

This pair of reports sparked a general interest in the use of cobaloximes for HER in a variety of contexts, including photocatalytic[7–19] as well as electrocatalyic[3,5,6,20] systems in both aqueous and organic solvents. Despite the ubiquity of these reports, however, a consensus mechanism never developed.

There have been attempts to directly study the mechanism of cobaloxime-mediated HER, though the emerging picture has possibly become less clear rather than more. A 1971 report by Schrauzer and Holland[21] identifying a “hydridocobaloxime” prepared by reduction with $NaBH_4$ and stabilized by PBu_3 trans to the hydride (Chart 2) has formed the basis for

mechanistic work from this apparent trapped intermediate. However, Artero et al. called into question the assignment of this complex as a classical metal hydride based on its purple color and the downfield ^{1}H NMR resonance (~6 ppm) assigned as that of the hydride; a Co(III) hydride would be expected to be pale yellow with a hydride resonance upfield of 0 ppm.[22] After repeating the experimental measurements and performing theoretical calculations, Artero reassigned the product as the ligand-protonated Co(I) tautomer of the original formulation with a hydride resonance of ~-5 ppm.

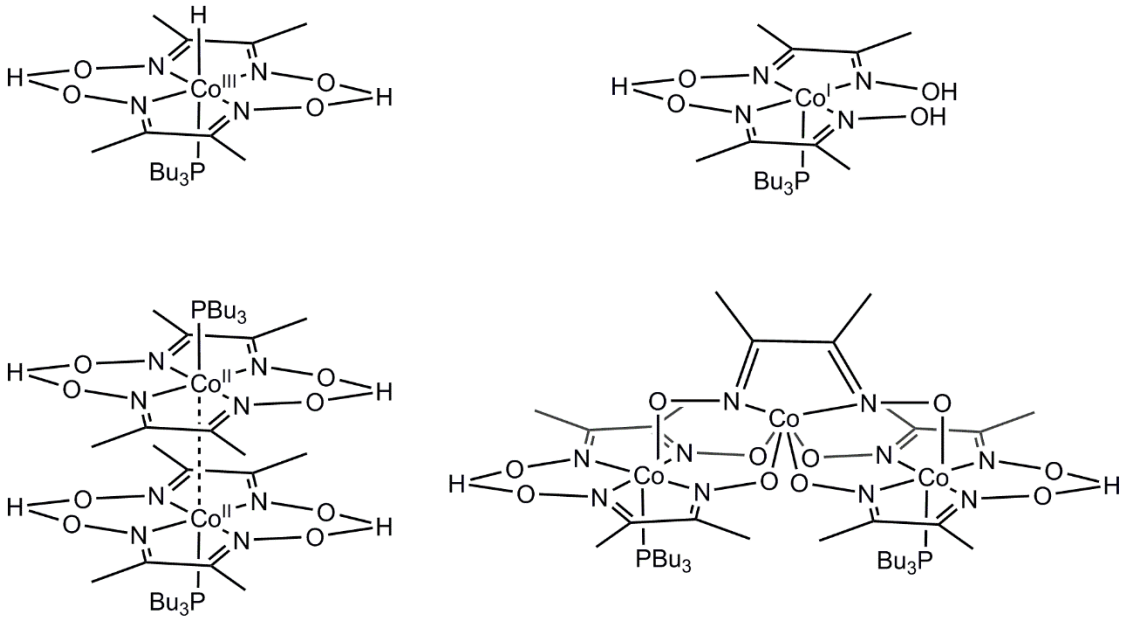

Chart 2: Assignments of the structure of "hydridocobaloxime". Top left, original assignment by Schrauzer and Holland;[21] top right, reassignment by Artero et al.;[22] bottom, major and minor products as assigned by Peters et al.[23]

More recently, the Peters group has again repeated that experimental characterization and found that the purple material which results from the $NaBH_4$ reduction of $Co(dmgH)_2Cl(PBu_3)$ does not correspond to a "hydridocobalxime" at all.[23] Instead, the major product was confirmed by X-ray crystallography to be the Co-Co bonded dimer $[Co(dmgH)_2(PBu_3)]_2$, with the apparent hydride signal arising from a paramagnetic trinuclear minor product. Alarmingly, this result invalidates mechanistic work which relied on this

incorrectly assigned “hydride”, including studies which measured the rate of H_2 evolution from the material upon addition of acid[24] as well as studies which assigned the spectra of various intermediates based on the spectrum of “hydridocobaloxime”.[25]

The most direct inspection of the mechanism of cobaloxime-mediated HER is a contribution from Dempsey and Gray in 2010 utilizing a strong photoacid and transient absorption spectroscopy to rapidly protonate $[Co^{I}(dmgBF_2)_2(MeCN)]^-$, allowing for the observation of the formation and decay of two intermediates prior to H_2 evolution and generation of the Co(II).[26] These intermediates were proposed to correspond first to the Co(III) hydride which results from protonation of the Co(I) anion, followed by the intermediate Co(II) hydride which results from reduction by excess Co(I). This final species is ultimately protonated again to release H_2. This result demonstrated that further reduction of a Co(III) hydride is possible under catalytic conditions and may be necessary in order to render the metal hydride reactive enough to produce hydrogen. This pathway has more recently been proposed under electrocatalytic conditions based on foot-of-the-wave analysis and other electroanalytical chemistry methods.[27,28] With this possibility under consideration, a second homolytic path (Scheme 1, violet arrow) may be added to the possibilities first proposed by Schrauzer.

Also complicating the picture is the possibility for ligand noninnocence. The Peters group has investigated related macrocycles in which the oxime oxygens and bridging atoms on one half of the macrocycle have been replaced by hydrocarbon linkers (Chart 3), and these studies have highlighted the importance of ligand protonation in H-bridged cobaloxime systems.[29] Aqueous HER catalysis by these complexes shows a Nernstian response consistent with a one-proton, one-electron process, while catalysis by $Co(dmgBF_2)_2$ complexes in MeCN does not, suggesting that protonation likely occurs on the ligand.

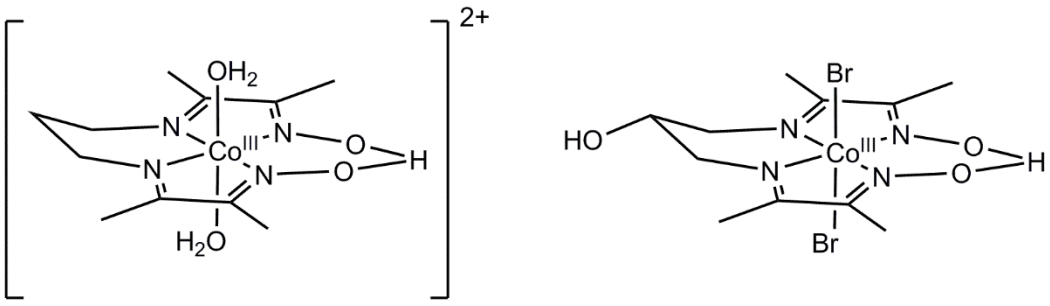

Chart 3: Cobalt diimine-dioxime complexes.

Additionally, a report by the Norton group concerning high-pressure spectroscopy of $Co(dmgBF_2)_2(MeCN)_2$ under 70 atm H_2 features slow growth of optical and ^1H NMR spectral features consistent with a solvent-assisted ligand-protonated product, suggesting that a ligand-protonated species could figure into catalysis even in the fluoroborated cobaloximes.[30] Electrochemical analysis of $Co(dmgBF_2)_2(MeCN)_2$ under high pressures of H_2, however, cast doubt on this hypothesis, as the $Co^{II/I}$ couple is positioned ca. 300 mV more negative than at 1 atm, which suggests that ligand-protonated species would not be the observed catalyst even if it is generated.[27]

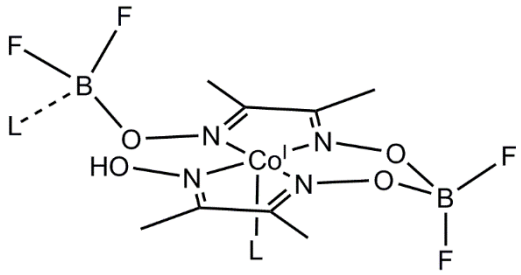

Figure 1: Proposed structure of the high-pressure reaction between H_2 and $Co(dmgBF_2)_2(MeCN)_2$ (L = MeCN).

History of Cobaloximes as Hydrogenation and HOR Catalysts

In the 1970s, the Simándi and Yamaguchi groups reported the first reactions of cobaloximes with dihydrogen, which resulted in decomposition via hydrogenation of the macrocyclic ligand.[31–34] This decomposition can be outcompeted by catalytic hydrogenation if an

alternate substrate such as a Schiff base[35] or styrene[32] is present. Simándi et al. reported that the rate law for hydrogenation of styrene in MeOH and 1:1 MeOH:H_2O is second-order in $Co(dmgH)_2$ and first-order in H_2, suggesting that the turnover-limiting step is homolytic activation of H_2. They also reported that coordination of an axial pyridine in lieu of solvent (MeOH/H_2O) enhanced the reaction rate by two orders of magnitude, highlighting the importance of understanding the effect of the axial ligands in cobaloxime systems. Complicating the matter, under most conditions the resting state of the cobaloxime is Co(II), a labile oxidation state that lends the molecule to readily undergo axial ligand substitution, leading to speciation if more than one viable ligand exists in solution.[36] Similar axial ligand effects have surfaced in more recent years in both the HER[12,37,38] and H_2 activation[39] literature.

Simándi et al. also studied the reaction of $Co(dmgH)_2$ complexes with H_2 in the presence of strong Brønsted base and found it competent for HOR catalysis.[31] As with styrene, the observed rate law is termolecular, but the HOR rate is enhanced relative to styrene hydrogenation, which implies that they cannot have the same intermediate in the rate-limiting step. Simándi et al. propose that deprotonation of one of the macrocyclic bridges produces a more active species for H_2 activation, a suggestion which mirrors more recent observations of ligand protonation in HER.

Norton et al. have more recently developed $Co(dmgBF_2)_2$ complexes under H_2 as H-atom transfer catalysts for radical cyclizations.[40] Kinetics experiments with a modified trityl radical and with TEMPO as H-atom acceptors resulted in a rate law second-order in Co, first-order in H_2, and independent of acceptor concentration or identity. This result suggests that substitution of BF_2 at the bridging position does not change the turnover-limiting H_2 activation found by Simándi et al. Further detailed mechanistic work from the Norton group has established that only the pentacoordinate $Co(dmgBF_2)_2L$ is active, and that the identity of L can have a dramatic effect on the rate of reaction.[39] Stronger donor ligands which labilize the trans ligand can case as much as an order of magnitude rate enhancement. By contrast, the rate is slowed by an order of magnitude by PPh_3, which only singly ligates

$Co(dmgBF_2)_2$, which they attribute to enforcement of a pseudo-boat conformation in the macrocycle rather than the pseudo-chair observed in most crystal structures. The pseudo-boat conformation may be sterically congested enough to slow bimolecular activation of H_2.

Studies of HOR in organic solvent with fluoroborated cobaloximes have been limited to a stoichiometric demonstration by the Peters group that with $Co(dmgBF_2)_2(MeCN)_2$, but not $Co(dpgBF_2)_2(MeCN)_2$, some degree of reversibility is possible using the conjugate bases of the acids used for HER catalysis.[20] The reaction approaches an unfavorable (K_{eq} = 0.03 $atm^{-1/2}$) equilibrium over the course of 34 with anisosbestic behavior, which the authors attribute to decomposition of the complex.

Taken together, these reports display that the rate cobaloxime-mediated H_2 activation in both HOR and hydrogenation reactions are markedly sensitive to changes in both the macrocycle and axial ligands. The third-order rate constants found by Simándi et al. range from ~10-3200 $M^{-2}s^{-1}$ for styrene hydrogenation by $Co(dmgH)_2$, depending on the solvent and presence of added pyridine.[32] When the reaction is instead HOR with strong base, they found a third-order rate constant of ~2200 $M^{-2}s^{-1}$.[31] In MeCN, Norton et al. found a third-order rate constant of ~110 $M^{-2}s^{-1}$ for radical hydrogenation.[40] This relatively slow oxidation of H_2 in acetonitrile contrasts with the fast second-order rates (k_{app} = 7000 $M^{-1}s^{-1}$) observed for $Co(dmgBF_2)_2(MeCN)_2$-catalyzed HER.[6] Additional research is needed to clarify the mechanism of cobaloxime-mediated HER and HOR and the factors governing the reaction rates.

Results

Scheme 2

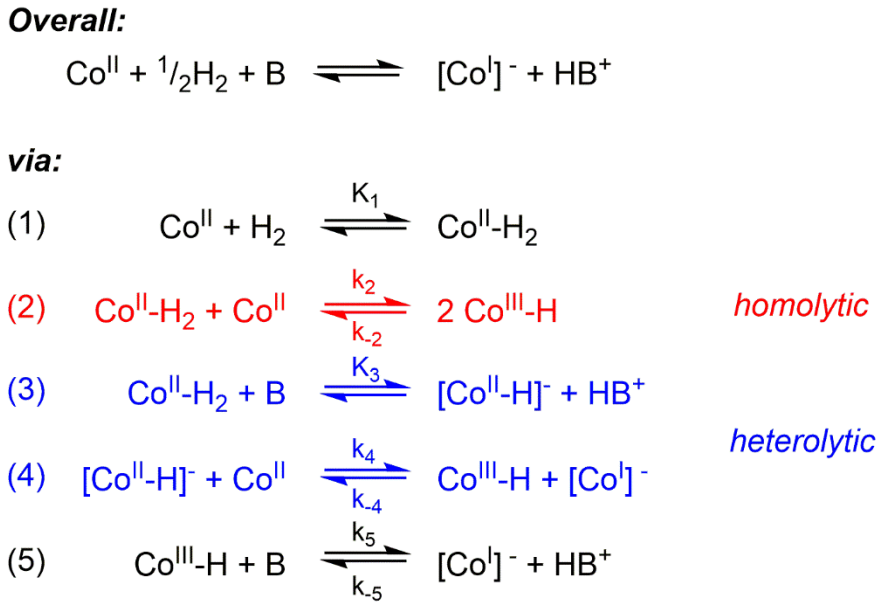

The stoichiometric oxidation of hydrogen to protons by cobaloximes may proceed either via bimetallic homolytic H-H bond cleavage or deprotonation (heterolysis), and the balance of data in the literature suggests that both pathways are accessible (Scheme 2). Using the pre-equilibrium approximation for equations (1) and (3) and the steady-state approximation for [Co^{III}-H], a rate law emerges which is second-order in Co regardless of the dominant pathway (Equation 6). In this work, kinetic studies of $Co(dmgBF_2)_2L_2$-mediated HOR were undertaken with the goal of determining whether this approximate rate law is appropriate and, if so, to measure the rate constants related to each pathway. By better understanding the bifurcation between these two pathways, insight may be gained into the microscopic-reverse HER.

$$(6) \qquad \frac{d[Co^I]^-}{dt} = \left\{K_1 k_2 + K_1 K_3 k_4 \frac{[B]}{[HB^+]}\right\}[Co^{II}]^2[H_2]$$

Selection of Base and Initial Kinetic Experiments

Co(II) species are kinetically labile, and cobaloximes in this oxidation state rapidly exchange axial ligands. In order to simplify kinetic analysis and avoid solution speciation, a non-coordinating base was sought which would ensure that solvent was the only source of spectator axial ligands. The optical spectra of $Co(dmgBF_2)_2(MeCN)_2$ solutions in MeCN were not altered by addition of *N*,*N*-dimethylaniline or 1,8-bis(dimethylamino)naphthalene ("proton sponge"), indicating neither displaces axial MeCN. Proton sponge is a relatively strong base (conjugate acid pK_a in MeCN = 18.2[41]), which favors the products side of the equilibrium, and an easy-to-handle solid at room temperature, making it an ideal candidate for initial studies.

Addition of an atmosphere of H_2 to a MeCN solution containing $Co(dmgBF_2)_2(MeCN)_2$ and excess proton sponge resulted in the appearance of optical bands at 553 and 628 nm, consistent with the known spectrum of $[Co(dmgBF_2)_2MeCN]^-$ after an induction period of three hours (Figure 2).[26] The $[Co(dmgBF_2)_2MeCN]^-$ spectrum continued to grow in isosbestically over the course of three days until all of the $Co(dmgBF_2)_2(MeCN)_2$ had been converted to $[Co(dmgBF_2)_2MeCN]^-$. The reaction did not reverse when the H_2 atmosphere was removed and was not altered by the presence of the conjugate acid.

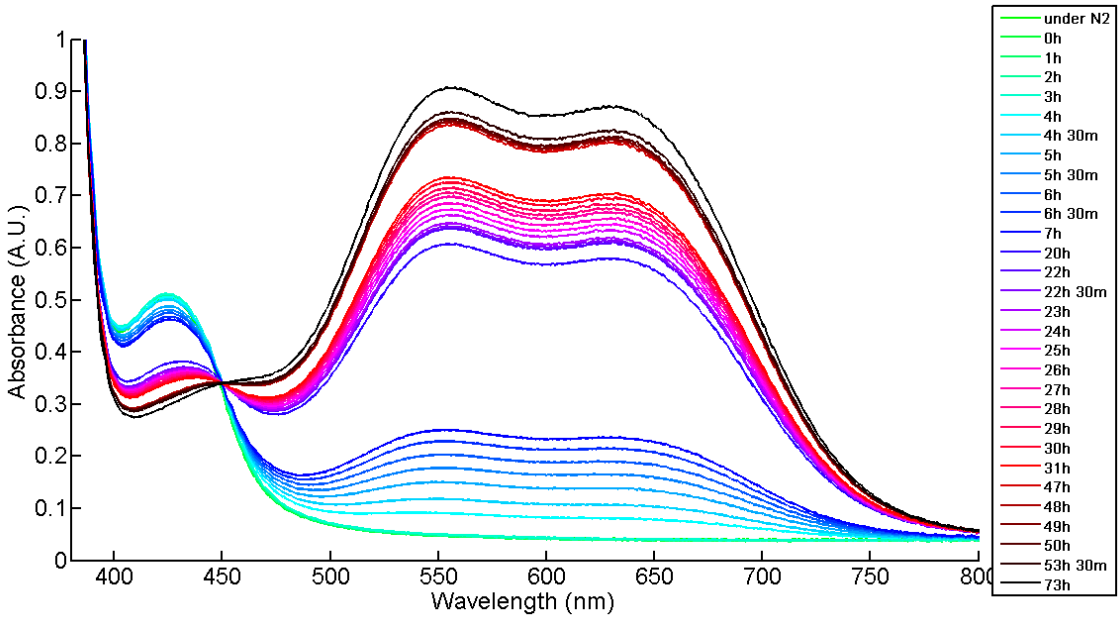

Figure 2: Time-dependent optical spectra of 1.9 mM $Co(dmgBF_2)_2(MeCN)_2$ and 36 mM proton sponge in MeCN under 1 atm H_2.

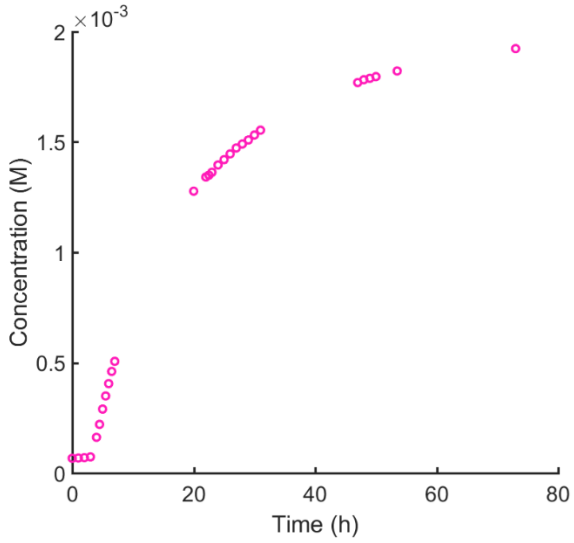

Figure 3: Concentration of Co(I) over time based on absorption at 553 nm.

Varying the concentration of both the Co species and the base produced variable induction periods with no distinct pattern, but all reactions proceeded to completion over the course of 2-3 days. Plots of the natural logarithm, inverse, and inverse-square of concentration vs. time were all nonlinear even when the induction period was excluded from the data.

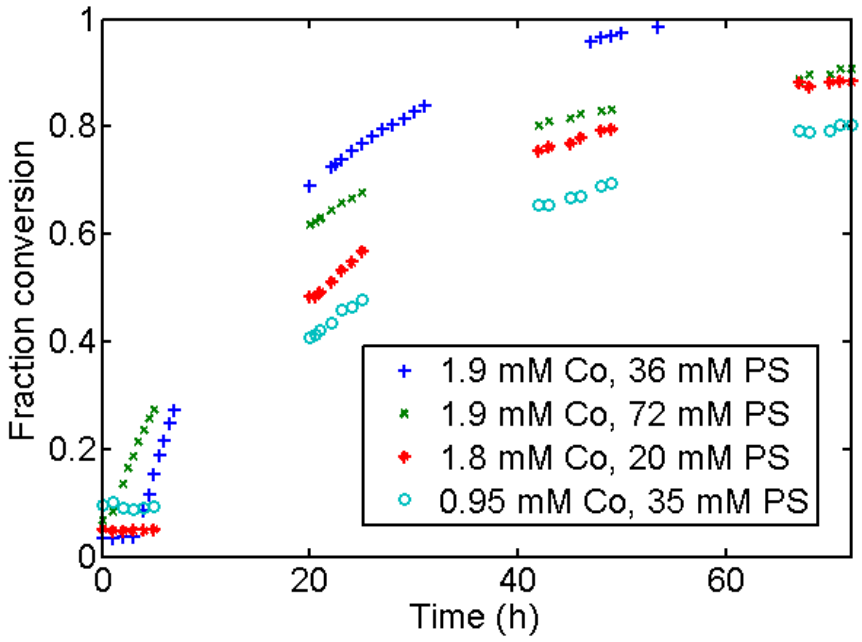

Figure 4: Comparison of data from runs with different initial concentrations of $Co(dmgBF_2)_2(MeCN)_2$ (Co) and proton sponger (PS).

Initial Rate Experiments Using Proton Sponge

The initial rate method is ideal for studying slow reactions, and was pursued along with higher concentration experiments to expedite data collection (Table 1, additional data in Supporting Data). The initial concentration of each reactant was systematically varied, and the average of a linear fit of the absorption data for the two Co(I) bands used to calculate the initial rate for each condition, truncating any observed induction period. The initial rate was not affected by variations in initial concentration of proton sponge. However, doubling the

initial pressure of H_2 resulted in a doubling of the initial rate, and the initial rate varied with variations in the initial concentration of $Co(dmgBF_2)_2(MeCN)_2$. A natural log-log plot of the initial rate vs. concentration was linear with a slope of 2.03 (Figure 5).

Table 1: Initial rate data for the reaction of $Co(dmgBF_2)_2(MeCN)_2$ (Co), proton sponge (B) and H_2.

Entry	$[Co]_0$ (mM)	$[B]_0$ (mM)	$P(H_2)$ (atm)	Initial Rate ($M/s \times 10^7$)
1	5.8	8.5	1.0	3.4
2	6.0	4.3	1.0	3.3
3	6.0	2.1	1.0	3.2
4	4.6	2.2	1.0	1.9
5	3.0	2.1	1.0	0.91
6	1.7	2.2	1.0	0.23
7	5.8	25.2	1.0	4.4
8	6.2	19.7	0.50	1.9
9	6.3	19.7	0.25	0.86

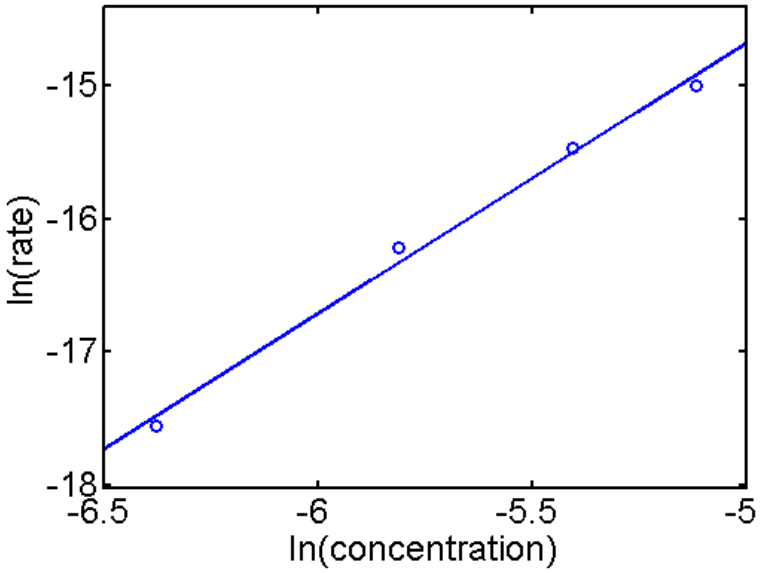

Figure 5: Rate vs. concentration log-log plot for Co-varied runs and fit line. Slope = 2.03, R^2 = 0.999.

Extension to N,N-dimethylaniline

Further initial rate experiments were pursued using *N*,*N*-dimethylaniline in order to understand the effect of base strength (conjugate acid pK_a in MeCN = 11.4[42]) on the kinetics of $Co(dmgBF_2)_2(MeCN)_2$-mediated HOR. Induction periods prior to the appearance of $[Co(dmgBF_2)_2MeCN]^-$ bands were frequently observed. The concentration vs. time data became nonlinear within minutes, and the reaction did not proceed to completion after 24 h. After three days, the solution had reached equilibrium with an equilibrium constant of 1.3 x 10^{-5} $atm^{-1/2}$. Removal of H_2 resulted in a slow diminution of the $[Co(dmgBF_2)_2MeCN]^-$ spectrum.

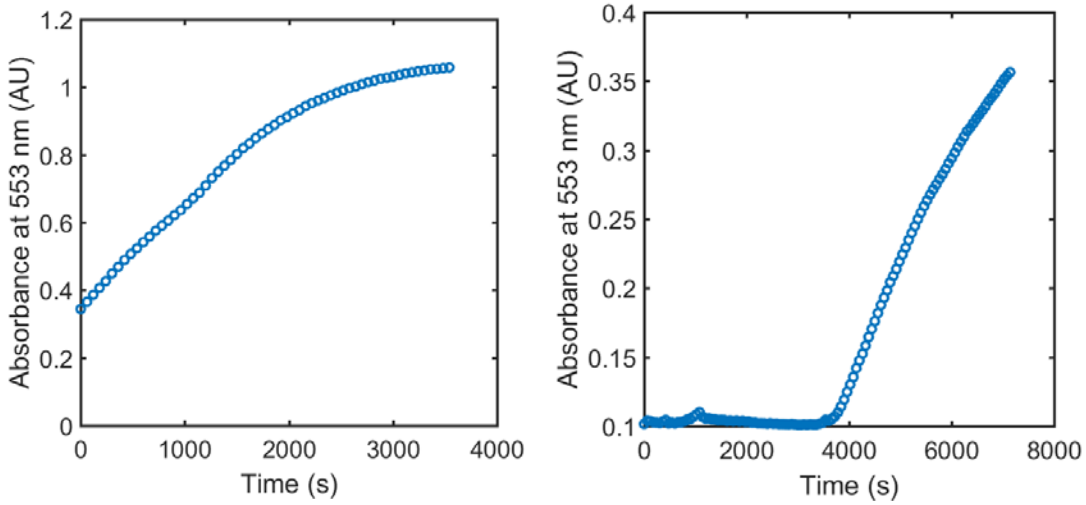

Figure 6: Example plots of absorbance over time for Co(dmgBF-$_2$)$_2$(MeCN)$_2$ and *N*,*N*-dimethylaniline under H_2.

Discussion

Observed Induction Period

The variable induction periods observed in these experiments likely occur due to trace O_2 present in solution. Blue solutions of [Co(dmgBF$_2$)$_2$MeCN]$^-$ are rapidly converted to yellow Co(dmgBF$_2$)$_2$(MeCN)$_2$ on exposure to air, and the induction periods observed were considerably longer when an ordinary Schlenk line (pressure ca. 50 mTorr) was used to degas the reaction vessel than when a high vacuum line (pressure ca. 5 μTorr) was used. The induction period is then produced by rapid reoxidation of [Co(dmgBF$_2$)$_2$MeCN]$^-$ as it is produced at early time points. If this is the case, initial rate data recorded after the induction period ends should still be valid, since the reaction of interest is rate-limiting and therefore the induction period is simply obscuring the beginning of the linear data region. However, rigorous exclusion of oxygen or monitoring of the production of products not affected by trace oxygen (i.e. conjugate acid) would be desirable to verify this hypothesis and ensure the reliablility of the data collected. Additionally, for experiments with bases such as *N*,*N*-dimethylaniline which approach equilibrium rapidly relative to the length of the induction

period, enough of the linear data region may be obscured to render initial rates difficult to reliably extract.

The source of the O_2 is unclear, as solutions were prepared in a nitrogen-filled glovebox in Kontes valve-equipped cuvettes which were sufficiently gastight to prevent detectable leakage of H_2 and degassed on a high-vacuum line before H_2 addition from a line flushed with gas for several minutes. These conditions would ordinarily be considered rigorously free of O_2; it is possible that this reaction is simply slow enough to observe the effects of unavoidable traces of O_2 which remain despite the most rigorous efforts to eliminate it.

Rate Law of HOR

The initial rate data for $Co(dmgBF_2)_2(MeCN)_2$-mediated HOR indicates a reaction that is second-order in Co, first-order in H_2, and zero-order in proton sponge, with a rate constant of $3.8 \pm .5\ M^{-2}s^{-1}$. This rate law suggests that only the homolytic pathway is accessed in this reaction, and the rate constant is smaller by two orders of magnitude than that measured by Norton with radical scavengers.[40]

The complete dominance of the homolytic pathway is unexpected, given that proton sponge is sufficiently basic to make the reaction irreversible, as evidenced by the final concentration of $[Co(dmgBF_2)_2MeCN]^-$ being equal to the initial concentration of $Co(dmgBF_2)_2(MeCN)_2$, the observation that the reaction does not reverse when the H_2 atmosphere is removed, and the lack of any effect on the reaction when the conjugate acid is present in solution. It is possible, then, that the pK_a of the Co(III) hydride species is less than 18.2 in MeCN, but the pK_a of the dihydrogen adduct is much higher. Recent work examining the relationship between acid identity and hydride formation rates in a related Co complex identified a departure from the linear free energy relationship with pK_a when the acidic proton is sterically encumbered, as in *N,N*-dimethylanilinium.[43] It is therefore also possible that the selection of a sterically encumbered base in order to preclude solution speciation has resulted

in a much slower deprotonation rate than would be expected based on pH, to the point where heterolysis cannot compete with homolysis.

Further research would be needed to distinguish these effects. Alternate strategies for circumventing solution speciation, such as using a strong non-solvent axial ligand to push the speciation equilibrium far to one side or operating in a noncoordinating solvent such as CH_2Cl_2 would allow for unencumbered bases to be examined and analyzed unambiguously based on conjugate acid pK_a.

Conclusion

Initial rate data suggests that the HOR mediated by $Co(dmgBF_2)_2(MeCN)_2$ using proton sponge as the base proceeds by homolytic cleavage of the H-H bond. More experiments varying the base are needed to contextualize these results, as well as better methodology with respect to the exclusion of oxygen.

References

(1) Schrauzer, G. N.; Windgassen, R. J. Über Cobaloxime(II) Und Deren Beziehung Zum Vitamin B12r. *Chem. Ber.* **1966**, *99* (2), 602–610. https://doi.org/10.1002/cber.19660990234.

(2) Schrauzer, G. N.; Windgassen, R. J. Alkylcobaloximes and Their Relation to Alkylcobalamins. *J. Am. Chem. Soc.* **1966**, *88* (16), 3738–3743. https://doi.org/10.1021/ja00968a012.

(3) Razavet, M.; Artero, V.; Fontecave, M. Proton Electroreduction Catalyzed by Cobaloximes: Functional Models for Hydrogenases. *Inorg. Chem.* **2005**, *44* (13), 4786–4795. https://doi.org/10.1021/ic050167z.

(4) Connolly, P.; Espenson, J. H. Cobalt-Catalyzed Evolution of Molecular Hydrogen. *Inorg. Chem.* **1986**, *25* (16), 2684–2688. https://doi.org/10.1021/ic00236a006.

(5) Dempsey, J. L.; Brunschwig, B. S.; Winkler, J. R.; Gray, H. B. Hydrogen Evolution Catalyzed by Cobaloximes. *Acc. Chem. Res.* **2009**, *42* (12), 1995–2004. https://doi.org/10.1021/ar900253e.

(6) Hu, X.; Cossairt, B. M.; Brunschwig, B. S.; Lewis, N. S.; Peters, J. C. Electrocatalytic Hydrogen Evolution by Cobalt Difluoroboryl-Diglyoximate Complexes. *Chem. Commun.* **2005**, No. 37, 4723–4725. https://doi.org/10.1039/B509188H.

(7) Zhang, P.; Jacques, P.-A.; Chavarot-Kerlidou, M.; Wang, M.; Sun, L.; Fontecave, M.; Artero, V. Phosphine Coordination to a Cobalt Diimine–Dioxime Catalyst Increases Stability during Light-Driven H2 Production. *Inorg. Chem.* **2012**, *51* (4), 2115–2120. https://doi.org/10.1021/ic2019132.

(8) Li, L.; Duan, L.; Wen, F.; Li, C.; Wang, M.; Hagfeldt, A.; Sun, L. Visible Light Driven Hydrogen Production from a Photo-Active Cathode Based on a Molecular Catalyst and Organic Dye-Sensitized p-Type Nanostructured NiO. *Chem. Commun.* **2012**, *48* (7), 988–990. https://doi.org/10.1039/C2CC16101J.

(9) Guttentag, M.; Rodenberg, A.; Kopelent, R.; Probst, B.; Buchwalder, C.; Brandstätter, M.; Hamm, P.; Alberto, R. Photocatalytic H2 Production with a Rhenium/Cobalt System in Water under Acidic Conditions. *Eur. J. Inorg. Chem.* **2012**, *2012* (1), 59–64. https://doi.org/10.1002/ejic.201100883.

(10) Utschig, L. M.; Silver, S. C.; Mulfort, K. L.; Tiede, D. M. Nature-Driven Photochemistry for Catalytic Solar Hydrogen Production: A Photosystem I–Transition Metal Catalyst Hybrid. *J. Am. Chem. Soc.* **2011**, *133* (41), 16334–16337. https://doi.org/10.1021/ja206012r.

(11) Probst, B.; Guttentag, M.; Rodenberg, A.; Hamm, P.; Alberto, R. Photocatalytic H2 Production from Water with Rhenium and Cobalt Complexes. *Inorg. Chem.* **2011**, *50* (8), 3404–3412. https://doi.org/10.1021/ic102317u.

(12) McCormick, T. M.; Han, Z.; Weinberg, D. J.; Brennessel, W. W.; Holland, P. L.; Eisenberg, R. Impact of Ligand Exchange in Hydrogen Production from Cobaloxime-Containing Photocatalytic Systems. *Inorg. Chem.* **2011**, *50* (21), 10660–10666. https://doi.org/10.1021/ic2010166.

(13) Dong, J.; Wang, M.; Zhang, P.; Yang, S.; Liu, J.; Li, X.; Sun, L. Promoting Effect of Electrostatic Interaction between a Cobalt Catalyst and a Xanthene Dye on Visible-Light-Driven Electron Transfer and Hydrogen Production. *J. Phys. Chem. C* **2011**, *115* (30), 15089–15096. https://doi.org/10.1021/jp2040778.

(14) Zhang, P.; Wang, M.; Dong, J.; Li, X.; Wang, F.; Wu, L.; Sun, L. Photocatalytic Hydrogen Production from Water by Noble-Metal-Free Molecular Catalyst Systems Containing Rose Bengal and the Cobaloximes of BFx-Bridged Oxime Ligands. *J. Phys. Chem. C* **2010**, *114* (37), 15868–15874. https://doi.org/10.1021/jp106512a.

(15) Zhang, P.; Wang, M.; Li, C.; Li, X.; Dong, J.; Sun, L. Photochemical H2 Production with Noble-Metal-Free Molecular Devices Comprising a Porphyrin Photosensitizer and a Cobaloxime Catalyst. *Chem. Commun.* **2009**, *46* (46), 8806–8808. https://doi.org/10.1039/C0CC03154B.

(16) Probst, B.; Rodenberg, A.; Guttentag, M.; Hamm, P.; Alberto, R. A Highly Stable Rhenium−Cobalt System for Photocatalytic H2 Production: Unraveling the Performance-Limiting Steps. *Inorg. Chem.* **2010**, *49* (14), 6453–6460. https://doi.org/10.1021/ic100036v.

(17) Berben, L. A.; Peters, J. C. Hydrogen Evolution by Cobalt Tetraimine Catalysts Adsorbed on Electrode Surfaces. *Chem. Commun.* **2010**, *46* (3), 398–400. https://doi.org/10.1039/B921559J.

(18) Probst, B.; Kolano, C.; Hamm, P.; Alberto, R. An Efficient Homogeneous Intermolecular Rhenium-Based Photocatalytic System for the Production of H2. *Inorg. Chem.* **2009**, *48* (5), 1836–1843. https://doi.org/10.1021/ic8013255.

(19) Du, P.; Schneider, J.; Luo, G.; Brennessel, W. W.; Eisenberg, R. Visible Light-Driven Hydrogen Production from Aqueous Protons Catalyzed by Molecular Cobaloxime Catalysts. *Inorg. Chem.* **2009**, *48* (11), 4952–4962. https://doi.org/10.1021/ic900389z.

(20) Hu, X.; Brunschwig, B. S.; Peters, J. C. Electrocatalytic Hydrogen Evolution at Low Overpotentials by Cobalt Macrocyclic Glyoxime and Tetraimine Complexes. *J. Am. Chem. Soc.* **2007**, *129* (29), 8988–8998. https://doi.org/10.1021/ja067876b.

(21) Schrauzer, G. N.; Holland, R. J. Hydridocobaloximes. *J. Am. Chem. Soc.* **1971**, *93* (6), 1505–1506. https://doi.org/10.1021/ja00735a040.

(22) Bhattacharjee, A.; Chavarot-Kerlidou, M.; Andreiadis, Eugen. S.; Fontecave, M.; Field, M. J.; Artero, V. Combined Experimental–Theoretical Characterization of the Hydrido-Cobaloxime [HCo(DmgH)2(PnBu3)]. *Inorg. Chem.* **2012**, *51* (13), 7087–7093. https://doi.org/10.1021/ic2024204.

(23) Lacy, D. C.; Roberts, G. M.; Peters, J. C. The Cobalt Hydride That Never Was: Revisiting Schrauzer's "Hydridocobaloxime." *J. Am. Chem. Soc.* **2015**, *137* (14), 4860–4864. https://doi.org/10.1021/jacs.5b01838.

(24) Chao, T.-H.; Espenson, J. H. Mechanism of Hydrogen Evolution from Hydridocobaloxime. *J. Am. Chem. Soc.* **1978**, *100* (1), 129–133. https://doi.org/10.1021/ja00469a022.

(25) Szajna-Fuller, E.; Bakac, A. Catalytic Generation of Hydrogen with Titanium Citrate and a Macrocyclic Cobalt Complex. *Eur. J. Inorg. Chem.* **2010**, *2010* (17), 2488–2494. https://doi.org/10.1002/ejic.200901176.

(26) Dempsey, J. L.; Winkler, J. R.; Gray, H. B. Mechanism of H2 Evolution from a Photogenerated Hydridocobaloxime. *J. Am. Chem. Soc.* **2010**, *132* (47), 16774–16776. https://doi.org/10.1021/ja109351h.

(27) Wiedner, E. S.; Bullock, R. M. Electrochemical Detection of Transient Cobalt Hydride Intermediates of Electrocatalytic Hydrogen Production. *J. Am. Chem. Soc.* **2016**, *138* (26), 8309–8318. https://doi.org/10.1021/jacs.6b04779.

(28) Rountree, E. S.; Martin, D. J.; McCarthy, B. D.; Dempsey, J. L. Linear Free Energy Relationships in the Hydrogen Evolution Reaction: Kinetic Analysis of a Cobaloxime Catalyst. *ACS Catal.* **2016**, *6* (5), 3326–3335. https://doi.org/10.1021/acscatal.6b00667.

(29) McCrory, C. C. L.; Uyeda, C.; Peters, J. C. Electrocatalytic Hydrogen Evolution in Acidic Water with Molecular Cobalt Tetraazamacrocycles. *J. Am. Chem. Soc.* **2012**, *134* (6), 3164–3170. https://doi.org/10.1021/ja210661k.

(30) Estes, D. P.; Grills, D. C.; Norton, J. R. The Reaction of Cobaloximes with Hydrogen: Products and Thermodynamics. *J. Am. Chem. Soc.* **2014**, *136* (50), 17362–17365. https://doi.org/10.1021/ja508200g.

(31) Simándi, L. I.; Budó-Záhonyi, É.; Szeverényi, Z. Effect of Strong Base on the Activation of Molecular Hydrogen by Pyridinebis(Dimethylglyoximato)Cobalt(II). *Inorg. Nucl. Chem. Lett.* **1976**, *12* (3), 237–241. https://doi.org/10.1016/0020-1650(76)80158-4.

(32) Simándi, L. I.; Szeverényi, Z.; Budó-Záhonyi, É. Activation of Molecular Hydrogen by Cobaloxime(II) Derivatives. *Inorg. Nucl. Chem. Lett.* **1975**, *11* (11), 773–777. https://doi.org/10.1016/0020-1650(75)80098-5.

(33) Yamaguchi, T.; Miyagawa, R. The Effect of Pyridine on the Hydrogen Absorption Process of Bis(Dimethylglyoximato)Cobalt(Ii). *Chem. Lett.* **1978**, *7* (1), 89–92. https://doi.org/10.1246/cl.1978.89.

(34) Yamaguchi, T.; Tsumura, T. The Effect of Triphenylphosphine on the Hydrogenation Reaction of Bis(Dimethylglyoximato)Cobalt(Ii). *Chem. Lett.* **1973**, *2* (4), 409–412. https://doi.org/10.1246/cl.1973.409.

(35) Yamaguchi, T.; Nakayama, M.; Tsumura, T. The Effect of Base Strength of Schiff Bases on Their Catalytic Hydrogenation with Bis(Dimethylglyoximato)Cobalt(Ii). *Chem. Lett.* **1972**, *1* (12), 1231–1234. https://doi.org/10.1246/cl.1972.1231.

(36) Lawrence, M. A. W.; Celestine, M. J.; Artis, E. T.; Joseph, L. S.; Esquivel, D. L.; Ledbetter, A. J.; Cropek, D. M.; Jarrett, W. L.; Bayse, C. A.; Brewer, M. I.; et al. Computational, Electrochemical, and Spectroscopic Studies of Two Mononuclear Cobaloximes: The Influence of an Axial Pyridine and Solvent on the Redox Behaviour and Evidence for Pyridine Coordination to Cobalt(I) and Cobalt(II) Metal Centres. *Dalton Trans.* **2016**, *45* (25), 10326–10342. https://doi.org/10.1039/C6DT01583B.

(37) Basu, D.; Mazumder, S.; Niklas, J.; Baydoun, H.; Wanniarachchi, D.; Shi, X.; Staples, R. J.; Poluektov, O.; Schlegel, H. B.; Verani, C. N. Evaluation of the Coordination Preferences and Catalytic Pathways of Heteroaxial Cobalt Oximes towards Hydrogen Generation. *Chem. Sci.* **2016**, *7* (5), 3264–3278. https://doi.org/10.1039/C5SC04214C.

(38) Panagiotopoulos, A.; Ladomenou, K.; Sun, D.; Artero, V.; Coutsolelos, A. G. Photochemical Hydrogen Production and Cobaloximes: The Influence of the Cobalt Axial N-Ligand on the System Stability. *Dalton Trans.* **2016**, *45* (15), 6732–6738. https://doi.org/10.1039/C5DT04502A.

(39) Li, G.; Estes, D. P.; Norton, J. R.; Ruccolo, S.; Sattler, A.; Sattler, W. Dihydrogen Activation by Cobaloximes with Various Axial Ligands. *Inorg. Chem.* **2014**, *53* (19), 10743–10747. https://doi.org/10.1021/ic501975r.

(40) Li, G.; Han, A.; Pulling, M. E.; Estes, D. P.; Norton, J. R. Evidence for Formation of a Co–H Bond from (H2O)2Co(DmgBF2)2 under H2: Application to Radical Cyclizations. *J. Am. Chem. Soc.* **2012**, *134* (36), 14662–14665. https://doi.org/10.1021/ja306037w.

(41) Ozeryanskii, V. A.; Pozharskii, A. F.; Milgizina, G. R.; Howard, S. T. Synthesis and Properties of 5,6-Bis(Dimethylamino)Acenaphthylene: The First Proton Sponge with Easily-Modified Basicity. *J. Org. Chem.* **2000**, *65* (22), 7707–7709. https://doi.org/10.1021/jo001171p.

(42) Tshepelevitsh, S.; Kütt, A.; Lõkov, M.; Kaljurand, I.; Saame, J.; Heering, A.; Plieger, P. G.; Vianello, R.; Leito, I. On the Basicity of Organic Bases in Different Media. *Eur. J. Org. Chem.* **2019**, *2019* (40), 6735–6748. https://doi.org/10.1002/ejoc.201900956.

(43) Elgrishi, N.; Kurtz, D. A.; Dempsey, J. L. Reaction Parameters Influencing Cobalt Hydride Formation Kinetics: Implications for Benchmarking H2-Evolution Catalysts. *J. Am. Chem. Soc.* **2017**, *139* (1), 239–244. https://doi.org/10.1021/jacs.6b10148.

(44) Pangborn, A. B.; Giardello, M. A.; Grubbs, R. H.; Rosen, R. K.; Timmers, F. J. Safe and Convenient Procedure for Solvent Purification. *Organometallics* **1996**, *15* (5), 1518–1520. https://doi.org/10.1021/om9503712.

Methods

General Considerations

Unless stated otherwise, all manipulations were carried out in a nitrogen-filled glovebox or under nitrogen or argon using standard Schlenk techniques. Dry, air-free solvents were obtained from a Grubbs-type solvent purification system.[44] $Co(dmgBF_2)_2(MeCN)_2$ was synthesized by a literature method[26] and its purity confirmed by cyclic voltammetry prior to use. Proton sponge and *N*,*N*-dimethylaniline were ordered from Sigma-Aldrich and used as received. UV-Vis spectra were recorded on a Cary Bio 50 spectrometer.

General Procedure for Kinetics Experiments

A solution of $Co(dmgBF_2)_2(MeCN)_2$ and base (proton sponge or *N*,*N*-dimethylaniline) was prepared in MeCN. A 1 mm path length, Kontes valve-sealed cuvette equipped with a side-arm bulb and a stirbar was charged with the solution and degassed on a high-vacuum line by the freeze-pump-thaw method twice. The solution was allowed to warm to room temperature before H_2 was added to the desired pressure. The reaction was monitored by UV-Vis spectroscopy by tipping the solution into the cuvette at the desired intervals and was stirred in the side-arm bulb between spectra.

Supporting Data

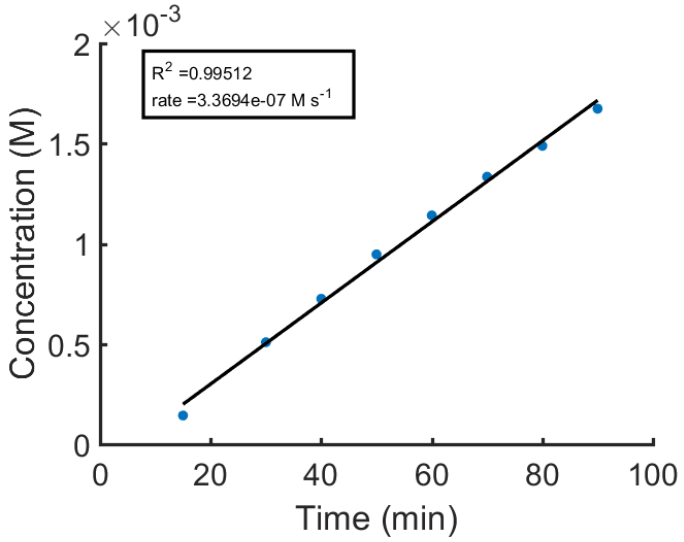

Figure S1: Initial rate plot for Table 1 entry 1, calculated based on absorbance at 553 nm.

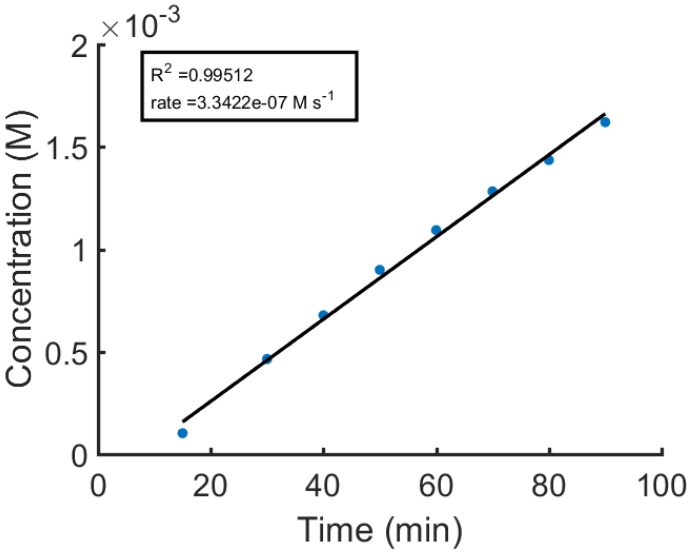

Figure S2: Initial rate plot for Table 1 entry 1, calculated based on absorbance at 628 nm.

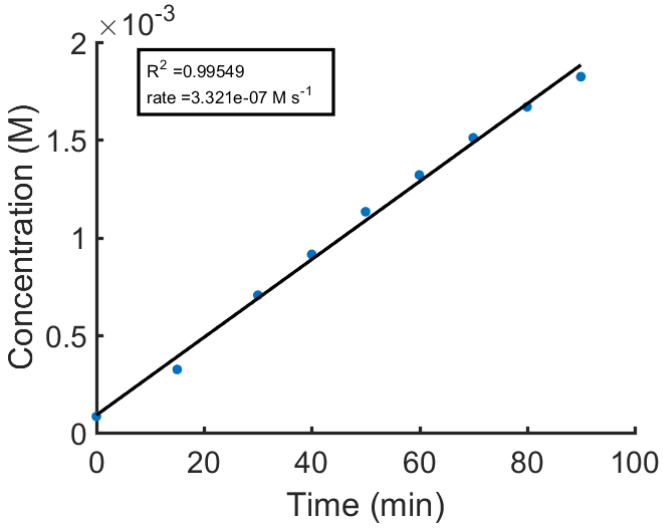

Figure S3: Initial rate plot for Table 1 entry 2, calculated based on absorbance at 553 nm.

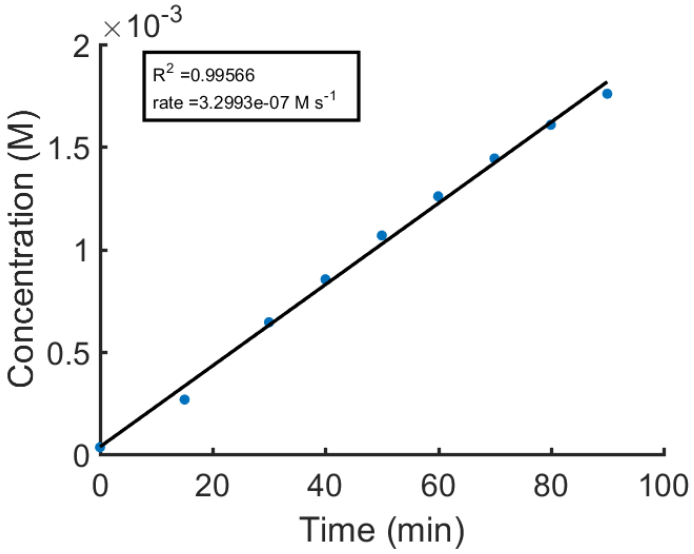

Figure S4: Initial rate plot for Table 1 entry 2, calculated based on absorbance at 628 nm.

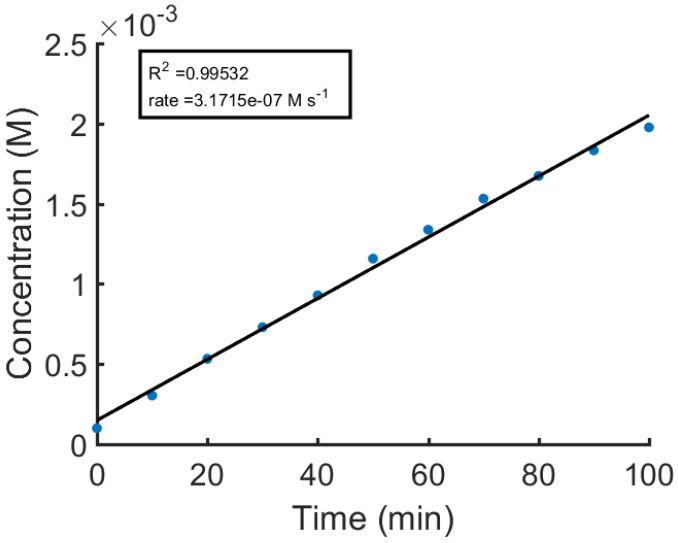

Figure S5: Initial rate plot for Table 1 entry 3, calculated based on absorbance at 553 nm.

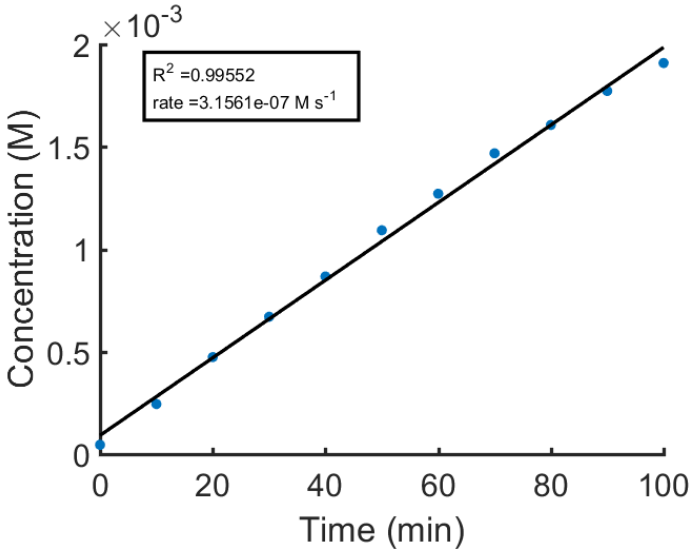

Figure S6: Initial rate plot for Table 1 entry 3, calculated based on absorbance at 628 nm.

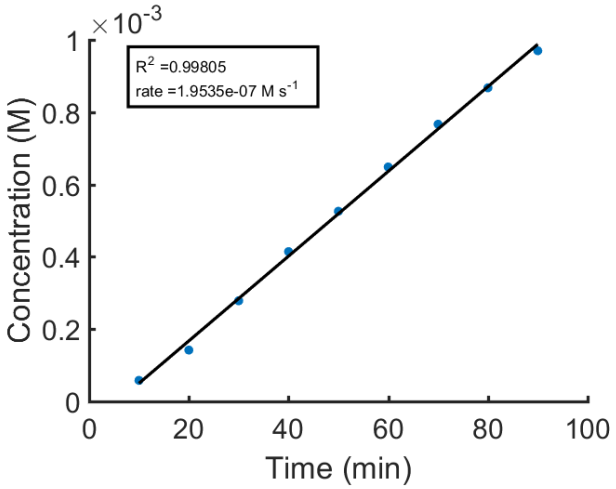

Figure S7: Initial rate plot for Table 1 entry 4, calculated based on absorbance at 553 nm.

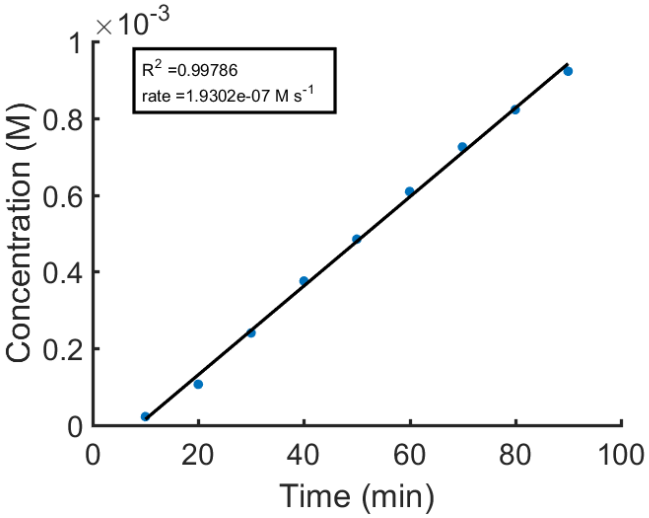

Figure S8: Initial rate plot for Table 1 entry 4, calculated based on absorbance at 628 nm.

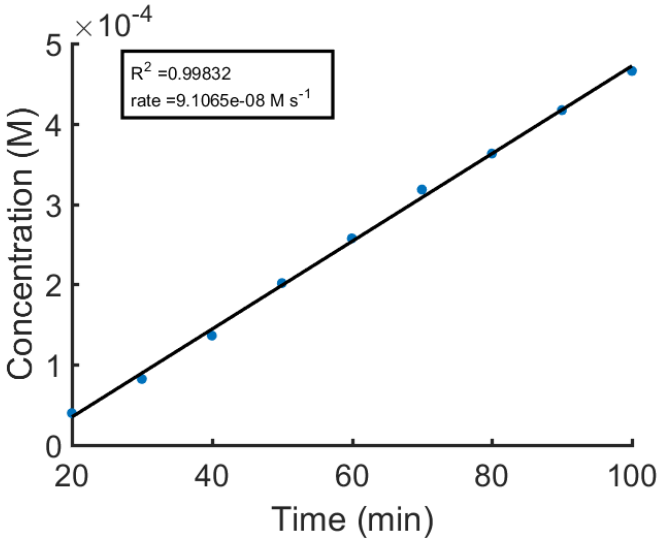

Figure S9: Initial rate plot for Table 1 entry 5, calculated based on absorbance at 553 nm.

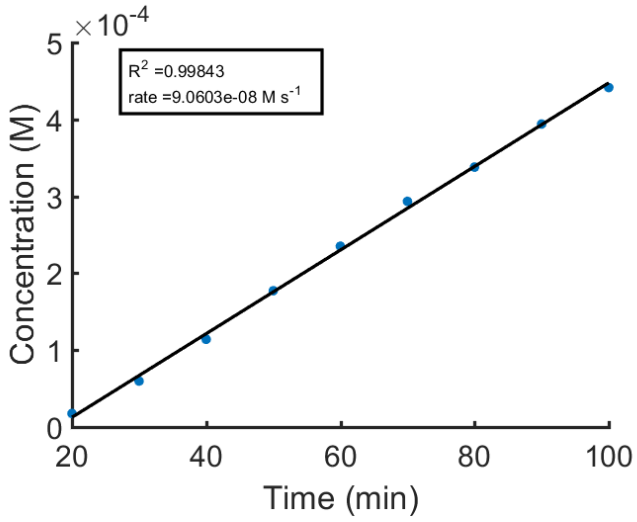

Figure S10: Initial rate plot for Table 1 entry 5, calculated based on absorbance at 628 nm.

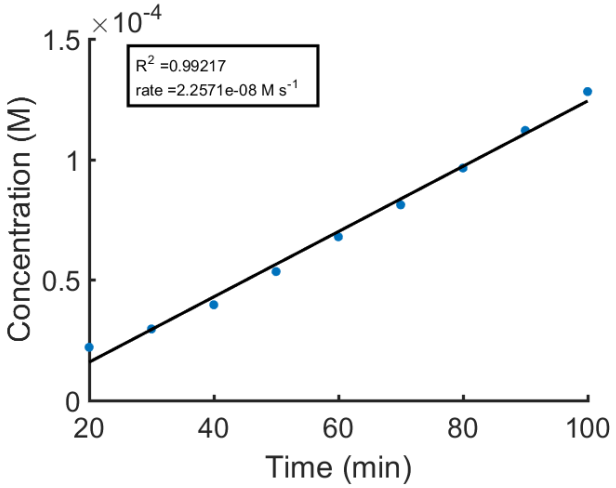

Figure S11: Initial rate plot for Table 1 entry 6, calculated based on absorbance at 553 nm.

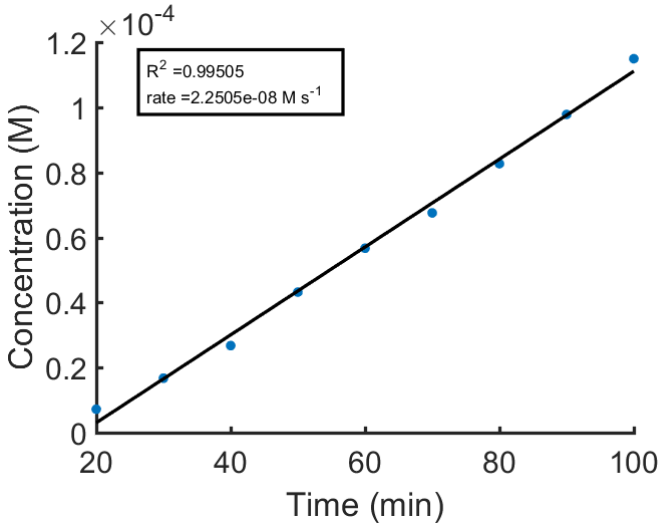

Figure S12: Initial rate plot for Table 1 entry 6, calculated based on absorbance at 628 nm.

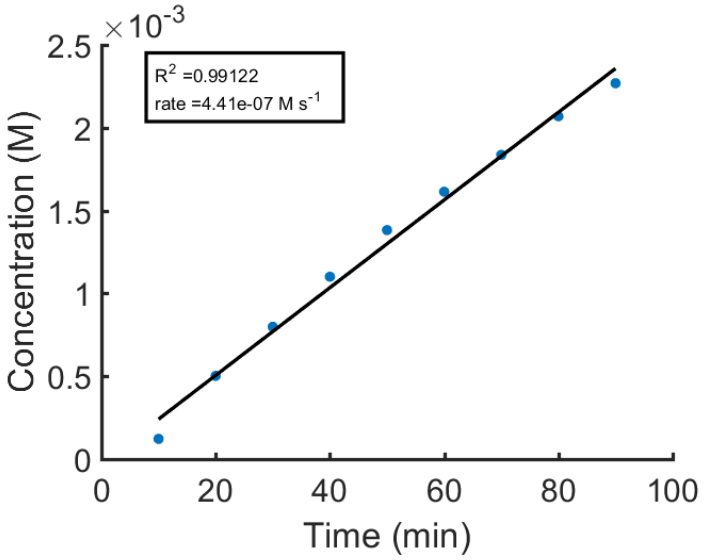

Figure S13: Initial rate plot for Table 1 entry 7, calculated based on absorbance at 553 nm.

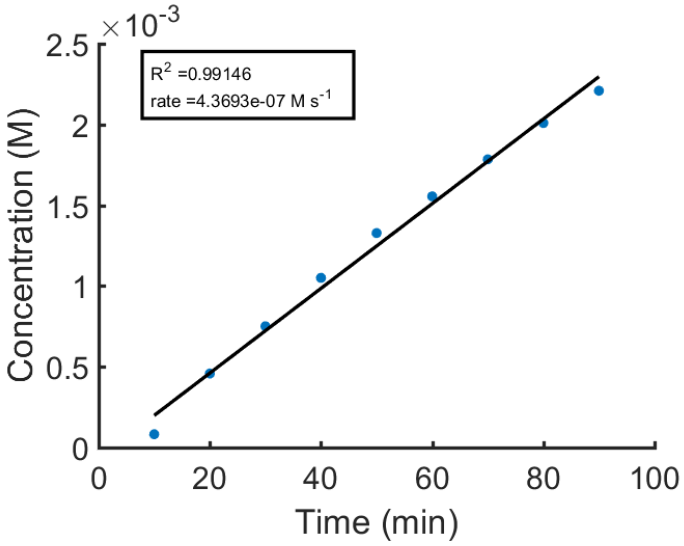

Figure S14: Initial rate plot for Table 1 entry 7, calculated based on absorbance at 628 nm.

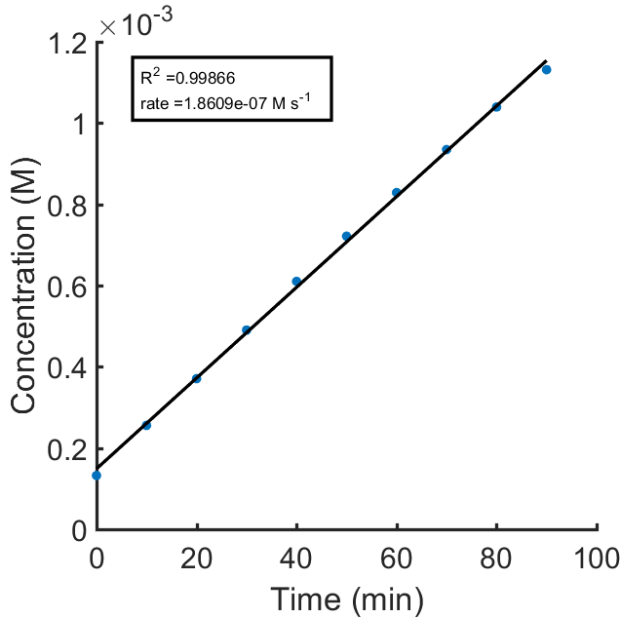

Figure S15: Initial rate plot for Table 1 entry 8, calculated based on absorbance at 553 nm.

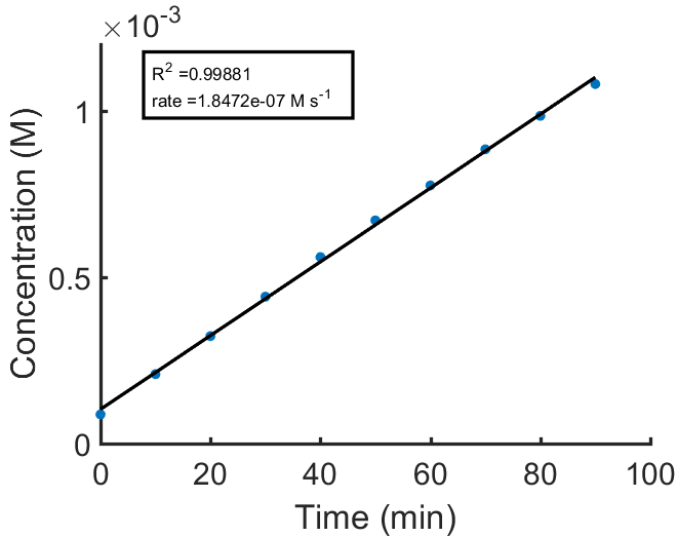

Figure S16: Initial rate plot for Table 1 entry 8, calculated based on absorbance at 628 nm.

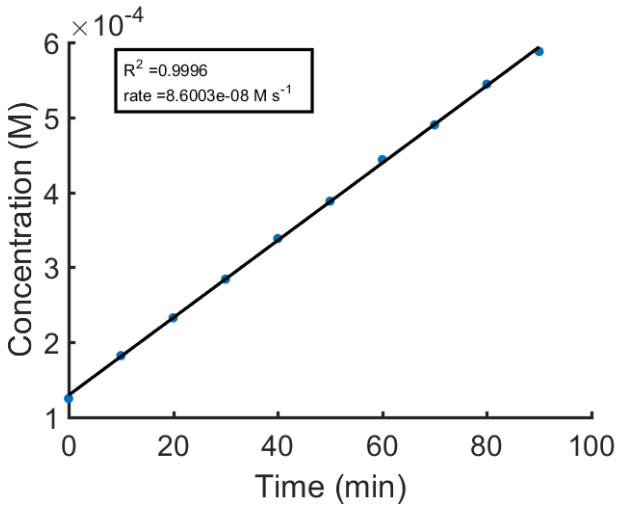

Figure S17: Initial rate plot for Table 1 entry 9, calculated based on absorbance at 553 nm

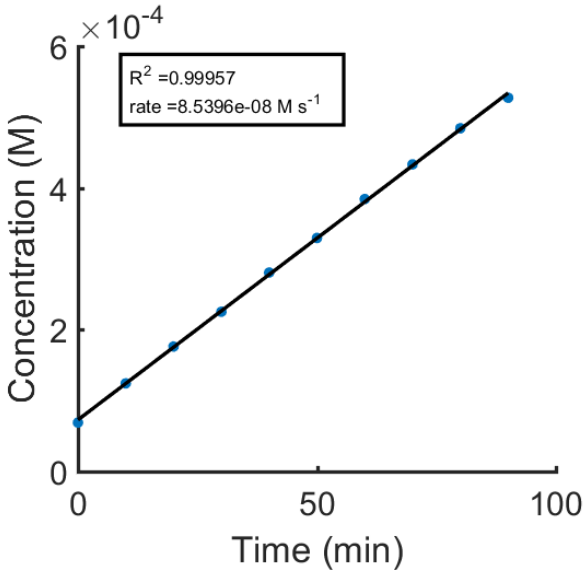

Figure S18: Initial rate plot for Table 1 entry 9, calculated based on absorbance at 628 nm.

CHAPTER 3

SYNTHESIS, SPECTROSCOPY AND BORONATION OF A NEW HETEROLEPTIC RUTHENIUM CYANIDE COMPLEX

Introduction

[Ru(diimine)(CN)$_4$]$^{2-}$ complexes

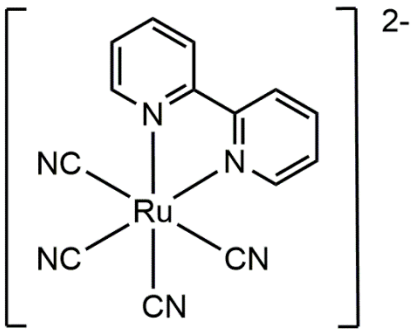

Figure 1: Structure of [Ru(bpy)(CN)$_4$]$^{2-}$.

Inspired by mounting evidence that the long-lived metal-to-ligand charge transfer (MLCT) excited state of [Ru(bpy)$_3$]$^{2+}$ featured an electron localized on just one bpy ligand, Scandola et al. first synthesized [Ru(bpy)(CN)$_4$]$^{2-}$ (Figure 1) in 1986 as a minimalistic model of Ru(II) diimine photosensitizers.[1] They observed that the luminescence and excited-state properties were very similar to [Ru(bpy)$_3$]$^{2+}$, but that the spectroscopic properties also featured strong solvatochromism. The magnitude of

the solvatochromism is driven largely by specific solvent interactions with the cyanide ligands. In a systematic study of Ru-polypyridyl-cyanide complexes with 1-5 cyanides, Meyer et al. found that shifts in the C-N stretching frequency, MLCT absorption energy, and emission energy all correlated with the Gutmann acceptor number of the solvent and increased as a function of the number of cyanide ligands.[2]

These solvatochromic properties have driven much of the interest in $[Ru(bpy)(CN)_4]^{2-}$ and related $[Ru(diimine)(CN)_4]^{2-}$ complexes,[3–5] and several applications have been reported. PPN_2 $Ru(bpy)(CN)_4$ (PPN = bis(triphenylphosphine)iminium) can be used as a humidity sensor, as it reversibly turns from purple to yellow on exposure to water vapor.[6] Solvent-tunable dye sensitized solar cells have been produced using a carboxylate-modified bpy to append the molecule to TiO_2.[7]

The exposed lone pair on the cyanide nitrogen in $[Ru(diimine)(CN)_4]^{2-}$ complexes has also been exploited to form supramolecular assemblies through hydrogen bonding[8–13] or coordination to other metal centers.[14–21] These assemblies often have interesting luminescence or energy-transfer properties, and one such assembly has been exploited as a sensor and chemodosimeter for amines released during food spoilage.[15,16]

Borane Modification of Metal Cyanide Complexes

In 1963, Shriver observed that a number of cyanometallates could absorb an equivalent of borane per cyanide, resulting in a ca. 100 cm^{-1} shift in the C-N stretch to higher frequencies.[22] For the homoleptic cyanometallates, he found that the d-d transitions were unaffected by the coordination of borane, but the spectrum of $Fe(phen)_2(CN)_2$, which is dominated by MLCT transitions, blueshifted dramatically. This pair of observations indicates that formation of the borane adduct stabilizes metal-centered orbitals, but has no strong effect on the ligand-based orbitals. As a

result, one expects that d-d transitions should remain relatively constant, MLCT transitions should blueshift, and ligand-to-metal charge transfer (LMCT) transitions should redshift on boronation; electrochemically, the same orbital shifts should produce anodic shifts in metal-centered redox processes while minimally affecting ligand-centered redox processes.

While this area of research had been fairly dormant since Shriver's work, it became of interest to the Gray group as a way of tuning the potential of cyanometallates in order to produce high-voltage redox flow battery electrolytes. As expected, McNicholas et al. found that addition of boranes to ferricyanide anodically shift the $Fe^{II/III}$ couple.[23] By examining cyclic voltammagrams containing substoichiometric BPh_3, which coordinates reversibly to the cyanides, they determined that there is a linear relationship between the number of boranes coordinated and the magnitude of the shift. Each equivalent of BPh_3 shifts the ferricyanide couple by ca. 260 mV, and for BCF, which coordinates irreversibly, a more dramatic 350 mV shift was observed. These observations were in line with previous publications which showed similar shifts in $Os^{II/III}$ [24] and $Re^{I/II}$ couples[25] on addition of the same boranes to cyanide ligands.

As of this writing, the study of boronation of homoleptic cyanometallates is very active within the Gray group, and manuscripts are now in preparation describing synthesis and spectroscopy of Co, Mn, Cr, Fe, Ru, Os, Ni, and Pt isocyanoborate complexes.[26–28]

Previous Work on Boronation of $[Ru(bpy)(CN)_4]^{2-}$ and related complexes

In an effort to develop symmetric redox flow battery electrolytes, the boronation of Fe(II) and Ru(II) cyanometallates containing bpy and phen has also been studied recently in the Gray group.[26,29] $[Ru(bpy)(CN)_4]^{2-}$, $[Fe(bpy)(CN)_4]^{2-}$, and $[Fe(phen)(CN)_4]^{2-}$ were each boronated with both BPh_3 and BCF. In each case,

boronation produces a shift to higher frequency of the C-N stretches, a blueshift in the MLCT-dominated optical spectrum, and an anodic shift of the $M^{II/III}$ couple, with more dramatic shifts for BCF than BPh_3, reflecting its higher Lewis acidity. In the case of $[Ru(bpy)(CN)_4]^{2-}$, boronation also results in a luminescent excited state that is two orders of magnitude longer-lived, although the BPh_3 adduct undergoes photodecomposition with loss of the borane.

Although a redox flow battery has not yet been successfully created from it, this research resulted in the synthesis of $[Ru(bpy)(CN\text{-}BCF)_4]^{2-}$, which in MeCN has two reversible redox events separated by more than 3.5 V. This voltage would greatly improve upon the working voltages of existing flow battery systems. The following work represents an effort to improve the reductive stability of this molecule.

Results & Discussion

Synthesis and Spectroscopy of $[Ru(^{CF3}bpy)(CN)_4]^{2-}$

$K_2Ru(^{CF3}bpy)(CN)_4$ (^{CF3}bpy = 4,4'-bis(trifluoromethyl)-2,2'-bipyridine) was synthesized analogously to other $K_2Ru(diimine)(CN)_4$ complexes[30] and converted to the PPN salt by precipitation from aqueous solution. $PPN_2Ru(^{CF3}bpy)(CN)_4$ is received initially as a brick-red solid which is soluble in polar organic solvents and turns dark green when fully dehydrated. The complex was characterized by ^1H and ^{19}F NMR spectroscopy, solid-state IR spectroscopy, elemental analysis, and X-ray crystallography.

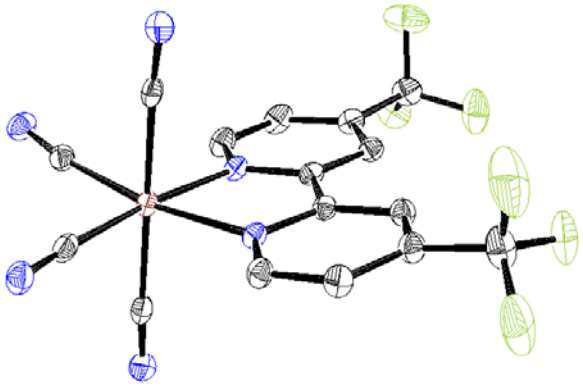

Figure 2: Molecular structure of $PPN_2Ru(^{CF3}bpy)(CN)_4$. Thermal ellipsoids set at 50% probability. Cations, hydrogen atoms, and solvent molecules omitted for clarity.

The X-ray crystallographic data (Figure 2) reveals a negligible difference in metal-ligand contacts between $[Ru(^{CF3}bpy)(CN)_4]^{2-}$ and the parent bpy complex,[6] which suggests that there is minimal difference in backbonding, despite the more electron-deficient bipyridine ligand. The C-N stretches detected in the solid state by FT-IR spectroscopy (Figure 3) support this interpretation. Typical complexes in this family have three closely-spaced strong peaks between 2030-2060 cm^{-1} and a weaker peak around 2090 cm^{-1}; the closely-spaced peaks were not resolved, but the observed peaks at 2062 and 2090 cm^{-1} are in line with related complexes.

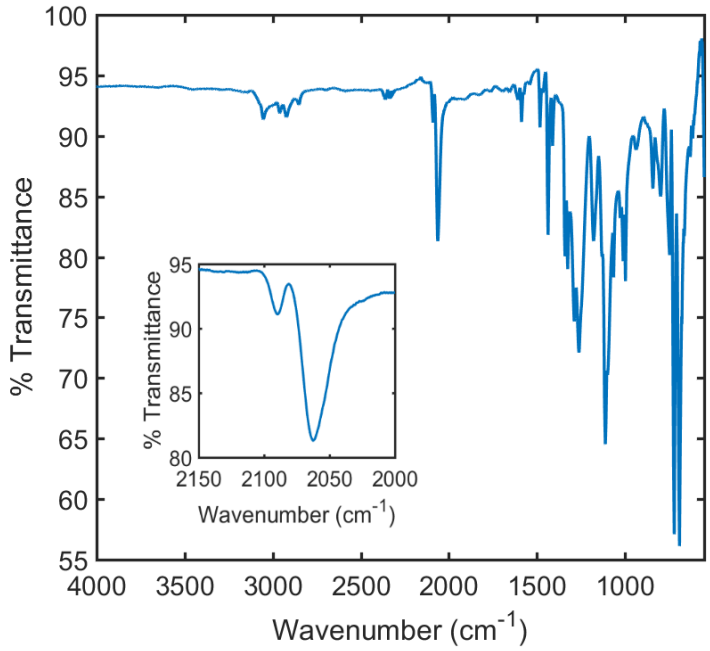

Figure 3: IR spectrum of $PPN_2Ru(^{CF3}bpy)(CN)_4$ with C-N stretches highlighted in inset.

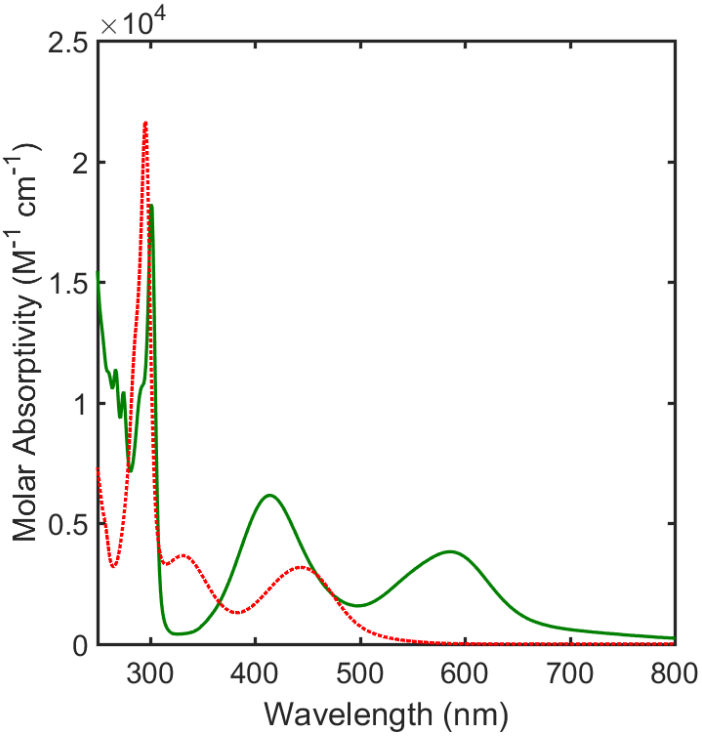

Figure 4: UV-Vis spectra of $[Ru(^{CF3}bpy)(CN)_4]^{2-}$ in water (red broken trace, K salt) and acetonitrile (green solid trace, PPN salt).

$[Ru(diimine)(CN)_4]^{2-}$ complexes are well-known for their solvatochromism, which results both from having a ground-state dipole which interacts with polar solvents and the ability to accept hydrogen bonds at the N-termini of the cyanide ligands.[5] Likewise, $[Ru(^{CF3}bpy)(CN)_4]^{2-}$ displays strong solvatochromism, with the lowest-energy MLCT transition redshifting ca. 5500 cm^{-1} when the solvent is changed from water to acetonitrile (Figure 4). In water, the spectrum displays three distinct bands, which can be assigned as two MLCT transitions and a ^{CF3}bpy-based π-π* transition based on their extinction coefficients (~10^3 $M^{-1}cm^{-1}$ for MLCT transitions and ~10^4 for π-π*). Both MLCT transitions are dramatically shifted by the change in solvent, but the π-π* transition shifts only slightly (ca. 550 cm^{-1}), indicating that cyanide lone pair interactions are able to shift the d(Ru) orbitals while minimally affecting the

^{CF3}bpy orbitals. The absorption bands are also redshifted relative to most other [Ru(diimine)$(CN)_4]^{2-}$ complexes (Table 1), reflecting the low-lying π orbitals of ^{CF3}bpy relative to bpy and other commonly-used diimines. In this respect, ^{CF3}bpy displays similar electronic properties to bpz, but without the exposed lone pairs which hydrogen bond with water.

Table 1: Comparison of room temperature photophysical data for [Ru(^{CF3}bpy)$(CN)_4]^{2-}$ and selected [Ru(diimine)$(CN)_4]^{2-}$ complexes. ^{R}bpy indicates R in the 4,4' positions of bipyridine.

Diimine ligand	Solvent	λ_{max} (nm)(ε (M^{-1} cm^{-1}))	λ_{em} (nm) (τ (ns))	Reference
bpy	H_2O	400	610(101)	1
	H_2O	404(4100)	624(100)	11
	MeCN	535	790(7)	8
^{Me}bpy	H_2O	392	600(115)	31
	MeCN	530	780(7)	31
bpym	D_2O	437(2200)	(3.4)	19
	MeCN	575	(0.25)	19
bpz	H_2O	465(5700)	704(5)	32
	MeCN	554		32
^{HOOC}bpy	MeCN	515	750	7
^{CF3}bpy	H_2O	443(3170)	706	This work
	MeCN	589(3770)	N.O. below 930	This work

While [Ru(diimine)$(CN)_4]^{2-}$ displays weak luminescence in aqueous solution (Figure S6), no luminescence was observed in the solid state or 2-MeTHF solution at room temperature or 77 K, suggesting that the emission in the dehydrated form may be redshifted beyond the 930 nm detection limit of the instruments used.

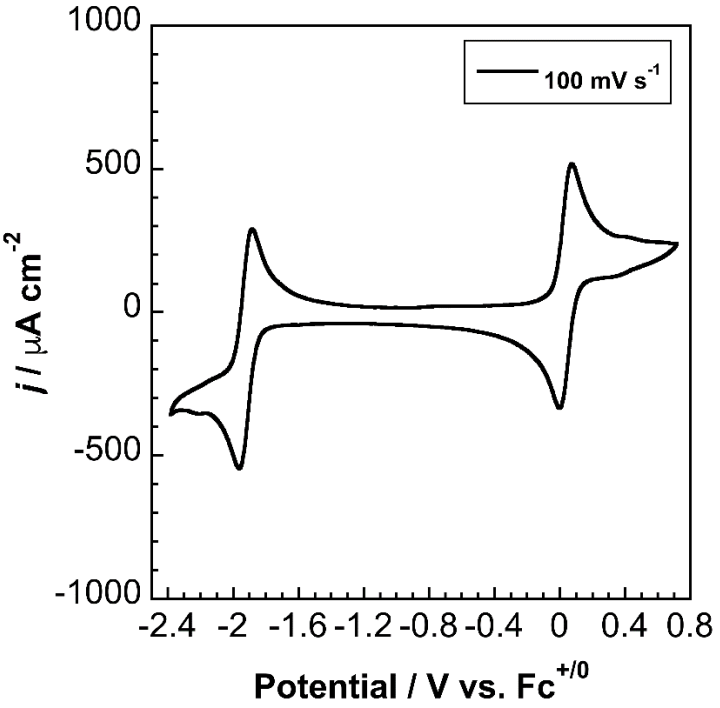

Figure 5: Cyclic voltammagram of 33 mM PPN_2 $Ru(^{CF3}bpy)(CN)_4$ in 0.2 M Bu_4NPF_6-supported acetonitrile. Working electrode: glassy carbon. Counter electrode: Pt wire.

The cyclic voltammagram of PPN_2 $Ru(^{CF3}bpy)(CN)_4$ in 0.2 M Bu_4NPF_6-supported acetonitrile displays two redox events at 0.05 and -1.92 V vs. $Fc^{+/0}$ corresponding to oxidation of the metal center to Ru(III) and reduction of the ^{CF3}bpy ligand, respectively (Figure 5). The peak current ratios for both waves are close to unity and the peak-to-peak separations are ca. 79 mV and independent of scan rate, indicating diffusion-controlled reversible electron transfer. While the parent bpy complex features a second irreversible reduction presumed to be deligation of bpy^{2-},[33] no such reduction or decomposition is observed for $[Ru(^{CF3}bpy)(CN)_4]^{2-}$. The reductive stability of ^{CF3}bpy in this system is accompanied by a 330 mV anodic shift in the $bpy^{0/-}$ couple relative to the parent complex and a 230 mV anodic shift in the $Ru^{2+/3+}$

couple. These shifts indicate that not only is ^{CF3}bpy more easily reduced than bpy, but that inductive effects result in a harder to oxidize Ru center.

Boronation with BCF and Spectroscopy

The tris(pentafluorophenyl)borane (BCF) adduct PPN_2 Ru(^{CF3}bpy)(CN-BCF)$_4$ was prepared in inert atmosphere by mixing DCM solutions of PPN_2 Ru(^{CF3}bpy)(CN)$_4$ and BCF and heating. On addition of the colorless BCF solution, the dark green PPN_2 Ru(^{CF3}bpy)(CN)$_4$ solution rapidly turns yellow. The resulting complex is an air-stable, luminescent yellow solid which is extremely soluble in polar organic solvents and has been characterized by ^{1}H, ^{19}F, and ^{11}B NMR spectroscopy, solid state IR spectroscopy, elemental analysis, and X-ray crystallography.

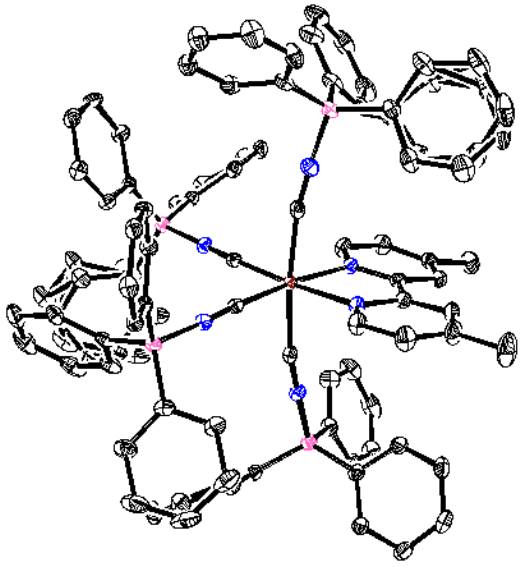

Figure 6: Molecular structure of PPN_2 Ru(^{CF3}bpy)(CN-BCF)$_4$. Thermal ellipsoids set at 50% probability. Cations, hydrogen and fluorine atoms, and solvent molecules omitted for clarity.

On addition of the borane, there is negligible change in the C-N distances and only a small shortening (ca. 0.05 Å) of the Ru-C distances (Figure 6). This observation is in line with the trends observed on addition of BCF to ferricyanide,[23] and likely results from a balancing of the bond-lengthening effect of N-donation to the borane and the bond-shortening effect of increased backbonding from Ru to the more π-acidic isocyanoborate. Crystallization of the related heteroleptic borane adducts has been stymied by their high solubility,[26,29] so more direct comparisons are not currently possible. Presumably due to steric crowding, the axial isocyanoborate ligands bow significantly (Ru-C-N bond angle 170°) over the plane of the bipyridine ligand, while those in the plane of the bipyridine remain close to linear. However, the crystal structure of PPN[Fe(phen)(CN-BPh_3)$_4$] does not display the same bowing effect (Ru-C-N = 176°), so there may be an electronic or crystal packing effect at play.

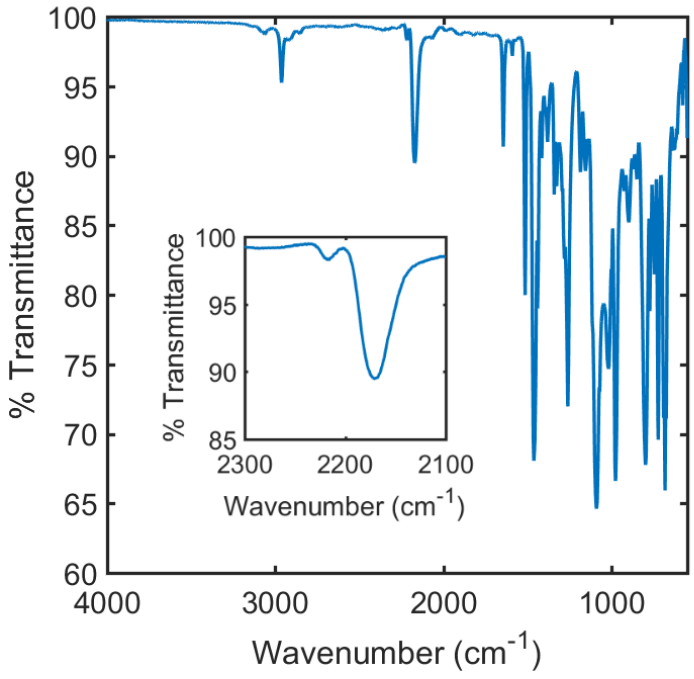

Figure 7: IR spectrum of $PPN_2Ru(^{CF3}bpy)(CN\text{-}BCF)_4$ with CN stretches highlighted in inset.

The C-N stretches in $[Ru(^{CF3}bpy)(CN\text{-}BCF)_4]^{2-}$ are shifted to much higher frequency (> 100 cm^{-1}, Figure 7). This observation, which indicates that the C-N bond is strengthened by coordination of the borane, is also in line with the shifts observed in ferricyanide[23] and other heteroleptic Ru complexes.[26,29]

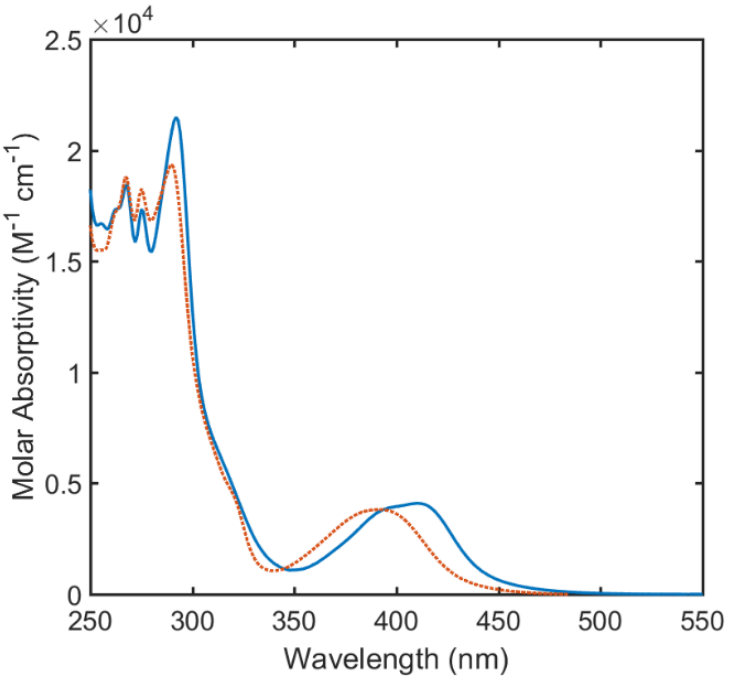

Figure 8: UV-Vis spectra for $PPN_2Ru(^{CF3}bpy)(CN\text{-}BCF)_4$ in DCM (blue solid trace) and MeCN (orange broken trace).

Addition of the boranes to $[Ru(^{CF3}bpy)(CN)_4]^{2-}$ induces a large blueshift in the optical absorption maximum, as the stronger Lewis acidity of BCF relative to water induces the cyanide ligands to become much better π acceptors. This strong ligand field lowers the energy of the Ru-d(π) orbitals, while minimally affecting the ^{CF3}bpy π orbitals, resulting in a blueshift in MeCN of the lowest-energy MLCT by nearly 8500 cm^{-1}. The boronated complex displays solvatochromism (Figure 8), with a slightly redshifted and split MLCT in DCM, indicating there is still a dipole in the ground state. $[Ru(^{CF3}bpy)(CN\text{-}BCF)_4]^{2-}$ is also brightly emissive at 545 nm, with a long

excited-state lifetime of 3.4 μs and high quantum yield of 14.4%, and is photostable for weeks in solution under room lights.

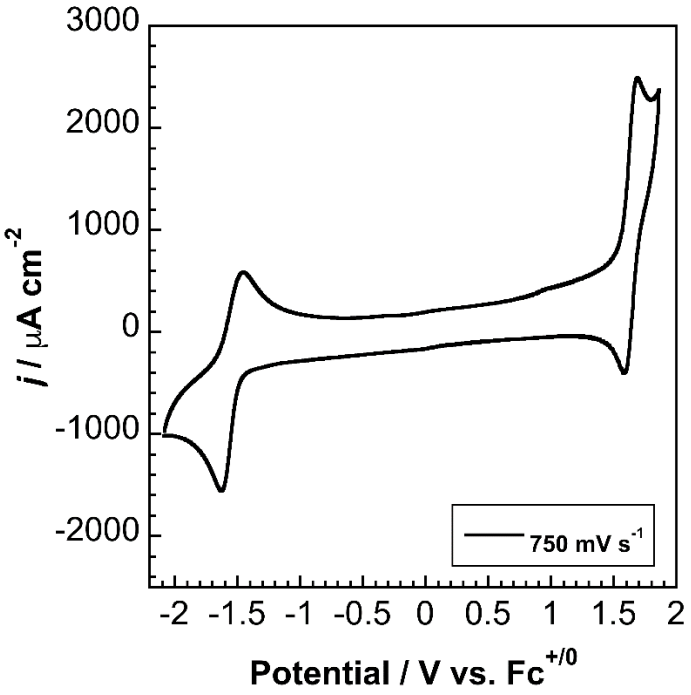

Figure 9: Cyclic voltammagram of 2.3 mM PPN_2 $Ru(^{CF3}bpy)(CN\text{-}BCF)_4$ in 0.2 M Bu_4NPF_6-supported acetonitrile. Working electrode: glassy carbon. Counter electrode: Pt wire.

Electrochemically, boronation with BCF induces a large anodic shift of 1.58 V in the potential of the $Ru^{2+/3+}$ couple along with a 390 mV anodic shift of the $^{CF3}bpy^{0/.-}$ couple (Figure 9), comparable to the shifts observed for the parent bpy complex.[26,29] While the peak current ratio for the $^{CF3}bpy^{0/.-}$ remains near-unity, the peak-to-peak separation increases with increasing scan rate, indicating that the electron transfer is reversible but slow on the timescale of the scan rates used. The heterogeneous charge-transfer rate constant (k_0) determined by Nicholson analysis (see Figure S5) of the appropriate variable scan rate data is 0.009 cm s^{-1}. The peak current ratios for the

$Ru^{2+/3+}$ couple deviate significantly from unity (average for all scan rates measured = 0.79) and decreases as the scan rate decreases, indicating a loss of reversibility attributable to an EC mechanism. Because the $Ru^{2+/3+}$ couple occurs very near the edge of the stability window for Bu_4NPF_6-supported MeCN, it is impossible to determine whether this electrochemical irreversibility is inherent to $PPN_2Ru(^{CF3}bpy)(CN\text{-}BCF)_4$ or a result of solvent or supporting electrolyte decomposition.

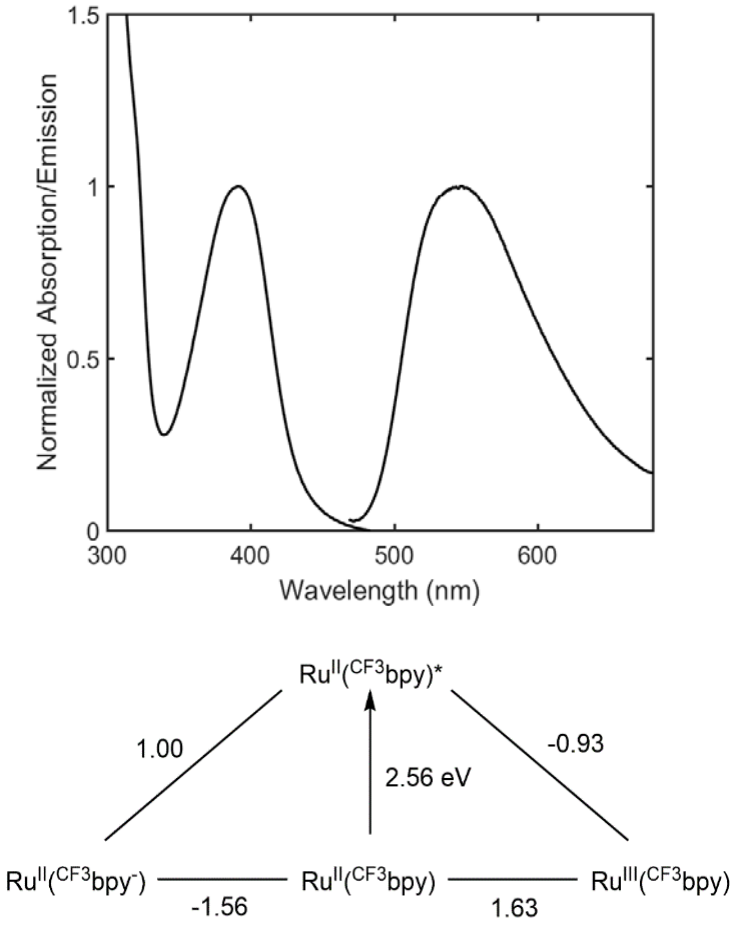

Figure 10: Top: room temperature absorption and emission data for $[Ru(^{CF3}bpy)(CN\text{-}BCF)_4]^{2-}$ in acetonitrile. Bottom: Modified Latimer diagram with potentials given in V vs. $Fc^{+/0}$.

Combining the electrochemical and photophysical data, a modified Latimer diagram can be constructed (Figure 10) to estimate the excited-state redox potentials for $[Ru(^{CF3}bpy)(CN\text{-}BCF)_4]^{2-}$. $[Ru(^{CF3}bpy)(CN\text{-}BCF)_4]^{2-}$ is expected to be a strong excited-state oxidant and modest excited state reductant, with an excited state oxidation potential comparable to $[Ru(bpz)_3]^{2+}$.[34]

Conclusion

A new member of the $[Ru(diimine)(CN)_4]^{2-}$ has been synthesized using the ^{CF3}bpy ligand, and it displays spectroscopic properties expected for an electron-withdrawing diimine. Notably, the library of $[Ru(diimine)(CN)_4]^{2-}$ complexes with electron-withdrawing diimine ligands is currently limited to bis(diazines) and ^{HOOC}bpy. $[Ru(^{CF3}bpy)(CN)_4]^{2-}$ represents an addition to this library that is nonreactive to protons, which may be desirable for certain applications.

The borane adduct $[Ru(^{CF3}bpy)(CN\text{-}BCF)_4]^{2-}$ has also been synthesized, and it represents an important step toward high voltage symmetric redox flow battery electrolytes with a voltage difference of 3.2 V. While the $Ru^{2+/3+}$ couple occurs too close to the edge of the solvent stability window to be useful as a flow battery electrolyte, the enhanced stability of the $^{CF3}bpy^{0/-}$ couple indicates that a different isocyanoborato complex of ^{CF3}bpy such as $Ru(^{CF3}bpy)_2(CN\text{-}BCF)_2$ might be able to achieve the right balance of properties.

$[Ru(^{CF3}bpy)(CN\text{-}BCF)_4]^{2-}$ also has luminescence properties that suggest it may be a useful photoredox catalyst. With 1 V of oxidizing power vs. $Fc^{+/0}$, it may be a competent catalyst for photooxidations that currently utilize $[Ru(bpz)_3]^{2+}$ or $[Ir[dF(CF_3)ppy]_2(dtbbpy)]^{+}$ as catalysts.

References

(1) Bignozzi, C. A.; Chiorboli, C.; Indelli, M. T.; Rampi Scandola, M. A.; Varani, G.; Scandola, F. Simple Poly(Pyridine)Ruthenium(II) Photosensitizer: (2,2'-Bipyridine)Tetracyanoruthenate(II). *J. Am. Chem. Soc.* **1986**, *108* (24), 7872–7873. https://doi.org/10.1021/ja00284a084.

(2) Timpson, C. J.; Bignozzi, C. A.; Sullivan, B. P.; Kober, E. M.; Meyer, T. J. Influence of Solvent on the Spectroscopic Properties of Cyano Complexes of Ruthenium(II). *J. Phys. Chem.* **1996**, *100* (8), 2915–2925. https://doi.org/10.1021/jp953179m.

(3) Shen, C.; Yu, F.; Chu, W.-K.; Xiang, J.; Tan, P.; Luo, Y.; Feng, H.; Guo, Z.-Q.; Leung, C.-F.; Lau, T.-C. Synthesis, Structures and Photophysical Properties of Luminescent Cyanoruthenate(II) Complexes with Hydroxylated Bipyridine and Phenanthroline Ligands. *RSC Adv.* **2016**, *6* (90), 87389–87399. https://doi.org/10.1039/C6RA16319J.

(4) Herrera, J.-M.; Pope, S. J. A.; Meijer, A. J. H. M.; Easun, T. L.; Adams, H.; Alsindi, W. Z.; Sun, X.-Z.; George, M. W.; Faulkner, S.; Ward, M. D. Photophysical and Structural Properties of Cyanoruthenate Complexes of Hexaazatriphenylene. *J. Am. Chem. Soc.* **2007**, *129* (37), 11491–11504. https://doi.org/10.1021/ja072672w.

(5) Ward, M. D. [Ru(Bipy)(CN)4]2− and Its Derivatives: Photophysical Properties and Its Use in Photoactive Supramolecular Assemblies. *Coord. Chem. Rev.* **2006**, *250* (23), 3128–3141. https://doi.org/10.1016/j.ccr.2006.02.012.

(6) Evju, J. K.; Mann, K. R. Synthesis and Spectroscopic Investigations of a Crystalline Humidity Sensor: Bis(Triphenylphosphine)Iminium 2,2'-Bipyridyltetracyanoruthenate. *Chem. Mater.* **1999**, *11* (6), 1425–1433. https://doi.org/10.1021/cm980323i.

(7) Argazzi, R.; Bignozzi, C. A.; Yang, M.; Hasselmann, G. M.; Meyer, G. J. Solvatochromic Dye Sensitized Nanocrystalline Solar Cells. *Nano Lett.* **2002**, *2* (6), 625–628. https://doi.org/10.1021/nl0255395.

(8) Rampi, M. A.; Indelli, M. T.; Scandola, F.; Pina, F.; Parola, A. J. Photophysics of Supercomplexes. Adduct between Ru(Bpy)(CN)42- and the [32]Ane-N8H88+ Polyaza Macrocycle. *Inorg. Chem.* **1996**, *35* (11), 3355–3361. https://doi.org/10.1021/ic951590i.

(9) Borsarelli, C. D.; Braslavsky, S. E.; Indelli, M. T.; Scandola, F. Photophysics of Supercomplexes. A Laser-Induced Optoacoustic Study of the Adducts between Ru(Bpy)(CN)42− and Polyaza Macrocycles. *Chem. Phys. Lett.* **2000**, *317* (1), 53–58. https://doi.org/10.1016/S0009-2614(99)01360-3.

(10) Pina, F.; Parola, A. J. Photochemistry of Supramolecular Species Involving Anionic Coordination Compounds and Polyammonium Macrocyclic Receptors. *Coord. Chem. Rev.* **1999**, *185–186*, 149–165. https://doi.org/10.1016/S0010-8545(98)00265-3.

(11) Simpson, N. R. M.; Ward, M. D.; Morales, A. F.; Barigelletti, F. Solvatochromism as a Mechanism for Controlling Intercomponent Photoinduced Processes in a Bichromophoric Complex Containing [Ru(Bpy)3]2+ and [Ru(Bpy)(CN)4]2− Units. *J. Chem. Soc. Dalton Trans.* **2002**, No. 12, 2449–2454. https://doi.org/10.1039/B201597H.

(12) Loiseau, F.; Marzanni, G.; Quici, S.; Indelli, M. T.; Campagna, S. An Artificial Antenna Complex Containing Four Ru(Bpy)32+-Type Chromophores as Light-Harvesting Components and a Ru(Bpy)(CN)42− Subunit as the Energy Trap. A Structural Motif Which Resembles the Natural Photosynthetic Systems. *Chem. Commun.* **2003**, No. 2, 286–287. https://doi.org/10.1039/B211122E.

(13) Bergamini, G.; Saudan, C.; Ceroni, P.; Maestri, M.; Balzani, V.; Gorka, M.; Lee, S.-K.; van Heyst, J.; Vögtle, F. Proton-Driven Self-Assembled Systems Based on Cyclam-Cored Dendrimers and [Ru(Bpy)(CN)4]2-. *J. Am. Chem. Soc.* **2004**, *126* (50), 16466–16471. https://doi.org/10.1021/ja0450814.

(14) Derossi, S.; Baca, S. G.; Miller, T. A.; Adams, H.; Jeffery, J. C.; Ward, M. D. Formation and Structural Chemistry of the Unusual Cyanide-Bridged Dinuclear Species [Ru2(NN)2(CN)7]3− (NN=2,2'-Bipyridine or 1,10-Phenanthroline). *Inorganica Chim. Acta* **2009**, *362* (4), 1282–1288. https://doi.org/10.1016/j.ica.2008.06.017.

(15) Chow, C.-F.; Lam, M. H. W.; Wong, W.-Y. Design and Synthesis of Heterobimetallic Ru(II)–Ln(III) Complexes as Chemodosimetric Ensembles for the Detection of Biogenic Amine Odorants. *Anal. Chem.* **2013**, *85* (17), 8246–8253. https://doi.org/10.1021/ac401513j.

(16) Chow, C.-F.; Kong, H.-K.; Leung, S.-W.; Chiu, B. K. W.; Koo, C.-K.; Lei, E. N. Y.; Lam, M. H. W.; Wong, W.-T.; Wong, W.-Y. Heterobimetallic Ru(II)−Eu(III) Complex as Chemodosimeter for Selective Biogenic Amine Odorants Detection in Fish Sample. *Anal. Chem.* **2011**, *83* (1), 289–296. https://doi.org/10.1021/ac102393f.

(17) Lazarides, T.; Easun, T. L.; Veyne-Marti, C.; Alsindi, W. Z.; George, M. W.; Deppermann, N.; Hunter, C. A.; Adams, H.; Ward, M. D. Structural and Photophysical Properties of Adducts of [Ru(Bipy)(CN)4]2- with Different Metal Cations: Metallochromism and Its Use in Switching Photoinduced Energy Transfer. *J. Am. Chem. Soc.* **2007**, *129* (13), 4014–4027. https://doi.org/10.1021/ja068436n.

(18) Baca, S. G.; Adams, H.; Sykes, D.; Faulkner, S.; Ward, M. D. Three-Component Coordination Networks Based on [Ru(Phen)(CN)4]2− Anions, near-Infrared Luminescent Lanthanide(III) Cations, and Ancillary Oligopyridine Ligands: Structures and Photophysical Properties. *Dalton Trans.* **2007**, No. 23, 2419–2430. https://doi.org/10.1039/B702235B.

(19) Adams, H.; Alsindi, W. Z.; Davies, G. M.; Duriska, M. B.; Easun, T. L.; Fenton, H. E.; Herrera, J.-M.; George, M. W.; Ronayne, K. L.; Sun, X.-Z.; et al. New Members of the [Ru(Diimine)(CN)4]2− Family: Structural, Electrochemical and Photophysical Properties. *Dalton Trans.* **2006**, *0* (1), 39–50. https://doi.org/10.1039/B509042C.

(20) Davies, G. M.; Pope, S. J. A.; Adams, H.; Faulkner, S.; Ward, M. D. Structural and Photophysical Properties of Coordination Networks Combining [Ru(Bipy)(CN)4]2- Anions and Lanthanide(III) Cations: Rates of Photoinduced Ru-to-Lanthanide Energy Transfer and Sensitized Near-Infrared Luminescence. *Inorg. Chem.* **2005**, *44* (13), 4656–4665. https://doi.org/10.1021/ic050512k.

(21) Hidalgo-Luangdilok, Carmela.; Bocarsly, A. B.; Woods, R. E. Electrochemically-Modulated Photoluminescence at the Chemically Derivatized Electrode: [CdRu(CN)4 (Bipyridine)]0/+ Modified Electrodes. *J. Phys. Chem.* **1990**, *94* (5), 1918–1924. https://doi.org/10.1021/j100368a037.

(22) Shriver, D. F. Preparation and Structures of Metal Cyanide-Lewis Acid Bridge Compounds. *J. Am. Chem. Soc.* **1963**, *85* (10), 1405–1408. https://doi.org/10.1021/ja00893a011.

(23) J. McNicholas, B.; H. Grubbs, R.; R. Winkler, J.; B. Gray, H.; Despagnet-Ayoub, E. Tuning the Formal Potential of Ferrocyanide over a 2.1 V Range. *Chem. Sci.* **2019**, *10* (12), 3623–3626. https://doi.org/10.1039/C8SC04972F.

(24) Chu, W.-K.; Yiu, S.-M.; Ko, C.-C. Neutral Luminescent Bis(Bipyridyl) Osmium(II) Complexes with Improved Phosphorescent Properties. *Organometallics* **2014**, *33* (23), 6771–6777. https://doi.org/10.1021/om500630c.

(25) Chu, W.-K.; Ko, C.-C.; Chan, K.-C.; Yiu, S.-M.; Wong, F.-L.; Lee, C.-S.; Roy, V. A. L. A Simple Design for Strongly Emissive Sky-Blue Phosphorescent Neutral Rhenium Complexes: Synthesis, Photophysics, and Electroluminescent Devices. *Chem. Mater.* **2014**, *26* (8), 2544–2550. https://doi.org/10.1021/cm4038654.

(26) Ngo, D. X.; Grubbs, R. H.; Gray, H. B.; McNicholas, B. J. Electronic Structures and Photophysics of [M(Diimine)(CN-BR3)4]2- (M = Fe, Ru) Complexes. **Manuscript in Preparation**.

(27) McNicholas, B.; Winkler, J. R.; Gray, H. B. Electronic Structure of Boronated, Group VIII Hexacyanometalates and Their Utility in Non-Aqueous Redox Flow Batteries and Cold Climate Energy Storage. **Manuscript in preparation**.

(28) Nie, C.; McNicholas, B. J.; Gray, H. B.; Grubbs, R. H. **Manuscript In Preparation**.

(29) Ngo, D. X. High Voltage Fe(II) and Ru(II) Symmetric Redox Flow Battery Electrolytes. Senior Thesis, California Institute of Technology, Pasadena, CA, 2019.

(30) Jiwan, J. L. H.; Wegewijs, B.; Indelli, M. T.; Scandola, F.; Braslavsky, S. E. Volume Changes Associated with Intramolecular Electron Transfer during MLCT State Formation. Time-Resolved Optoacoustic Studies of Ruthenium Cyano Complexes. *Recl. Trav. Chim. Pays-Bas-J. R. Neth. Chem. Soc.* **1995**, *114* (11–12), 542-.

(31) Indelli, M. T.; Ghirotti, M.; Prodi, A.; Chiorboli, C.; Scandola, F.; McClenaghan, N. D.; Puntoriero, F.; Campagna, S. Solvent Switching of Intramolecular Energy Transfer in Bichromophoric Systems: Photophysics of (2,2'-Bipyridine)Tetracyanoruthenate(II)/Pyrenyl Complexes. *Inorg. Chem.* **2003**, *42* (18), 5489–5497. https://doi.org/10.1021/ic034185x.

(32) Garcia Posse, M. E.; Katz, N. E.; Baraldo, L. M.; Polonuer, D. D.; Colombano, C. G.; Olabe, J. A. Comparative Bonding and Photophysical Properties of 2,2'-Bipyridine and 2,2'-Bipyrazine in Tetracyano Complexes Containing Ruthenium and Osmium. *Inorg. Chem.* **1995**, *34* (7), 1830–1835. https://doi.org/10.1021/ic00111a034.

(33) Roffia, S.; Ciano, M. Electrochemical Behaviour of Dicyanobis(2,2'-Bipyridine) Ruthenium(II) and Dicyanobis(1,10-Phenanthroline) Ruthenium(II) Complexes. *J. Electroanal. Chem. Interfacial Electrochem.* **1977**, *77* (3), 349–359. https://doi.org/10.1016/S0022-0728(77)80280-5.

(34) Prier, C. K.; Rankic, D. A.; MacMillan, D. W. C. Visible Light Photoredox Catalysis with Transition Metal Complexes: Applications in Organic Synthesis. *Chem. Rev.* **2013**, *113* (7), 5322–5363. https://doi.org/10.1021/cr300503r.

(35) Krause, R. A.; Violette, C. An Improved Synthesis of Potassium Hexacyanoruthenate(II). *Inorganica Chim. Acta* **1986**, *113* (2), 161–162. https://doi.org/10.1016/S0020-1693(00)82239-2.

(36) Bard, A. J.; Faulkner, L. R. *Electrochemical Methods: Fundamentals and Applications*, 2nd ed.; John Wiley & Sons: Hoboken, NJ, 2001.

(37) Nicholson, R. S. Theory and Application of Cyclic Voltammetry for Measurement of Electrode Reaction Kinetics. *Anal. Chem.* **1965**, *37* (11), 1351–1355. https://doi.org/10.1021/ac60230a016.

(38) Lavagnini, I.; Antiochia, R.; Magno, F. An Extended Method for the Practical Evaluation of the Standard Rate Constant from Cyclic Voltammetric Data. *Electroanalysis* **2004**, *16* (6), 505–506. https://doi.org/10.1002/elan.200302851.

(39) Sattler, W.; Ener, M. E.; Blakemore, J. D.; Rachford, A. A.; LaBeaume, P. J.; Thackeray, J. W.; Cameron, J. F.; Winkler, J. R.; Gray, H. B. Generation of Powerful Tungsten Reductants by Visible Light Excitation. *J. Am. Chem. Soc.* **2013**, *135* (29), 10614–10617. https://doi.org/10.1021/ja4047119.

(40) Suzuki, K.; Kobayashi, A.; Kaneko, S.; Takehira, K.; Yoshihara, T.; Ishida, H.; Shiina, Y.; Oishi, S.; Tobita, S. Reevaluation of Absolute Luminescence Quantum Yields of Standard Solutions Using a Spectrometer with an Integrating Sphere and a Back-Thinned CCD Detector. *Phys. Chem. Chem. Phys.* **2009**, *11* (42), 9850–9860. https://doi.org/10.1039/B912178A.

(41) Crosby, G. A.; Demas, J. N. Measurement of Photoluminescence Quantum Yields. Review. *J. Phys. Chem.* **1971**, *75* (8), 991–1024. https://doi.org/10.1021/j100678a001.

Methods

General Considerations

Potassium hexacyanoruthenate(II) was synthesized by a known procedure[35]. 4,4'-trifluoromethyl-2,2'-bipyridine (^{CF3}bpy, Strem), bis(triphenylphosphine)iminium chloride (PPNCl, Millipore Sigma), and tris(pentafluorophenyl)borane (BCF, TCI) were used as received. NMR spectra were collected on a Varian 400 MHz spectrometer (δ in ppm, m: multiplet, s: singlet, d: doublet, t: triplet). UV-visible spectra were collected on a Cary 50 Bio or Cary 500 spectrometer. Solid-state infrared spectra were collected on a Thermo Scientific Nicolet iS5 FT-IR spectrometer with an iD5 ATR diamond.

Synthesis & Characterization

$PPN_2Ru(^{CF3}bpy)(CN)_4$

$K_2Ru(^{CF3}bpy)(CN)_4$ was synthesized with a modified version of the procedure published by Jiwan.[30] To a boiling solution of $K_4Ru(CN)_6$ (400 mg, .908 mmol) and ^{CF3}bpy (305 mg, 1.04 mmol) in 50 mL 1:1 methanol:water was added 400 μL 3.6 N H_2SO_4 (pH 4). The solution was refluxed for 24 h, over which time it slowly turned red, then cooled to room temperature and neutralized. Excess ^{CF3}bpy was removed by filtration and the solvent was removed. The remaining residue was purified by gel-filtration chromatography on a Sephadex G-15 column. Elution with water gave a main orange band free of excess $K_4Ru(CN)_6$. The main fraction was dried under vacuum to give $K_2Ru(^{CF3}bpy)(CN)_4$, yield 30%. The cation was exchanged by precipitation from concentrated aqueous solution with a saturated solution of PPNCl (307 mg, .535 mmol in 20 mL water). The resulting brick-red precipitate was collected by filtration and dried in a desiccator or under vacuum until it turned green, yield 326 mg (25%). Single crystals suitable for X-ray diffraction analysis were grown by slow evaporation from DCM solution. ^{1}H NMR (400 MHz, CD_2Cl_2): δ

10.02 (d, J = 8 Hz, 2H, 6,6'-H), 8.12 (s, 2H, 3,3'-H), 7.69-7.65 (m, 24H, PPN), 7.52-7.44 (m, 36H, PPN), 7.40 (d, J = 8 Hz, 2H, 5,5'-H). ^{19}F NMR (CD_2Cl_2): δ -64.71. IR (cm^{-1}, CN stretches) 2062, 2090. Anal. Calcd for $C_{88}H_{66}F_6N_8P_4Ru$: C, 67.13; H, 4.23; N, 7.12. Found: C, 64.21; H, 4.28; N, 5.55.

$PPN_2Ru(^{CF3}bpy)(CN\text{-}BCF)_4$

In a nitrogen-filled glovebox, $PPN_2Ru(^{CF3}bpy)(CN)_4$ (100 mg, 0.0637 mmol) and excess BCF (133 mg, 0.261 mmol) were each dissolved in minimal DCM. The two solutions were combined, causing a rapid color change from green to red to yellow. The solution was stirred for 1 h, then dried under vacuum. The resulting luminescent yellow solid was washed 3 x 10 mL hexanes, then dried thoroughly under vacuum. The resulting air-stable material was then further purified by flash chromatography on silica gel (eluent gradient from 100% hexanes to 90% dichloromethane in hexanes), affording 131 mg yellow product (0.0362 mmol, 56% yield). Single crystals suitable for X-ray diffraction analysis were grown from a saturated ethanol solution at –25°C. ^{1}H NMR (400 MHz, CD_2Cl_2): δ 9.22 (d, J = 4 Hz, 2H, 6,6'-H), 8.29 (s, 2H, 3,3'-H), 7.65-7.59 (m, 14H, PPN + 5,5'-H), 7.51-7.40 (m, 48H, PPN). ^{19}F NMR (CD_2Cl_2): δ -65.48 (s, 6F, CF_3), -134.54 (dd, 12F, *o*-F), -135.00 (dd, 12F, *o*-F), -161.57 (t, 6F, *p*-F), -162.03 (t, 6F, *p*-F), -167.01 (td, 12F, *m*-F), -167.29 (td, 12F, *m*-F). ^{11}B NMR (CD_2Cl_2): δ -14.09. IR (cm^{-1}, CN stretches) 2171, 2216. Anal. Calcd for $C_{160}H_{66}F_{66}N_8P_4Ru$: C, 53.05; H, 1.84; N, 3.09. Found: C, 51.69; H, 2.09; N, 2.76.

Electrochemical Measurements

Cyclic voltammagrams were taken in a nitrogen-filled glovebox with a Gamry Reference 600 potentiostat in a standard 3-electrode cell containing a 3 mm diameter glassy carbon working electrode, a 0.01 M $Ag^{+/0}$ in 0.1 M $TBAPF_6$/MeCN quasireference electrode, and a platinum wire counter electrode and compensated for 85% of the measured uncompensated resistance (R_u) value.

Diffusion coefficients were calculated from linear fits of plots of the peak current versus the square root of the scan rate using the Randles-Sevcik equation (Equation S1),[36] where i_p (A) is the peak current, n is the number of electrons transferred (1), F (C mol^{-1}) is the Faraday constant, C (mol cm^{-1}) is the bulk concentration of analyte, ν (V s^{-1}) is the scan rate, D_O (cm^2 s^{-1}) is the diffusion coefficient of the oxidized analyte, R (J mol^{-1} K^{-1}) is the ideal gas constant, and T (K) is the temperature.

$$i_p = 0.446nFAC\left(\frac{nF\nu D_O}{RT}\right)^{1/2} \quad \text{(S1)}$$

The heterogeneous electron transfer rate constant (k_0) for the $^{CF3}bpy^{0/\cdot-}$ couple of $PPN_2Ru(^{CF3}bpy)(CN\text{-}BCF)_4$ was determined using Nicholson's kinetic parameter Ψ[37] along with Lavagnini's numerical interpretation of Ψ[38] (Equations S2 and S3).

$$\Psi = k_0\left(\frac{\pi Dn\nu F}{RT}\right)^{-1/2} \quad \text{(S2)}$$

$$\Psi = \frac{-.06288 + .0021\chi}{1 - 0.017\chi} \quad \text{(S3)}$$

χ (mV) is the peak-to-peak separation. For sufficiently fast scan rates with respect to the electron transfer (i.e. in the region where χ is observed to vary with scan rate, where Ψ becomes small), plots of Ψ vs. $\nu^{-1/2}$ become linear, and k_0 may be calculated from the slope. For the other electrochemical couples observed, χ did not vary with the scan rates used, and would have required very high (> 3 V/s) scan rates for this analysis.

Photophysical Measurements

Steady-state and time-resolved spectroscopic measurements were carried out in the Beckman Institute Laser Resource Center (California Institute of Technology) using methods described previously.[39]

Quantum yields (φ_{PL}) were measured by comparison of deaerated, optically dilute solutions of the molecule of interest to $[Ru(bpy)_3](PF_6)_2$ in aerated and deaerated MeCN (φ_{PL} = 0.018 for aerated solutions and 0.095 for aerated solutions[40]) according to Equation S4.[41]

$$\varphi = \varphi_{ref} \frac{A_{ref}}{A} \frac{I}{I_{ref}} \frac{\eta^2}{{\eta_{ref}}^2} \quad \text{(S4)}$$

Subscript "ref" refers to the reference solutions, A are the absorbances at the exciting wavelength (450 nm for all measurements), I are the integrated emission intensities, and η are the refractive indices of the solvents used. Absorption measurements were taken before and after emission spectra to ensure there was no photodecomposition. Emission spectra were taken twice with different integration times to ensure there were no significant differences.

The resulting luminescence decay traces were fitted as an exponential decay to determine the excited state lifetimes (τ).

Supporting Data

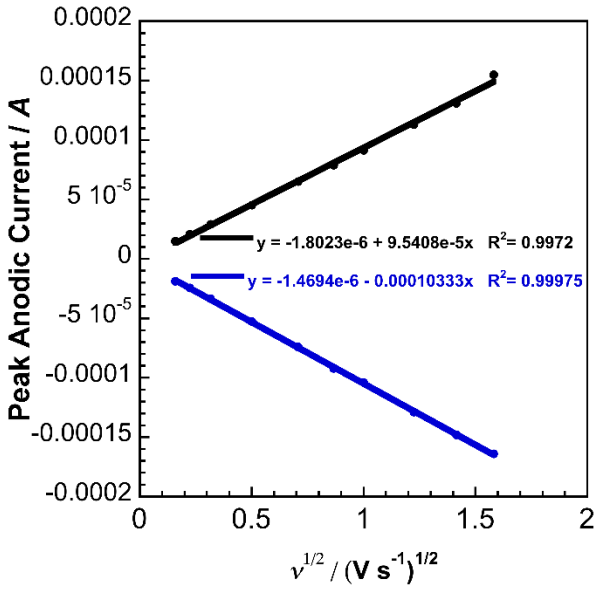

Figure S1: Randles-Sevcik plot for $PPN_2Ru(^{CF3}bpy)(CN)_4$; D = 5.7 x 10^{-6} cm^2 s^{-1}.

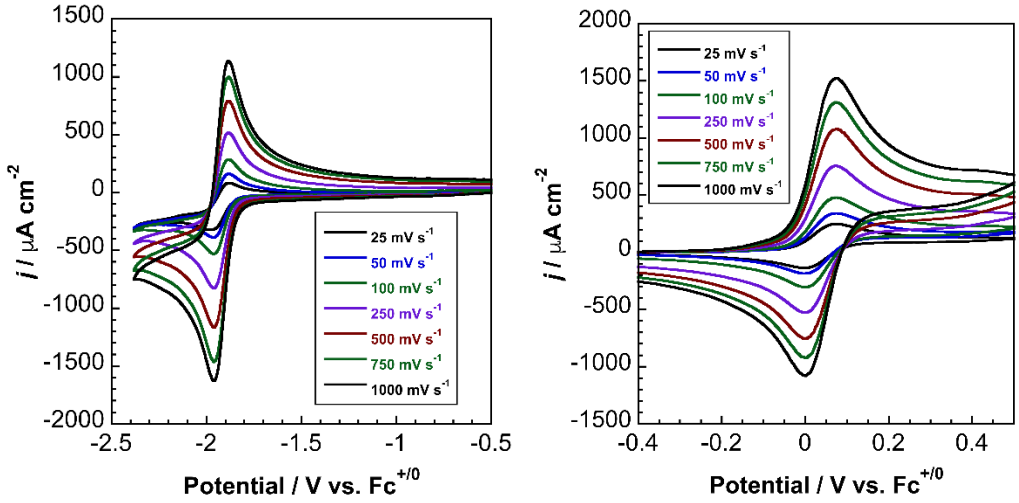

Figure S2: Variable scan rate cyclic voltammagrams for $PPN_2Ru(^{CF3}bpy)(CN)_4$. 33 mM PPN_2 $Ru(^{CF3}bpy)(CN)_4$ in 0.2 M Bu_4NPF_6-supported acetonitrile. Working electrode: glassy carbon. Counter electrode: Pt wire.

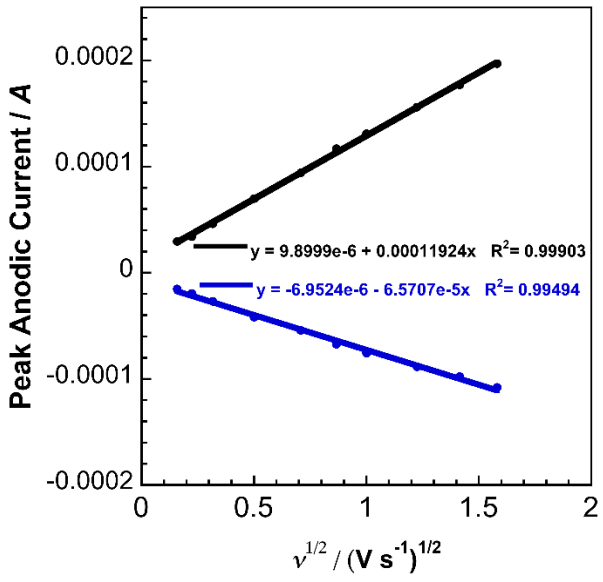

Figure S3: Randles-Sevcik plot for $PPN_2Ru(^{CF3}bpy)(CN\text{-}BCF)_4$; D = 7.4 x 10^{-6} cm^2 s^{-1} (top), 2.4 x 10^{-6} cm^2 s^{-1} (bottom).

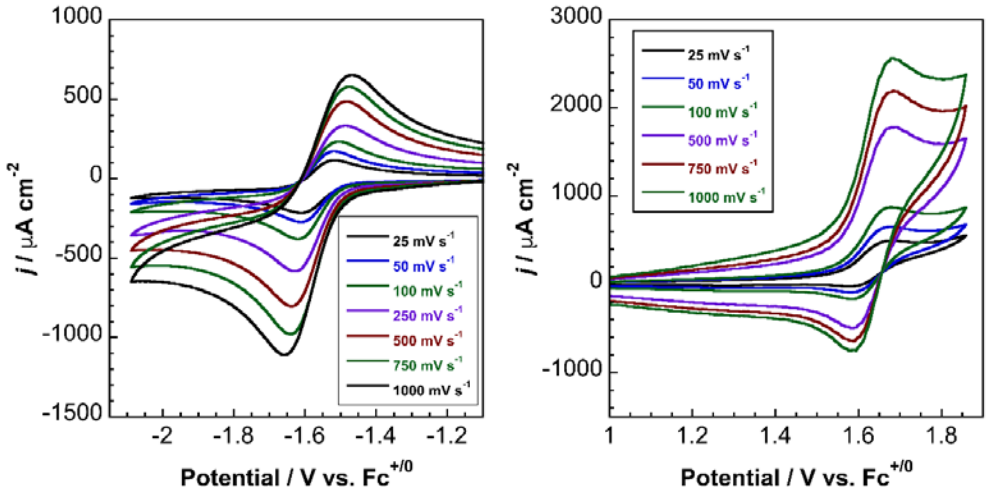

Figure S4: Variable scan rate cyclic voltammetry of $PPN_2Ru(^{CF3}bpy)(CN\text{-}BCF)_4$. . 2.3 mM $PPN_2Ru(^{CF3}bpy)(CN\text{-}BCF)_4$ in 0.2 M Bu_4NPF_6-supported acetonitrile. Working electrode: glassy carbon. Counter electrode: Pt wire.

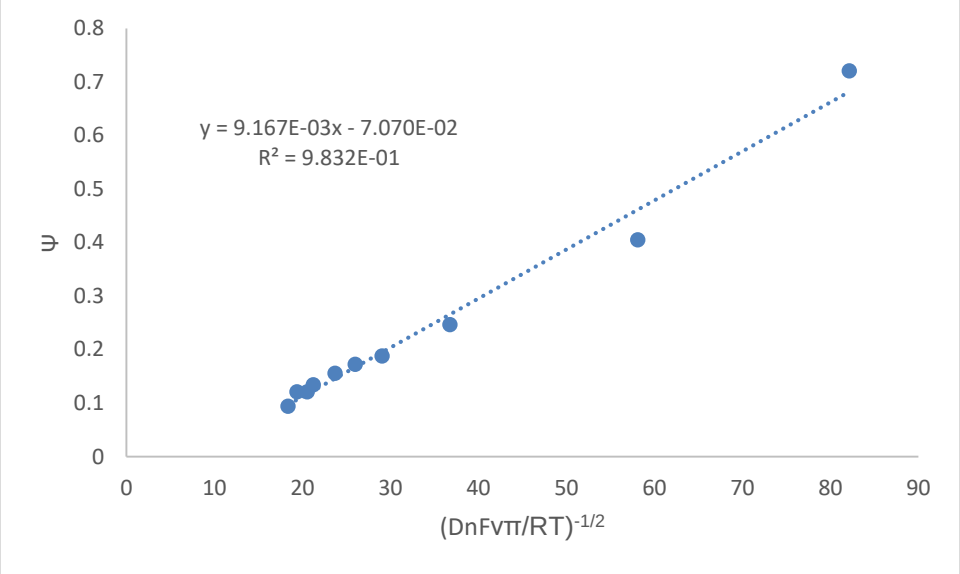

Figure S5: Nicholson analysis of the $^{CF3}bpy^{0/\cdot-}$ couple of $PPN_2Ru(^{CF3}bpy)(CN\text{-}BCF)_4$, with a slope of k_0.

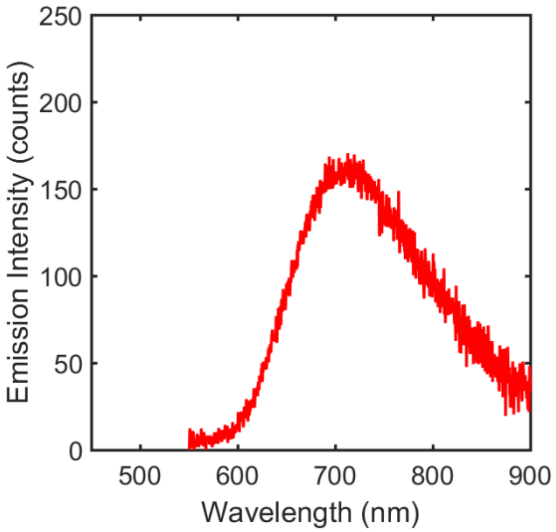

Figure S6: Steady-state emission spectrum of aqueous $K_2Ru(^{CF3}bpy)(CN)_4$ excited at 400 nm.

Table S1: Measurement of quantum yield for $PPN_2Ru(^{CF3}bpy)(CN\text{-}BCF)_4$.

Sample	A_{450}	I	φ_{ref}	φ_{sample} *wrt*
Aerated $[Ru(bpy)_3]^{2+}$ *1*	0.0747	8.30×10^5	0.018	0.132
Deaerated $[Ru(bpy)_3]^{2+}$ *1*	0.1043	5.08×10^6	0.095	0.159
Sample 1	0.0467	3.79×10^6	-	-
Aerated $[Ru(bpy)_3]^{2+}$ *2*	0.0743	1.10×10^6	0.018	0.131
Deaerated $[Ru(bpy)_3]^{2+}$ *2*	0.0961	6.43×10^6	0.095	0.153
Sample 2	0.0464	5.00×10^6	-	-
				0.144 average

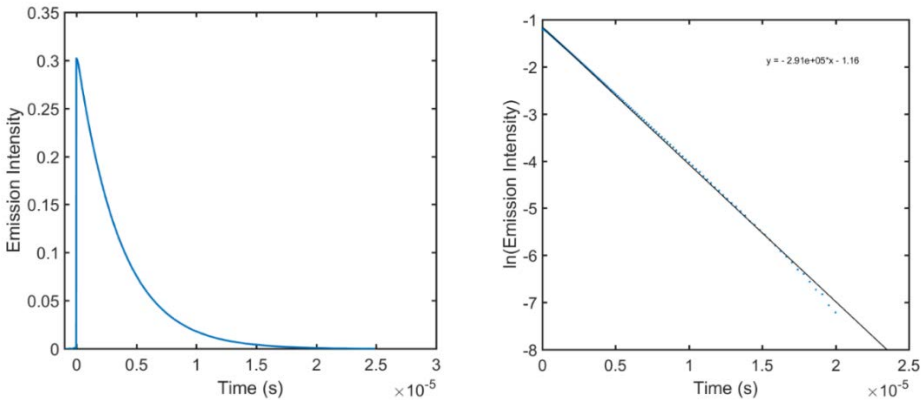

Figure S7: Left, time-resolved luminescence data for $PPN_2Ru(^{CF3}bpy)(CN\text{-}BCF)_4$. Right, linear fit to determine lifetime. The slope of the fit is the inverse of $\tau = 3.44$ μs.

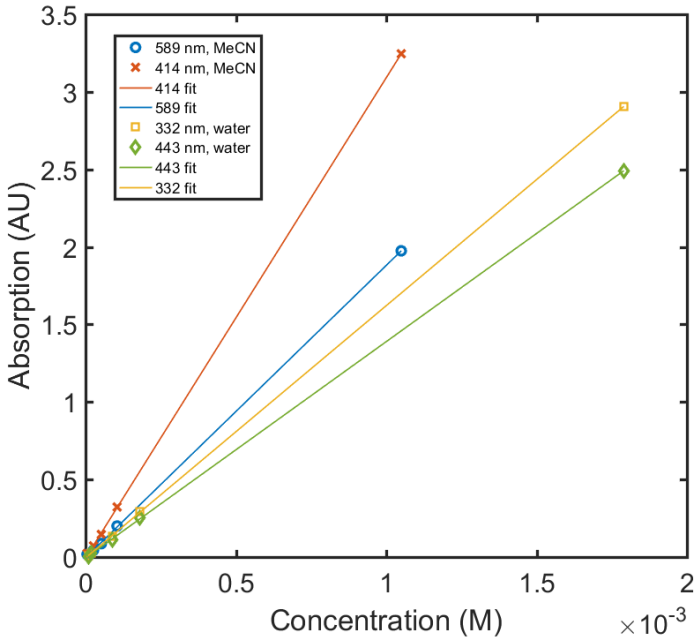

Figure S8: Dilution series for molar absorptivity of $[Ru(^{CF3}bpy)(CN)_4]^{2-}$ (K salt in water, PPN salt in MeCN) and linear fits. All measurements in 5 mm cuvette. Extinction coefficients are ε_{332} = 3660 $M^{-1}cm^{-1}$, ε_{443} = 3170 $M^{-1}cm^{-1}$ in water and ε_{414} = 6190 $M^{-1}cm^{-1}$, ε_{589} = 3770 $M^{-1}cm^{-1}$ in MeCN.

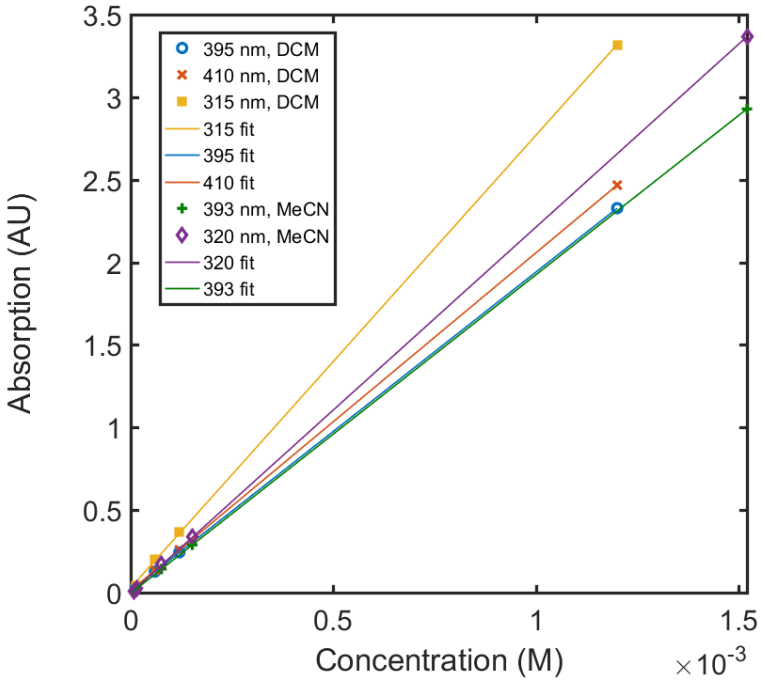

Figure S9: Dilution series for molar absorptivity of $PPN_2Ru(^{CF3}bpy)(CN\text{-}BCF)_4$ and linear fits. All measurements in 5 mm cuvette. Extinction coefficients are ε_{315} = 1460 $M^{-1}cm^{-1}$, ε_{395} = 958 $M^{-1}cm^{-1}$, ε_{410} = 1020 $M^{-1}cm^{-1}$ in DCM and ε_{320} = 3860 $M^{-1}cm^{-1}$, ε_{393} = 4440 $M^{-1}cm^{-1}$ in MeCN.

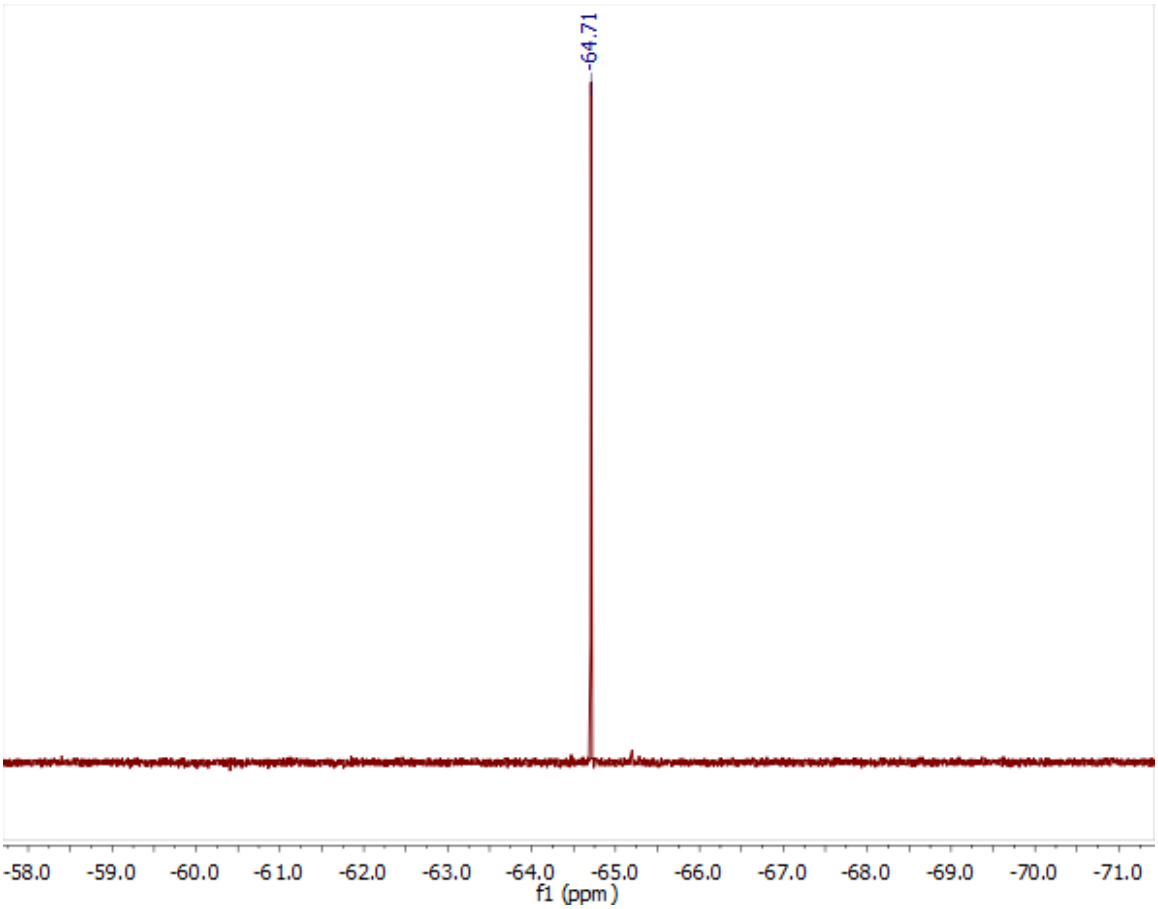

Figure S10: ^{19}F NMR spectrum of $PPN_2Ru(^{CF3}bpy)(CN)_4$ in CD_2Cl_2.

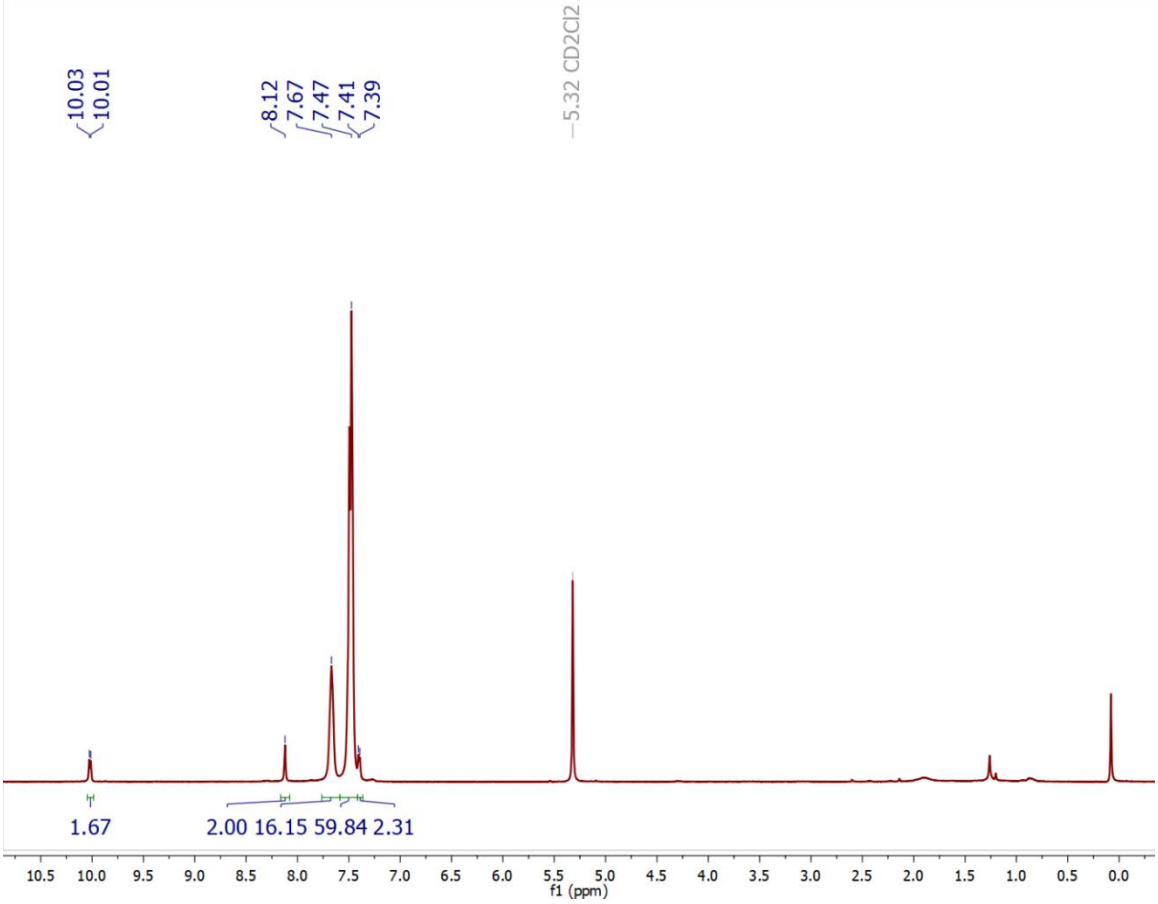

Figure S11: ^{1}H NMR spectrum of $PPN_2Ru(^{CF3}bpy)(CN)_4$ in CD_2Cl_2. Peaks upfield of 3 ppm are attributable to water, trace solvents, and silicone grease.

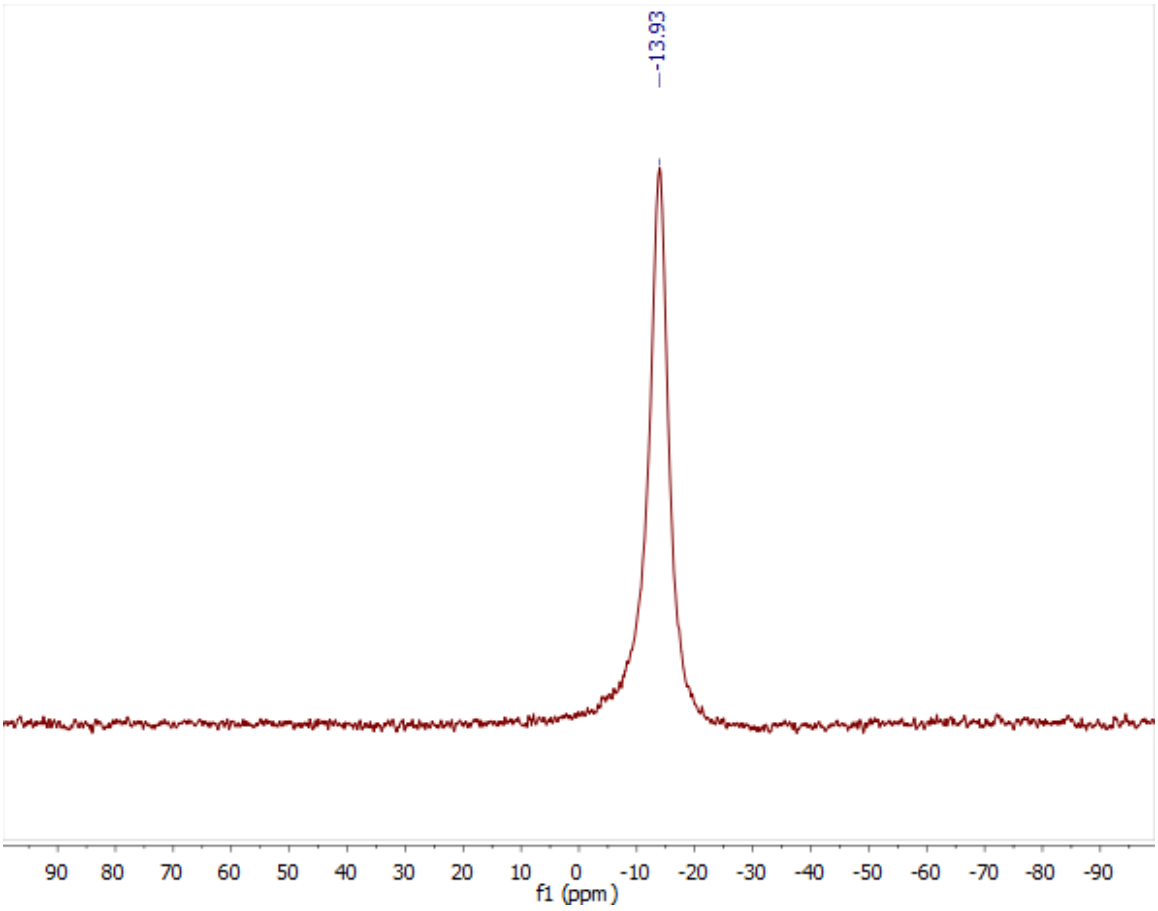

Figure S12: ^{11}B NMR spectrum of $PPN_2Ru(^{CF3}bpy)(CN\text{-}BCF)_4$ in CD_2Cl_2 acquired in a quartz NMR tube.

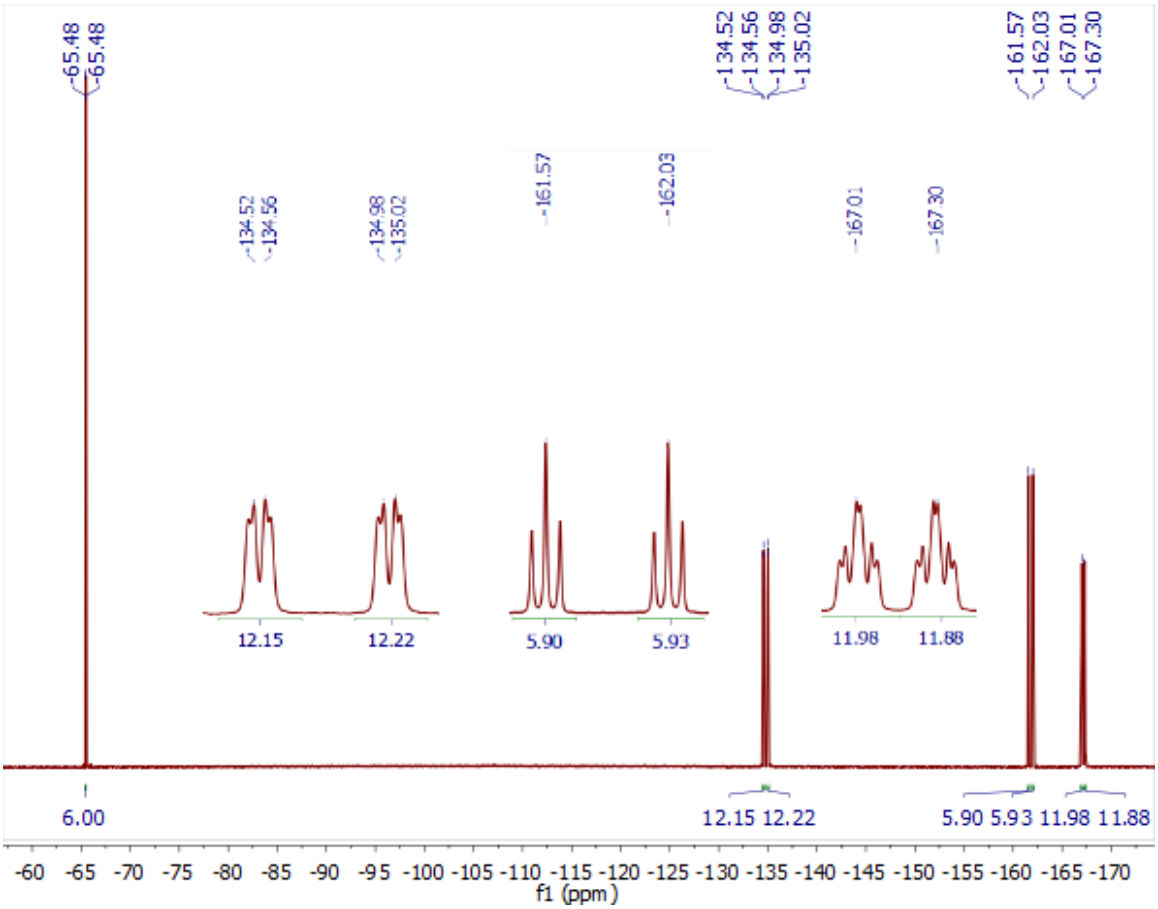

Figure S13: ^{19}F NMR spectrum of $PPN_2Ru(^{CF3}bpy)(CN\text{-}BCF)_4$ in CD_2Cl_2 with insets showing detail of BCF peaks.

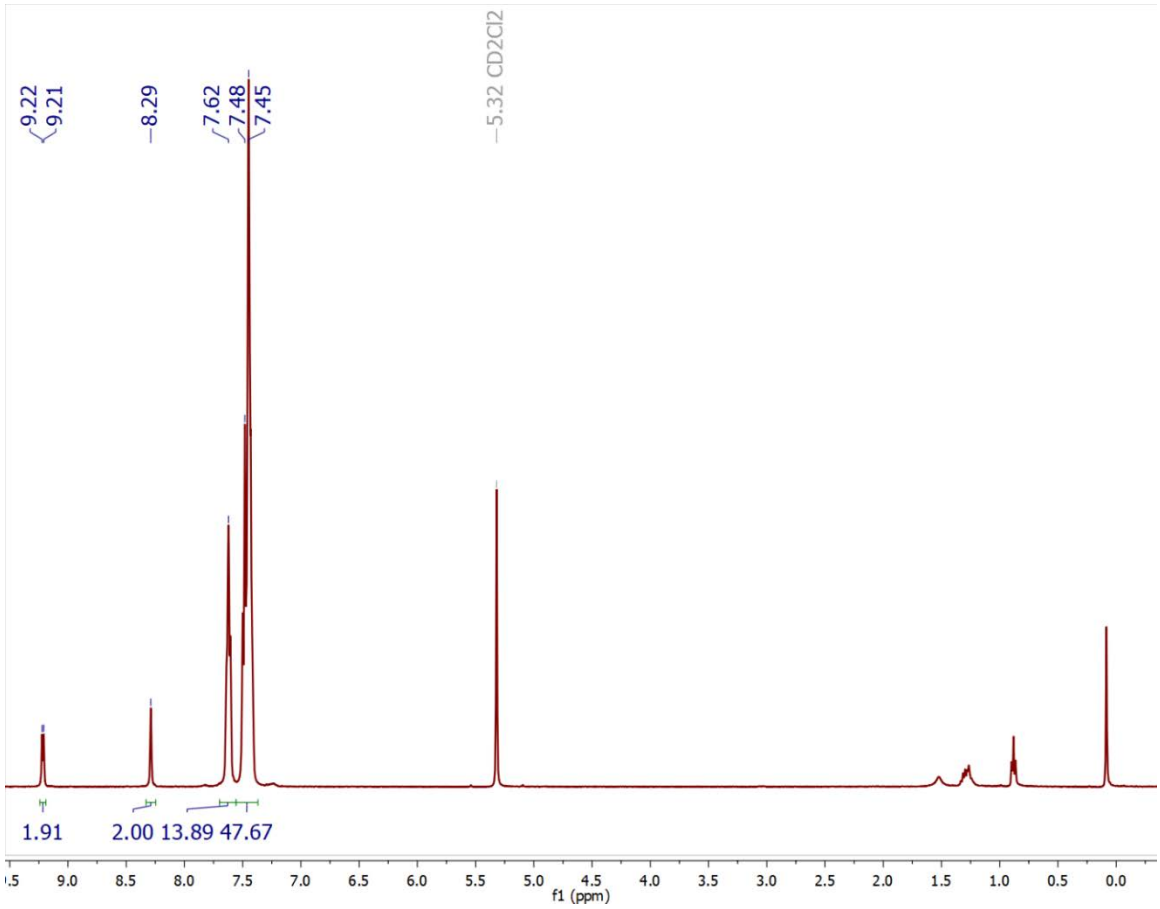

Figure S14: ^{1}H NMR spectrum of $PPN_2Ru(^{CF3}bpy)(CN\text{-}BCF)_4$ in CD_2Cl_2. Peaks upfield of 2 ppm are attributable to water, pentane, and silicone grease.

APPENDIX

Crystal Data

$PPN_2Ru(^{CF3}bpy)(CN)_4$

Table 1. Crystal data and structure refinement for v19188.

Identification code	v19188	
Empirical formula	C90.22 H70.45 Cl4.45 F6 N8 P4 Ru	
Formula weight	1763.39	
Temperature	100.01 K	
Wavelength	1.54178 Å	
Crystal system	Triclinic	
Space group	P-1	
Unit cell dimensions	a = 14.4682(16) Å	α= 104.716(5)°
	b = 14.6308(17) Å	β= 101.091(4)°
	c = 21.319(2) Å	γ = 105.092(6)°
Volume	4049.6(8) $Å^3$	
Z	2	
Density (calculated)	1.446 g/cm^3	
Absorption coefficient	4.214 mm^{-1}	
F(000)	1803	
Crystal size	0.26 x 0.23 x 0.07 mm^3	
Theta range for data collection	3.292 to 79.375°.	
Index ranges	$-18 \le h \le 18$, $-18 \le k \le 18$, $-27 \le l \le 25$	
Reflections collected	196069	

Independent reflections	16794 [R(int) = 0.0435]
Completeness to theta = 67.679°	99.6 %
Absorption correction	Semi-empirical from equivalents
Max. and min. transmission	1.0000 and 0.6998
Refinement method	Full-matrix least-squares on F^2
Data / restraints / parameters	16794 / 3 / 1075
Goodness-of-fit on F^2	1.081
Final R indices [I>2sigma(I)]	R1 = 0.0339, wR2 = 0.0783
R indices (all data)	R1 = 0.0373, wR2 = 0.0817
Extinction coefficient	n/a
Largest diff. peak and hole	0.743 and -0.937 e.$Å^{-3}$

Table 2. Atomic coordinates (x 10^5), equivalent isotropic displacement parameters ($Å^2$x 10^4), and population for v19188. U(eq) is defined as one third of the trace of the orthogonalized U^{ij} tensor.

	x	y	z	U(eq)	pop
Ru(1)	45462(2)	32209(2)	32147(2)	164(1)	1
F(1)	91407(11)	61245(17)	52808(9)	662(6)	1
F(2)	86565(14)	73757(13)	53059(9)	714(6)	1
F(3)	83829(9)	66006(11)	60068(6)	394(3)	1
F(4)	47136(12)	19524(12)	61075(8)	445(4)	1
F(5)	50334(11)	35255(11)	65956(6)	426(4)	1
F(6)	35186(10)	25435(10)	61844(7)	336(3)	1
N(1)	57172(11)	44418(11)	39063(8)	168(3)	1
N(2)	44080(11)	30596(11)	41383(8)	178(3)	1
N(3)	28847(12)	11226(13)	24313(9)	259(4)	1
N(4)	50189(13)	38045(12)	19468(8)	242(4)	1
N(5)	61750(12)	20869(13)	32206(8)	236(3)	1
N(6)	29843(13)	44400(13)	32600(9)	244(4)	1
C(1)	63788(14)	51207(14)	37447(9)	199(4)	1
C(2)	72338(14)	58029(14)	42083(10)	213(4)	1
C(3)	74264(14)	57990(14)	48720(10)	213(4)	1
C(4)	67457(14)	51358(14)	50573(9)	189(4)	1
C(5)	58956(13)	44635(13)	45605(9)	166(3)	1
C(6)	51363(13)	37123(13)	46959(9)	174(4)	1

C(7)	51563(14)	36511(14)	53405(9)	185(4)	1
C(8)	44035(15)	29050(14)	54083(10)	214(4)	1
C(9)	36391(16)	22605(15)	48432(11)	260(4)	1
C(10)	36642(15)	23631(15)	42220(10)	239(4)	1
C(11)	83926(16)	64723(17)	53739(11)	309(5)	1
C(12)	44228(16)	27452(16)	60747(11)	269(4)	1
C(13)	34720(14)	19137(14)	26794(9)	202(4)	1
C(14)	48137(14)	35513(14)	23903(10)	208(4)	1
C(15)	55656(14)	24668(13)	31992(9)	184(4)	1
C(16)	35352(14)	39885(14)	32245(9)	197(4)	1
P(1)	67865(3)	90701(3)	20102(2)	169(1)	1
P(2)	77912(3)	101220(3)	11525(2)	175(1)	1
N(7)	75261(12)	94480(13)	16056(8)	228(3)	1
C(17)	55407(14)	91013(15)	17491(9)	201(4)	1
C(18)	53712(15)	100132(15)	19613(10)	237(4)	1
C(19)	44377(16)	100897(18)	17289(12)	303(5)	1
C(20)	36646(17)	92440(20)	13041(12)	361(5)	1
C(21)	38197(17)	83308(19)	11108(12)	359(5)	1
C(22)	47588(16)	82526(16)	13196(10)	276(4)	1
C(23)	66956(14)	77873(14)	19183(10)	208(4)	1
C(24)	60693(15)	72262(15)	22065(10)	233(4)	1
C(25)	60154(17)	62415(15)	21326(11)	284(4)	1
C(26)	65817(19)	58103(17)	17746(13)	353(5)	1
C(27)	71980(20)	63572(18)	14792(14)	394(6)	1

C(28)	72561(17)	73473(16)	15512(12)	296(5)	1
C(29)	72746(14)	97990(14)	28941(9)	192(4)	1
C(30)	82215(15)	105111(15)	31265(11)	251(4)	1
C(31)	86106(17)	110626(16)	38089(11)	315(5)	1
C(32)	80624(18)	109060(16)	42574(11)	321(5)	1
C(33)	71165(17)	102017(16)	40276(10)	292(5)	1
C(34)	67182(15)	96472(15)	33479(10)	235(4)	1
C(35)	70075(14)	108762(14)	10521(10)	199(4)	1
C(36)	70200(15)	116017(15)	16302(10)	247(4)	1
C(37)	63708(16)	121439(15)	15971(11)	269(4)	1
C(38)	57064(15)	119760(16)	9814(12)	279(4)	1
C(39)	57018(15)	112781(16)	4037(11)	277(4)	1
C(40)	63519(14)	107199(15)	4344(10)	232(4)	1
C(41)	76969(14)	93400(14)	3260(9)	207(4)	1
C(42)	69772(15)	83920(15)	646(10)	247(4)	1
C(43)	68344(16)	77949(16)	-5916(11)	285(4)	1
C(44)	74020(20)	81416(18)	-9842(11)	363(5)	1
C(45)	81160(20)	90760(20)	-7270(13)	489(7)	1
C(46)	82759(19)	96768(17)	-694(12)	366(5)	1
C(47)	90511(14)	109529(14)	15232(9)	198(4)	1
C(48)	93517(16)	118815(16)	14293(11)	281(4)	1
C(49)	103328(17)	125099(17)	17265(13)	337(5)	1
C(50)	110072(16)	122226(18)	21161(12)	347(5)	1
C(51)	107113(16)	112940(20)	22057(12)	353(5)	1

C(52)	97386(15)	106593(17)	19113(11)	278(4)	1
P(3)	5024(4)	62485(4)	31836(3)	228(1)	1
P(4)	7117(4)	59281(4)	17572(3)	221(1)	1
N(8)	8696(13)	62742(13)	25386(9)	277(4)	1
C(53)	15586(14)	66411(14)	39049(10)	213(4)	1
C(54)	14760(16)	63649(15)	44762(11)	248(4)	1
C(55)	22676(17)	67842(15)	50596(11)	269(4)	1
C(56)	31393(16)	74778(15)	50705(11)	270(4)	1
C(57)	32294(16)	77394(16)	45001(11)	273(4)	1
C(58)	24430(15)	73253(15)	39145(10)	234(4)	1
C(59)	-1517(15)	71356(16)	33663(13)	299(5)	1
C(60)	-3310(20)	74200(20)	39906(17)	495(7)	1
C(61)	-8110(30)	81230(30)	41331(19)	620(10)	1
C(62)	-11110(20)	85410(20)	36526(17)	483(7)	1
C(63)	-9290(20)	82734(19)	30348(14)	443(6)	1
C(64)	-4566(19)	75661(18)	28864(13)	388(6)	1
C(65)	-2896(15)	50589(15)	31583(11)	247(4)	1
C(66)	1051(15)	42825(15)	31416(10)	249(4)	1
C(67)	-4823(15)	33724(15)	31590(10)	256(4)	1
C(68)	-14518(16)	32423(15)	31985(10)	262(4)	1
C(69)	-18540(16)	40023(16)	31940(12)	309(5)	1
C(70)	-12780(16)	49134(17)	31732(12)	311(5)	1
C(71)	17784(15)	56443(15)	15653(11)	260(4)	1
C(72)	20038(17)	57017(18)	9657(12)	324(5)	1

C(73)	27827(19)	54020(20)	7984(14)	411(6)	1
C(74)	33374(19)	50430(20)	12255(15)	433(6)	1
C(75)	31230(18)	49950(20)	18234(14)	395(6)	1
C(76)	23418(16)	52916(17)	19975(12)	321(5)	1
C(77)	5281(15)	68979(15)	14077(10)	231(4)	1
C(78)	12210(16)	78624(16)	17059(11)	269(4)	1
C(79)	10753(17)	86447(16)	14833(11)	291(4)	1
C(80)	2425(17)	84625(16)	9620(12)	304(5)	1
C(81)	-4425(17)	75050(17)	6580(11)	301(5)	1
C(82)	-3030(15)	67216(16)	8805(11)	257(4)	1
C(83)	-3668(15)	48408(15)	12968(10)	237(4)	1
C(84)	-3522(16)	40972(15)	7443(11)	268(4)	1
C(85)	-12164(17)	32928(16)	3838(11)	307(5)	1
C(86)	-20858(17)	32331(16)	5780(12)	311(5)	1
C(87)	-21012(16)	39672(16)	11287(12)	310(5)	1
C(88)	-12468(15)	47742(15)	14870(11)	276(4)	1
Cl(1)	38869(4)	87792(4)	28961(3)	302(2)	0.93(1)
Cl(2)	45630(5)	102685(5)	42351(3)	402(2)	0.93(1)
C(89)	43369(18)	100770(18)	33600(12)	300(5)	0.93(1)
Cl(3)	50678(16)	56800(15)	735(13)	805(6)	0.5
Cl(4)	53814(14)	38163(16)	1177(14)	874(6)	0.5
C(90)	47140(90)	45930(110)	2630(70)	2800(180)	0.5
Cl(5)	11699(9)	102985(9)	45590(6)	371(4)	0.46(1)
Cl(6)	17995(13)	98342(14)	33269(8)	340(4)	0.46(1)

C(91)	16830(50)	95430(40)	40720(30)	299(11)	0.46(1)
Cl(7)	9270(14)	107714(14)	37162(10)	431(6)	0.33(1)
Cl(8)	20340(16)	94144(16)	38323(15)	508(7)	0.33(1)
C(92)	13900(80)	98950(70)	32840(50)	300(20)	0.33(1)

Table 3. Bond lengths [Å] and angles [°] for v19188.

Ru(1)-N(1)	2.0881(15)
Ru(1)-N(2)	2.0822(16)
Ru(1)-C(13)	2.0091(19)
Ru(1)-C(14)	2.017(2)
Ru(1)-C(15)	2.060(2)
Ru(1)-C(16)	2.063(2)
F(1)-C(11)	1.337(3)
F(2)-C(11)	1.330(3)
F(3)-C(11)	1.318(3)
F(4)-C(12)	1.346(3)
F(5)-C(12)	1.330(3)
F(6)-C(12)	1.343(2)
N(1)-C(1)	1.352(2)
N(1)-C(5)	1.359(2)
N(2)-C(6)	1.361(2)
N(2)-C(10)	1.350(2)
N(3)-C(13)	1.160(3)
N(4)-C(14)	1.161(3)
N(5)-C(15)	1.158(3)
N(6)-C(16)	1.162(3)
C(1)-C(2)	1.374(3)
C(2)-C(3)	1.390(3)

C(3)-C(4)	1.384(3)
C(3)-C(11)	1.497(3)
C(4)-C(5)	1.393(3)
C(5)-C(6)	1.467(2)
C(6)-C(7)	1.395(3)
C(7)-C(8)	1.386(3)
C(8)-C(9)	1.390(3)
C(8)-C(12)	1.494(3)
C(9)-C(10)	1.376(3)
P(1)-N(7)	1.5761(16)
P(1)-C(17)	1.797(2)
P(1)-C(23)	1.804(2)
P(1)-C(29)	1.8062(19)
P(2)-N(7)	1.5753(17)
P(2)-C(35)	1.797(2)
P(2)-C(41)	1.798(2)
P(2)-C(47)	1.7969(19)
C(17)-C(18)	1.397(3)
C(17)-C(22)	1.397(3)
C(18)-C(19)	1.390(3)
C(19)-C(20)	1.387(3)
C(20)-C(21)	1.384(4)
C(21)-C(22)	1.390(3)
C(23)-C(24)	1.398(3)

C(23)-C(28)	1.395(3)
C(24)-C(25)	1.389(3)
C(25)-C(26)	1.385(3)
C(26)-C(27)	1.390(3)
C(27)-C(28)	1.396(3)
C(29)-C(30)	1.393(3)
C(29)-C(34)	1.396(3)
C(30)-C(31)	1.392(3)
C(31)-C(32)	1.380(4)
C(32)-C(33)	1.388(3)
C(33)-C(34)	1.389(3)
C(35)-C(36)	1.401(3)
C(35)-C(40)	1.393(3)
C(36)-C(37)	1.381(3)
C(37)-C(38)	1.391(3)
C(38)-C(39)	1.384(3)
C(39)-C(40)	1.400(3)
C(41)-C(42)	1.397(3)
C(41)-C(46)	1.387(3)
C(42)-C(43)	1.392(3)
C(43)-C(44)	1.377(3)
C(44)-C(45)	1.379(4)
C(45)-C(46)	1.391(3)
C(47)-C(48)	1.392(3)

C(47)-C(52)	1.395(3)
C(48)-C(49)	1.393(3)
C(49)-C(50)	1.378(4)
C(50)-C(51)	1.388(4)
C(51)-C(52)	1.386(3)
P(3)-N(8)	1.5721(19)
P(3)-C(53)	1.795(2)
P(3)-C(59)	1.804(2)
P(3)-C(65)	1.799(2)
P(4)-N(8)	1.5648(19)
P(4)-C(71)	1.792(2)
P(4)-C(77)	1.815(2)
P(4)-C(83)	1.804(2)
C(53)-C(54)	1.394(3)
C(53)-C(58)	1.397(3)
C(54)-C(55)	1.391(3)
C(55)-C(56)	1.390(3)
C(56)-C(57)	1.383(3)
C(57)-C(58)	1.389(3)
C(59)-C(60)	1.385(4)
C(59)-C(64)	1.392(3)
C(60)-C(61)	1.388(4)
C(61)-C(62)	1.378(4)
C(62)-C(63)	1.372(4)

C(63)-C(64)	1.386(4)
C(65)-C(66)	1.394(3)
C(65)-C(70)	1.398(3)
C(66)-C(67)	1.395(3)
C(67)-C(68)	1.388(3)
C(68)-C(69)	1.384(3)
C(69)-C(70)	1.393(3)
C(71)-C(72)	1.396(3)
C(71)-C(76)	1.397(3)
C(72)-C(73)	1.387(3)
C(73)-C(74)	1.389(4)
C(74)-C(75)	1.383(4)
C(75)-C(76)	1.392(3)
C(77)-C(78)	1.401(3)
C(77)-C(82)	1.395(3)
C(78)-C(79)	1.394(3)
C(79)-C(80)	1.387(3)
C(80)-C(81)	1.390(3)
C(81)-C(82)	1.393(3)
C(83)-C(84)	1.393(3)
C(83)-C(88)	1.396(3)
C(84)-C(85)	1.394(3)
C(85)-C(86)	1.387(3)
C(86)-C(87)	1.384(3)

C(87)-C(88)	1.387(3)
Cl(1)-C(89)	1.778(2)
Cl(2)-C(89)	1.766(3)
Cl(3)-C(90)	1.713(15)
Cl(4)-C(90)	1.682(15)
Cl(5)-C(91)	1.729(6)
Cl(6)-C(91)	1.774(5)
Cl(7)-C(92)	1.740(10)
Cl(8)-C(92)	1.753(10)

N(2)-Ru(1)-N(1)	77.38(6)
C(13)-Ru(1)-N(1)	169.04(7)
C(13)-Ru(1)-N(2)	93.38(7)
C(13)-Ru(1)-C(14)	94.05(8)
C(13)-Ru(1)-C(15)	88.31(7)
C(13)-Ru(1)-C(16)	92.10(7)
C(14)-Ru(1)-N(1)	95.26(7)
C(14)-Ru(1)-N(2)	172.56(7)
C(14)-Ru(1)-C(15)	89.53(7)
C(14)-Ru(1)-C(16)	89.81(7)
C(15)-Ru(1)-N(1)	85.99(6)
C(15)-Ru(1)-N(2)	91.02(7)
C(15)-Ru(1)-C(16)	179.25(7)
C(16)-Ru(1)-N(1)	93.71(7)

C(16)-Ru(1)-N(2)	89.59(7)
C(1)-N(1)-Ru(1)	125.27(12)
C(1)-N(1)-C(5)	118.10(16)
C(5)-N(1)-Ru(1)	115.99(12)
C(6)-N(2)-Ru(1)	116.38(12)
C(10)-N(2)-Ru(1)	125.25(13)
C(10)-N(2)-C(6)	118.37(16)
N(1)-C(1)-C(2)	122.72(17)
C(1)-C(2)-C(3)	118.78(18)
C(2)-C(3)-C(11)	119.92(18)
C(4)-C(3)-C(2)	119.78(17)
C(4)-C(3)-C(11)	120.22(18)
C(3)-C(4)-C(5)	118.33(17)
N(1)-C(5)-C(4)	122.22(17)
N(1)-C(5)-C(6)	114.74(16)
C(4)-C(5)-C(6)	123.03(17)
N(2)-C(6)-C(5)	114.71(16)
N(2)-C(6)-C(7)	121.94(17)
C(7)-C(6)-C(5)	123.34(17)
C(8)-C(7)-C(6)	118.39(17)
C(7)-C(8)-C(9)	119.79(18)
C(7)-C(8)-C(12)	121.17(18)
C(9)-C(8)-C(12)	118.96(18)
C(10)-C(9)-C(8)	118.80(18)

N(2)-C(10)-C(9)	122.61(18)
F(1)-C(11)-C(3)	111.25(19)
F(2)-C(11)-F(1)	105.0(2)
F(2)-C(11)-C(3)	111.78(18)
F(3)-C(11)-F(1)	107.54(19)
F(3)-C(11)-F(2)	107.0(2)
F(3)-C(11)-C(3)	113.79(17)
F(4)-C(12)-C(8)	111.10(17)
F(5)-C(12)-F(4)	107.15(19)
F(5)-C(12)-F(6)	106.95(17)
F(5)-C(12)-C(8)	113.34(17)
F(6)-C(12)-F(4)	105.46(16)
F(6)-C(12)-C(8)	112.37(18)
N(3)-C(13)-Ru(1)	172.28(18)
N(4)-C(14)-Ru(1)	175.11(17)
N(5)-C(15)-Ru(1)	176.21(16)
N(6)-C(16)-Ru(1)	177.03(17)
N(7)-P(1)-C(17)	116.71(9)
N(7)-P(1)-C(23)	107.03(9)
N(7)-P(1)-C(29)	110.15(9)
C(17)-P(1)-C(23)	107.30(9)
C(17)-P(1)-C(29)	106.52(9)
C(23)-P(1)-C(29)	108.92(9)
N(7)-P(2)-C(35)	114.43(9)

N(7)-P(2)-C(41)	109.29(9)
N(7)-P(2)-C(47)	109.10(9)
C(35)-P(2)-C(41)	107.79(9)
C(35)-P(2)-C(47)	107.44(9)
C(47)-P(2)-C(41)	108.65(9)
P(2)-N(7)-P(1)	146.60(12)
C(18)-C(17)-P(1)	118.40(15)
C(18)-C(17)-C(22)	119.86(19)
C(22)-C(17)-P(1)	121.69(16)
C(19)-C(18)-C(17)	120.38(19)
C(20)-C(19)-C(18)	119.4(2)
C(21)-C(20)-C(19)	120.4(2)
C(20)-C(21)-C(22)	120.7(2)
C(21)-C(22)-C(17)	119.2(2)
C(24)-C(23)-P(1)	121.08(15)
C(28)-C(23)-P(1)	119.40(15)
C(28)-C(23)-C(24)	119.52(18)
C(25)-C(24)-C(23)	120.10(19)
C(26)-C(25)-C(24)	120.3(2)
C(25)-C(26)-C(27)	120.1(2)
C(26)-C(27)-C(28)	119.9(2)
C(23)-C(28)-C(27)	120.0(2)
C(30)-C(29)-P(1)	119.61(15)
C(30)-C(29)-C(34)	119.70(18)

C(34)-C(29)-P(1)	120.69(15)
C(31)-C(30)-C(29)	120.0(2)
C(32)-C(31)-C(30)	120.2(2)
C(31)-C(32)-C(33)	120.0(2)
C(32)-C(33)-C(34)	120.4(2)
C(33)-C(34)-C(29)	119.71(19)
C(36)-C(35)-P(2)	117.88(15)
C(40)-C(35)-P(2)	122.39(15)
C(40)-C(35)-C(36)	119.60(19)
C(37)-C(36)-C(35)	120.69(19)
C(36)-C(37)-C(38)	119.6(2)
C(39)-C(38)-C(37)	120.3(2)
C(38)-C(39)-C(40)	120.4(2)
C(35)-C(40)-C(39)	119.37(19)
C(42)-C(41)-P(2)	118.57(15)
C(46)-C(41)-P(2)	121.74(16)
C(46)-C(41)-C(42)	119.58(19)
C(43)-C(42)-C(41)	120.14(19)
C(44)-C(43)-C(42)	119.9(2)
C(43)-C(44)-C(45)	120.2(2)
C(44)-C(45)-C(46)	120.7(2)
C(41)-C(46)-C(45)	119.6(2)
C(48)-C(47)-P(2)	121.22(15)
C(48)-C(47)-C(52)	119.56(18)

C(52)-C(47)-P(2)	119.21(15)
C(47)-C(48)-C(49)	119.8(2)
C(50)-C(49)-C(48)	120.5(2)
C(49)-C(50)-C(51)	119.8(2)
C(52)-C(51)-C(50)	120.3(2)
C(51)-C(52)-C(47)	120.0(2)
N(8)-P(3)-C(53)	109.52(9)
N(8)-P(3)-C(59)	110.65(10)
N(8)-P(3)-C(65)	116.31(10)
C(53)-P(3)-C(59)	105.67(10)
C(53)-P(3)-C(65)	106.69(9)
C(65)-P(3)-C(59)	107.41(10)
N(8)-P(4)-C(71)	110.15(10)
N(8)-P(4)-C(77)	111.03(10)
N(8)-P(4)-C(83)	114.13(10)
C(71)-P(4)-C(77)	108.35(9)
C(71)-P(4)-C(83)	107.57(10)
C(83)-P(4)-C(77)	105.33(9)
P(4)-N(8)-P(3)	151.97(12)
C(54)-C(53)-P(3)	121.17(15)
C(54)-C(53)-C(58)	120.01(19)
C(58)-C(53)-P(3)	118.43(15)
C(55)-C(54)-C(53)	119.96(19)
C(56)-C(55)-C(54)	119.8(2)

C(57)-C(56)-C(55)	120.3(2)
C(56)-C(57)-C(58)	120.3(2)
C(57)-C(58)-C(53)	119.54(19)
C(60)-C(59)-P(3)	120.69(18)
C(60)-C(59)-C(64)	119.1(2)
C(64)-C(59)-P(3)	120.18(19)
C(59)-C(60)-C(61)	120.3(3)
C(62)-C(61)-C(60)	120.0(3)
C(63)-C(62)-C(61)	120.3(3)
C(62)-C(63)-C(64)	120.1(2)
C(63)-C(64)-C(59)	120.2(3)
C(66)-C(65)-P(3)	118.89(16)
C(66)-C(65)-C(70)	119.98(19)
C(70)-C(65)-P(3)	121.11(16)
C(65)-C(66)-C(67)	119.6(2)
C(68)-C(67)-C(66)	120.2(2)
C(69)-C(68)-C(67)	120.11(19)
C(68)-C(69)-C(70)	120.3(2)
C(69)-C(70)-C(65)	119.7(2)
C(72)-C(71)-P(4)	120.56(16)
C(72)-C(71)-C(76)	120.0(2)
C(76)-C(71)-P(4)	119.30(17)
C(73)-C(72)-C(71)	119.9(2)
C(72)-C(73)-C(74)	120.2(2)

C(75)-C(74)-C(73)	120.1(2)
C(74)-C(75)-C(76)	120.4(2)
C(75)-C(76)-C(71)	119.5(2)
C(78)-C(77)-P(4)	118.24(15)
C(82)-C(77)-P(4)	122.04(15)
C(82)-C(77)-C(78)	119.63(19)
C(79)-C(78)-C(77)	120.2(2)
C(80)-C(79)-C(78)	119.7(2)
C(79)-C(80)-C(81)	120.5(2)
C(80)-C(81)-C(82)	120.1(2)
C(81)-C(82)-C(77)	119.90(19)
C(84)-C(83)-P(4)	121.78(16)
C(84)-C(83)-C(88)	119.76(19)
C(88)-C(83)-P(4)	118.40(16)
C(83)-C(84)-C(85)	119.9(2)
C(86)-C(85)-C(84)	119.9(2)
C(87)-C(86)-C(85)	120.4(2)
C(86)-C(87)-C(88)	120.1(2)
C(87)-C(88)-C(83)	120.0(2)
Cl(2)-C(89)-Cl(1)	110.79(13)
Cl(4)-C(90)-Cl(3)	117.3(8)
Cl(5)-C(91)-Cl(6)	112.9(3)
Cl(7)-C(92)-Cl(8)	111.4(5)

Symmetry transformations used to generate equivalent atoms:

Table 4. Anisotropic displacement parameters ($Å^2 x\ 10^4$) for v19188. The anisotropic displacement factor exponent takes the form: $-2\pi^2[\ h^2\ a^{*2}U^{11} + ...\ + 2\ h\ k\ a^*\ b^*\ U^{12}\ ]$

	U^{11}	U^{22}	U^{33}	U^{23}	U^{13}	U^{12}
Ru(1)	173(1)	152(1)	135(1)	22(1)	39(1)	30(1)
F(1)	200(7)	1136(16)	456(9)	49(10)	20(6)	155(8)
F(2)	684(11)	496(10)	497(10)	294(8)	-275(8)	-378(9)
F(3)	288(7)	517(8)	188(6)	81(6)	-5(5)	-96(6)
F(4)	607(9)	523(9)	541(9)	412(8)	367(8)	345(8)
F(5)	481(8)	472(8)	197(6)	126(6)	79(6)	-60(7)
F(6)	357(7)	422(7)	315(7)	188(6)	211(6)	112(6)
N(1)	186(7)	156(7)	155(7)	29(6)	66(6)	52(6)
N(2)	196(7)	155(7)	173(7)	32(6)	65(6)	50(6)
N(3)	200(8)	214(8)	296(9)	11(7)	27(7)	59(7)
N(4)	307(9)	216(8)	175(8)	48(7)	76(7)	48(7)
N(5)	224(8)	243(8)	218(8)	61(7)	49(6)	58(7)
N(6)	274(9)	240(8)	221(8)	67(7)	72(7)	92(7)
C(1)	232(9)	207(9)	152(8)	50(7)	74(7)	55(8)
C(2)	211(9)	210(9)	203(9)	77(7)	77(7)	21(8)
C(3)	187(9)	214(9)	203(9)	54(7)	31(7)	38(8)
C(4)	200(9)	200(9)	165(9)	62(7)	49(7)	57(7)
C(5)	181(8)	172(8)	156(8)	45(7)	64(7)	68(7)
C(6)	180(8)	166(8)	183(9)	43(7)	67(7)	68(7)

C(7)	197(9)	181(9)	184(9)	53(7)	66(7)	67(7)
C(8)	262(10)	205(9)	213(9)	84(8)	119(8)	82(8)
C(9)	280(10)	193(9)	287(11)	71(8)	136(8)	11(8)
C(10)	242(10)	190(9)	233(10)	32(8)	73(8)	13(8)
C(11)	240(10)	366(12)	238(10)	131(9)	29(8)	-40(9)
C(12)	319(11)	269(10)	269(10)	140(9)	137(9)	85(9)
C(13)	190(9)	228(9)	186(9)	42(7)	49(7)	88(8)
C(14)	185(9)	164(8)	206(9)	-13(7)	12(7)	44(7)
C(15)	194(9)	151(8)	134(8)	12(7)	32(7)	-18(7)
C(16)	229(9)	171(8)	139(8)	29(7)	47(7)	4(8)
P(1)	189(2)	149(2)	158(2)	47(2)	63(2)	29(2)
P(2)	176(2)	175(2)	154(2)	53(2)	54(2)	20(2)
N(7)	243(8)	241(8)	235(8)	113(7)	110(7)	71(7)
C(17)	211(9)	233(9)	157(8)	71(7)	64(7)	52(8)
C(18)	232(9)	249(10)	242(10)	86(8)	114(8)	58(8)
C(19)	295(11)	395(12)	322(11)	169(10)	162(9)	170(10)
C(20)	231(10)	547(15)	356(12)	215(11)	89(9)	134(10)
C(21)	262(11)	411(13)	278(11)	99(10)	-31(9)	-8(10)
C(22)	295(11)	261(10)	204(10)	54(8)	17(8)	36(9)
C(23)	246(9)	170(9)	192(9)	46(7)	68(7)	48(7)
C(24)	306(10)	200(9)	200(9)	62(7)	111(8)	65(8)
C(25)	371(12)	195(9)	281(11)	90(8)	125(9)	45(9)
C(26)	469(14)	203(10)	427(13)	106(9)	186(11)	126(10)
C(27)	504(14)	268(11)	521(15)	132(11)	306(12)	183(11)

C(28)	343(11)	241(10)	350(12)	105(9)	191(9)	90(9)
C(29)	240(9)	150(8)	176(9)	49(7)	41(7)	59(7)
C(30)	261(10)	204(9)	255(10)	97(8)	35(8)	23(8)
C(31)	337(11)	189(9)	305(11)	56(8)	-48(9)	23(9)
C(32)	468(13)	227(10)	202(10)	2(8)	-18(9)	152(10)
C(33)	411(12)	293(11)	189(10)	46(8)	87(9)	168(10)
C(34)	269(10)	219(9)	213(10)	54(8)	78(8)	82(8)
C(35)	174(8)	192(9)	209(9)	72(7)	60(7)	12(7)
C(36)	253(10)	236(10)	211(10)	49(8)	56(8)	37(8)
C(37)	285(10)	226(10)	294(11)	60(8)	130(8)	69(8)
C(38)	218(10)	245(10)	401(12)	128(9)	123(9)	68(8)
C(39)	193(9)	276(10)	309(11)	104(9)	14(8)	23(8)
C(40)	204(9)	236(9)	204(9)	60(8)	43(7)	9(8)
C(41)	227(9)	205(9)	172(9)	49(7)	52(7)	54(8)
C(42)	229(10)	242(10)	231(10)	53(8)	59(8)	37(8)
C(43)	259(10)	259(10)	248(10)	15(8)	8(8)	49(8)
C(44)	520(14)	319(12)	202(10)	22(9)	107(10)	113(11)
C(45)	750(19)	355(13)	328(13)	62(11)	342(13)	32(13)
C(46)	480(14)	263(11)	287(12)	40(9)	203(10)	-13(10)
C(47)	168(8)	211(9)	172(9)	37(7)	52(7)	14(7)
C(48)	234(10)	258(10)	318(11)	103(9)	60(8)	29(8)
C(49)	269(11)	224(10)	446(13)	54(9)	130(10)	-6(9)
C(50)	165(9)	397(13)	337(12)	-37(10)	72(8)	9(9)
C(51)	189(10)	501(14)	364(12)	113(11)	80(9)	125(10)

C(52)	210(10)	336(11)	316(11)	128(9)	105(8)	87(9)
P(3)	198(2)	208(2)	292(3)	133(2)	65(2)	40(2)
P(4)	194(2)	199(2)	241(2)	106(2)	18(2)	13(2)
N(8)	245(8)	272(9)	254(9)	115(7)	21(7)	-10(7)
C(53)	231(9)	184(9)	245(10)	72(8)	85(8)	82(8)
C(54)	313(10)	186(9)	277(10)	90(8)	127(8)	85(8)
C(55)	388(12)	228(10)	225(10)	82(8)	118(9)	128(9)
C(56)	324(11)	233(10)	230(10)	25(8)	51(8)	118(9)
C(57)	248(10)	251(10)	294(11)	65(8)	85(8)	55(8)
C(58)	247(10)	239(10)	230(10)	88(8)	99(8)	66(8)
C(59)	221(10)	249(10)	483(13)	195(10)	129(9)	68(8)
C(60)	617(17)	600(17)	750(20)	534(16)	513(16)	439(15)
C(61)	840(20)	750(20)	910(20)	650(20)	720(20)	588(19)
C(62)	426(14)	427(14)	830(20)	377(15)	308(14)	246(12)
C(63)	482(15)	341(13)	492(15)	142(11)	1(12)	199(12)
C(64)	405(13)	312(12)	383(13)	90(10)	-31(10)	135(10)
C(65)	248(10)	222(9)	274(10)	115(8)	71(8)	47(8)
C(66)	248(10)	231(10)	242(10)	82(8)	43(8)	49(8)
C(67)	291(10)	191(9)	233(10)	62(8)	19(8)	37(8)
C(68)	311(11)	205(9)	201(9)	61(8)	45(8)	-5(8)
C(69)	242(10)	281(11)	378(12)	107(9)	116(9)	18(9)
C(70)	276(11)	256(10)	445(13)	157(10)	145(10)	81(9)
C(71)	214(9)	245(10)	297(11)	130(8)	30(8)	26(8)
C(72)	302(11)	373(12)	363(12)	215(10)	94(9)	121(10)

C(73)	393(13)	517(15)	447(14)	261(12)	195(11)	189(12)
C(74)	345(13)	493(15)	571(17)	254(13)	172(12)	200(12)
C(75)	310(12)	437(14)	500(15)	263(12)	60(10)	151(11)
C(76)	267(11)	352(12)	360(12)	201(10)	45(9)	74(9)
C(77)	243(9)	212(9)	246(10)	110(8)	65(8)	54(8)
C(78)	260(10)	242(10)	266(10)	97(8)	46(8)	26(8)
C(79)	341(11)	198(10)	320(11)	79(8)	122(9)	44(9)
C(80)	388(12)	248(10)	356(12)	155(9)	155(10)	137(9)
C(81)	304(11)	325(11)	306(11)	151(9)	62(9)	125(9)
C(82)	247(10)	235(10)	267(10)	97(8)	47(8)	45(8)
C(83)	224(9)	192(9)	261(10)	106(8)	16(8)	18(8)
C(84)	298(11)	244(10)	249(10)	121(8)	59(8)	36(8)
C(85)	379(12)	232(10)	256(11)	82(8)	47(9)	34(9)
C(86)	286(11)	232(10)	331(12)	119(9)	-10(9)	-11(9)
C(87)	241(10)	247(10)	416(13)	132(9)	54(9)	38(9)
C(88)	248(10)	203(9)	338(11)	91(8)	40(8)	36(8)
Cl(1)	276(3)	308(3)	285(3)	105(2)	74(2)	26(2)
Cl(2)	537(4)	326(3)	319(3)	78(2)	198(3)	70(3)
C(89)	307(12)	273(11)	347(13)	137(10)	125(10)	78(10)
Cl(3)	655(11)	556(10)	914(15)	-169(10)	211(11)	123(9)
Cl(4)	497(9)	722(12)	1400(20)	463(13)	251(11)	84(9)
C(90)	750(90)	4800(400)	930(100)	-860(170)	160(70)	-410(150)
Cl(5)	391(7)	283(6)	353(7)	6(5)	149(5)	30(5)
Cl(6)	312(9)	379(8)	276(6)	83(5)	83(7)	44(7)

C(91)	340(30)	270(20)	280(30)	69(19)	180(20)	40(20)
Cl(7)	470(11)	424(10)	537(12)	205(8)	248(9)	242(8)
Cl(8)	375(11)	451(12)	860(18)	382(12)	235(11)	183(9)
C(92)	300(50)	280(40)	380(40)	150(30)	150(40)	120(40)

Table 5. Hydrogen coordinates (x 10^4) and isotropic displacement parameters ($Å^2$x 10^{3}) for v19188.

	x	y	z	U(eq)
H(1)	6247	5127	3292	24
H(2)	7685	6269	4078	26
H(4)	6855	5139	5512	23
H(7)	5674	4110	5724	22
H(9)	3109	1758	4885	31
H(10)	3137	1927	3837	29
H(18)	5897	10584	2266	28
H(19)	4330	10716	1860	36
H(20)	3024	9291	1145	43
H(21)	3279	7752	833	43
H(22)	4868	7630	1172	33
H(24)	5680	7519	2453	28
H(25)	5588	5862	2328	34
H(26)	6549	5139	1731	42
H(27)	7579	6057	1229	47
H(28)	7678	7722	1350	36
H(30)	8601	10620	2819	30
H(31)	9256	11549	3967	38

H(32)	8332	11280	4723	39
H(33)	6739	10098	4337	35
H(34)	6070	9167	3192	28
H(36)	7480	11722	2049	30
H(37)	6378	12629	1992	32
H(38)	5254	12342	958	33
H(39)	5255	11177	-16	33
H(40)	6346	10239	38	28
H(42)	6584	8154	335	30
H(43)	6346	7149	-768	34
H(44)	7301	7736	-1433	44
H(45)	8503	9311	-1002	59
H(46)	8778	10314	108	44
H(48)	8889	12086	1163	34
H(49)	10538	13142	1660	40
H(50)	11673	12659	2323	42
H(51)	11178	11093	2470	42
H(52)	9540	10024	1974	33
H(54)	879	5890	4467	30
H(55)	2213	6597	5450	32
H(56)	3676	7774	5472	32
H(57)	3832	8205	4509	33
H(58)	2506	7506	3523	28
H(60)	-124	7133	4323	59

H(61)	-933	8315	4562	74
H(62)	-1446	9017	3749	58
H(63)	-1126	8573	2708	53
H(64)	-341	7375	2456	47
H(66)	771	4373	3118	30
H(67)	-218	2840	3144	31
H(68)	-1840	2630	3229	31
H(69)	-2526	3902	3205	37
H(70)	-1556	5434	3169	37
H(72)	1624	5946	673	39
H(73)	2937	5441	391	49
H(74)	3865	4830	1107	52
H(75)	3511	4758	2117	47
H(76)	2193	5255	2407	39
H(78)	1792	7984	2061	32
H(79)	1544	9299	1687	35
H(80)	139	8996	812	37
H(81)	-1007	7385	298	36
H(82)	-773	6068	674	31
H(84)	245	4138	614	32
H(85)	-1210	2786	6	37
H(86)	-2674	2685	332	37
H(87)	-2698	3919	1262	37
H(88)	-1260	5282	1862	33

H(89A)	4961	10399	3263	36
H(89B)	3840	10391	3216	36
H(90A)	4734	4771	746	335
H(90B)	4011	4221	1	335
H(91A)	1260	8837	3947	36
H(91B)	2350	9614	4345	36
H(92A)	1844	10212	3050	35
H(92B)	831	9341	2938	35

$PPN_2Ru(^{CF3}bpy)(CN\text{-}BCF)$

Table 1. Crystal data and structure refinement for D19108.

Identification code	D19108	
Empirical formula	C161 H69 B4 F66 N8 O0.50 P4 Ru	
Formula weight	3645.43	
Temperature	100(2) K	
Wavelength	0.71073 Å	
Crystal system	Triclinic	
Space group	P-1	
Unit cell dimensions	a = 16.024(6) Å	α= 73.248(14)°.
	b = 21.220(6) Å	β= 76.541(18)°.
	c = 23.585(10) Å	γ = 79.114(12)°.
Volume	7404(5) $Å^3$	
Z	2	
Density (calculated)	1.635 Mg/m^3	
Absorption coefficient	0.291 mm^{-1}	
F(000)	3626	
Crystal size	0.300 x 0.250 x 0.150 mm^3	
Theta range for data collection	1.523 to 30.508°.	
Index ranges	-22<=h<=22, -29<=k<=30, -33<=l<=33	
Reflections collected	246908	
Independent reflections	44916 [R(int) = 0.0493]	
Completeness to theta = 25.242°	99.9 %	
Absorption correction	Semi-empirical from equivalents	

Max. and min. transmission	1.0000 and 0.9509
Refinement method	Full-matrix least-squares on F^2
Data / restraints / parameters	44916 / 2373 / 2588
Goodness-of-fit on F^2	1.011
Final R indices [I>2sigma(I)]	R1 = 0.0395, wR2 = 0.0858
R indices (all data)	R1 = 0.0588, wR2 = 0.0936
Extinction coefficient	n/a
Largest diff. peak and hole	0.577 and -0.980 e.$Å^{-3}$

Table 2. Atomic coordinates (x 10^4) and equivalent isotropic displacement parameters ($Å^2$x 10^3) for D19108. U(eq) is defined as one third of the trace of the orthogonalized U^{ij} tensor.

	x	y	z	U(eq)
N(7)	8780(1)	8990(1)	1524(1)	21(1)
P(1)	8214(1)	8410(1)	1853(1)	22(1)
C(151)	7122(3)	8630(2)	1696(2)	31(1)
C(152)	6447(2)	8284(2)	2075(2)	52(1)
C(153)	5624(3)	8440(3)	1934(3)	75(2)
C(154)	5459(4)	8940(3)	1435(4)	75(2)
C(155)	6135(3)	9261(3)	1042(2)	51(1)
C(156)	6951(3)	9127(2)	1192(2)	32(1)
C(51B)	7158(7)	8517(6)	1709(4)	38(3)
C(52B)	6690(5)	7987(5)	1872(4)	44(2)
C(53B)	5862(5)	8092(5)	1753(4)	49(2)
C(54B)	5544(9)	8708(6)	1442(9)	65(3)
C(55B)	5976(7)	9274(5)	1322(7)	59(3)
C(56B)	6826(6)	9145(5)	1421(6)	46(2)
C(161)	8125(1)	8146(1)	2656(1)	25(1)
C(162)	7464(1)	8461(1)	3020(1)	39(1)
C(163)	7423(2)	8286(1)	3635(1)	43(1)
C(164)	8032(2)	7807(1)	3888(1)	41(1)
C(165)	8691(2)	7496(1)	3532(1)	43(1)

C(166)	8740(1)	7668(1)	2911(1)	34(1)
C(171)	8732(1)	7712(1)	1559(1)	26(1)
C(172)	8443(2)	7096(1)	1810(1)	59(1)
C(173)	8831(2)	6570(1)	1563(1)	72(1)
C(174)	9493(2)	6658(1)	1069(1)	48(1)
C(175)	9780(1)	7268(1)	816(1)	32(1)
C(176)	9404(1)	7797(1)	1064(1)	25(1)
P(2)	8881(1)	9700(1)	1568(1)	15(1)
C(181)	9956(1)	9693(1)	1680(1)	16(1)
C(182)	10494(1)	9097(1)	1823(1)	22(1)
C(183)	11331(1)	9101(1)	1888(1)	30(1)
C(184)	11633(1)	9693(1)	1809(1)	28(1)
C(185)	11100(1)	10289(1)	1671(1)	27(1)
C(186)	10263(1)	10290(1)	1606(1)	22(1)
C(191)	8754(1)	10296(1)	868(1)	18(1)
C(192)	8854(1)	10065(1)	355(1)	23(1)
C(193)	8783(1)	10514(1)	-196(1)	28(1)
C(194)	8626(1)	11187(1)	-239(1)	30(1)
C(195)	8532(1)	11420(1)	267(1)	27(1)
C(196)	8595(1)	10976(1)	822(1)	22(1)
C(201)	8144(1)	9991(1)	2166(1)	19(1)
C(202)	7328(1)	10319(1)	2077(1)	28(1)
C(203)	6742(1)	10514(1)	2549(1)	36(1)
C(204)	6961(1)	10376(1)	3111(1)	33(1)

C(205)	7765(1)	10044(1)	3203(1)	31(1)
C(206)	8363(1)	9855(1)	2731(1)	26(1)
N(8)	7002(1)	2040(1)	6124(1)	30(1)
P(3)	6539(1)	2750(1)	6176(1)	23(1)
C(211)	5422(1)	2885(1)	6105(1)	26(1)
C(212)	5217(1)	2885(1)	5565(1)	44(1)
C(213)	4355(2)	2986(1)	5506(1)	49(1)
C(214)	3708(1)	3087(1)	5983(1)	45(1)
C(215)	3909(1)	3085(1)	6517(1)	45(1)
C(216)	4767(1)	2982(1)	6583(1)	30(1)
C(221)	7061(1)	3414(1)	5640(1)	25(1)
C(222)	6633(1)	3928(1)	5253(1)	45(1)
C(223)	7091(1)	4409(1)	4828(1)	52(1)
C(224)	7968(1)	4378(1)	4797(1)	38(1)
C(225)	8389(1)	3882(1)	5199(1)	31(1)
C(226)	7940(1)	3398(1)	5617(1)	26(1)
C(231)	6572(1)	2805(1)	6916(1)	30(1)
C(232)	6606(1)	3412(1)	7020(1)	33(1)
C(233)	6597(1)	3448(1)	7601(1)	43(1)
C(234)	6544(1)	2883(2)	8072(1)	50(1)
C(235)	6514(1)	2281(1)	7973(1)	49(1)
C(236)	6531(1)	2234(1)	7392(1)	39(1)
P(4)	7356(1)	1602(1)	5660(1)	24(1)
C(241)	8358(1)	1125(1)	5843(1)	26(1)

C(242)	8533(1)	1046(1)	6411(1)	36(1)
C(243)	9301(1)	681(1)	6563(1)	40(1)
C(244)	9893(1)	402(1)	6150(1)	35(1)
C(245)	9728(1)	484(1)	5583(1)	38(1)
C(246)	8962(1)	844(1)	5424(1)	34(1)
C(251)	6586(1)	1060(1)	5718(1)	31(1)
C(252)	6791(1)	567(1)	5411(1)	38(1)
C(253)	6165(2)	185(1)	5431(1)	47(1)
C(254)	5335(2)	306(1)	5752(1)	50(1)
C(255)	5130(1)	784(1)	6059(1)	49(1)
C(256)	5754(1)	1164(1)	6052(1)	41(1)
C(261)	7590(1)	2048(1)	4879(1)	23(1)
C(262)	7044(1)	2087(1)	4484(1)	29(1)
C(263)	7220(1)	2462(1)	3895(1)	36(1)
C(264)	7934(1)	2800(1)	3693(1)	36(1)
C(265)	8472(1)	2773(1)	4083(1)	35(1)
C(266)	8306(1)	2395(1)	4674(1)	29(1)
Ru(1)	7376(1)	6311(1)	8127(1)	13(1)
C(1)	8012(1)	5760(1)	7552(1)	16(1)
N(1)	8449(1)	5406(1)	7286(1)	18(1)
B(1)	9054(1)	4920(1)	6940(1)	17(1)
C(11)	8863(1)	4167(1)	7330(1)	18(1)
C(12)	8761(1)	3986(1)	7954(1)	21(1)
F(12)	8840(1)	4428(1)	8247(1)	28(1)

C(13)	8595(1)	3368(1)	8314(1)	26(1)
F(13)	8442(1)	3243(1)	8919(1)	35(1)
C(14)	8582(1)	2875(1)	8046(1)	27(1)
F(14)	8427(1)	2269(1)	8389(1)	37(1)
C(15)	8708(1)	3015(1)	7429(1)	25(1)
F(15)	8689(1)	2538(1)	7165(1)	35(1)
C(16)	8831(1)	3652(1)	7087(1)	20(1)
F(16)	8927(1)	3751(1)	6487(1)	26(1)
C(21)	10067(1)	4969(1)	6936(1)	20(1)
C(22)	10718(1)	4486(1)	6769(1)	25(1)
F(22)	10519(1)	4013(1)	6564(1)	36(1)
C(23)	11580(1)	4455(1)	6786(1)	33(1)
F(23)	12163(1)	3967(1)	6617(1)	54(1)
C(24)	11839(1)	4927(1)	6979(1)	35(1)
F(24)	12674(1)	4908(1)	6994(1)	52(1)
C(25)	11229(1)	5416(1)	7150(1)	31(1)
F(25)	11461(1)	5879(1)	7349(1)	47(1)
C(26)	10370(1)	5434(1)	7119(1)	26(1)
F(26)	9834(1)	5948(1)	7280(1)	40(1)
C(31)	8764(1)	5151(1)	6283(1)	18(1)
C(32)	9278(1)	5417(1)	5738(1)	22(1)
F(32)	10130(1)	5423(1)	5701(1)	32(1)
C(33)	8975(1)	5694(1)	5206(1)	27(1)
F(33)	9511(1)	5949(1)	4693(1)	40(1)

C(34)	8117(1)	5709(1)	5204(1)	31(1)
F(34)	7813(1)	5979(1)	4690(1)	48(1)
C(35)	7576(1)	5442(1)	5729(1)	30(1)
F(35)	6736(1)	5451(1)	5730(1)	48(1)
C(36)	7907(1)	5169(1)	6249(1)	22(1)
F(36)	7341(1)	4917(1)	6752(1)	30(1)
C(2)	6332(1)	6482(1)	7773(1)	15(1)
N(2)	5737(1)	6562(1)	7550(1)	17(1)
B(2)	5016(1)	6743(1)	7168(1)	16(1)
C(41)	4124(1)	7005(1)	7588(1)	15(1)
C(42)	4126(1)	7452(1)	7917(1)	18(1)
F(42)	4863(1)	7701(1)	7870(1)	27(1)
C(43)	3406(1)	7679(1)	8291(1)	21(1)
F(43)	3456(1)	8103(1)	8605(1)	32(1)
C(44)	2626(1)	7466(1)	8346(1)	21(1)
F(44)	1917(1)	7677(1)	8709(1)	29(1)
C(45)	2580(1)	7032(1)	8024(1)	20(1)
F(45)	1816(1)	6829(1)	8064(1)	32(1)
C(46)	3319(1)	6810(1)	7657(1)	16(1)
F(46)	3203(1)	6391(1)	7356(1)	24(1)
C(51)	4934(1)	6079(1)	6974(1)	19(1)
C(52)	4965(1)	5457(1)	7373(1)	24(1)
F(52)	5031(1)	5388(1)	7950(1)	33(1)
C(53)	4898(1)	4884(1)	7228(1)	36(1)

F(53)	4909(1)	4301(1)	7648(1)	56(1)
C(54)	4800(1)	4919(1)	6657(1)	40(1)
F(54)	4739(1)	4367(1)	6509(1)	65(1)
C(55)	4759(1)	5518(1)	6246(1)	36(1)
F(55)	4672(1)	5555(1)	5684(1)	58(1)
C(56)	4812(1)	6082(1)	6409(1)	27(1)
F(56)	4732(1)	6652(1)	5975(1)	42(1)
C(61)	5383(1)	7307(1)	6567(1)	17(1)
C(62)	6190(1)	7160(1)	6221(1)	22(1)
F(62)	6665(1)	6565(1)	6390(1)	29(1)
C(63)	6546(1)	7583(1)	5696(1)	31(1)
F(63)	7330(1)	7403(1)	5384(1)	45(1)
C(64)	6090(1)	8192(1)	5488(1)	36(1)
F(64)	6432(1)	8620(1)	4978(1)	54(1)
C(65)	5290(1)	8366(1)	5809(1)	31(1)
F(65)	4832(1)	8958(1)	5613(1)	47(1)
C(66)	4956(1)	7927(1)	6338(1)	21(1)
F(66)	4162(1)	8141(1)	6621(1)	25(1)
C(3)	7772(1)	7127(1)	7564(1)	14(1)
N(3)	8044(1)	7601(1)	7253(1)	17(1)
B(3)	8330(1)	8266(1)	6835(1)	15(1)
C(71)	8555(2)	8165(2)	6151(1)	17(1)
C(72)	9085(2)	7599(2)	6029(1)	22(1)
F(72)	9370(2)	7114(1)	6481(1)	31(1)

C(73)	9395(2)	7515(2)	5455(2)	31(1)
F(73)	9920(1)	6960(1)	5369(1)	47(1)
C(74)	9177(2)	8002(2)	4968(1)	35(1)
F(74)	9505(1)	7937(2)	4407(1)	58(1)
C(75)	8625(2)	8555(2)	5060(1)	32(1)
F(75)	8381(1)	9034(2)	4594(1)	48(1)
C(76)	8334(2)	8625(2)	5644(1)	23(1)
F(76)	7841(2)	9206(1)	5691(1)	32(1)
C(71A)	8552(6)	8293(6)	6113(5)	24(3)
C(72A)	8981(9)	7756(7)	5902(5)	30(3)
F(72A)	9228(10)	7192(7)	6288(6)	39(3)
C(73A)	9220(10)	7756(7)	5292(5)	32(2)
F(73A)	9662(9)	7219(6)	5134(6)	62(3)
C(74A)	9002(9)	8322(7)	4890(5)	33(2)
F(74A)	9242(9)	8353(8)	4294(4)	62(3)
C(75A)	8545(8)	8861(7)	5063(4)	30(2)
F(75A)	8317(6)	9428(7)	4658(4)	52(3)
C(76A)	8314(10)	8845(7)	5673(5)	22(2)
F(76A)	7930(8)	9410(6)	5816(5)	40(3)
C(81)	9223(1)	8371(1)	7014(1)	16(1)
C(82)	9940(1)	8604(1)	6601(1)	19(1)
F(82)	9935(1)	8808(1)	6004(1)	28(1)
C(83)	10702(1)	8654(1)	6758(1)	22(1)
F(83)	11364(1)	8889(1)	6328(1)	32(1)

C(84)	10773(1)	8475(1)	7354(1)	24(1)
F(84)	11504(1)	8517(1)	7517(1)	34(1)
C(85)	10076(1)	8256(1)	7785(1)	22(1)
F(85)	10124(1)	8096(1)	8371(1)	31(1)
C(86)	9324(1)	8216(1)	7610(1)	18(1)
F(86)	8656(1)	8026(1)	8063(1)	24(1)
C(91)	7505(1)	8824(1)	6964(1)	16(1)
C(92)	7497(1)	9379(1)	7163(1)	23(1)
F(92)	8230(1)	9528(1)	7250(1)	40(1)
C(93)	6751(1)	9809(1)	7290(1)	26(1)
F(93)	6786(1)	10342(1)	7481(1)	46(1)
C(94)	5972(1)	9692(1)	7226(1)	23(1)
F(94)	5246(1)	10096(1)	7361(1)	31(1)
C(95)	5945(1)	9154(1)	7020(1)	21(1)
F(95)	5194(1)	9040(1)	6931(1)	32(1)
C(96)	6699(1)	8739(1)	6899(1)	18(1)
F(96)	6630(1)	8226(1)	6691(1)	26(1)
C(4)	6843(1)	6801(1)	8767(1)	17(1)
N(4)	6630(1)	7018(1)	9181(1)	20(1)
B(4)	6431(1)	7300(1)	9745(1)	20(1)
C(101)	6386(2)	6686(2)	10367(2)	19(1)
C(102)	6468(3)	6785(2)	10905(2)	30(1)
F(102)	6475(3)	7406(2)	10940(1)	50(1)
C(103)	6574(3)	6278(2)	11415(2)	38(1)

F(103)	6669(3)	6416(2)	11918(1)	68(1)
C(104)	6571(3)	5631(2)	11412(2)	40(1)
F(104)	6695(3)	5133(2)	11897(2)	64(1)
C(105)	6443(5)	5502(2)	10909(3)	41(1)
F(105)	6413(4)	4876(2)	10893(2)	79(2)
C(106)	6334(6)	6027(3)	10404(3)	32(1)
F(106)	6169(4)	5848(2)	9938(2)	58(1)
C(01B)	6448(4)	6639(5)	10293(4)	29(2)
C(02B)	6748(5)	6628(4)	10811(3)	29(2)
F(02B)	6948(6)	7180(4)	10884(2)	52(2)
C(03B)	6848(5)	6051(4)	11278(3)	36(2)
F(03B)	7142(5)	6078(5)	11757(3)	64(2)
C(04B)	6645(6)	5483(4)	11234(4)	36(2)
F(04B)	6760(5)	4928(4)	11678(4)	59(2)
C(05B)	6287(9)	5494(5)	10764(5)	35(2)
F(05B)	6045(6)	4935(4)	10739(4)	58(2)
C(06B)	6190(11)	6055(5)	10317(6)	25(2)
F(06B)	5843(5)	6023(4)	9865(3)	38(2)
C(111)	7296(1)	7647(1)	9692(1)	24(1)
C(112)	8113(1)	7282(1)	9620(1)	26(1)
F(112)	8196(1)	6642(1)	9594(1)	31(1)
C(113)	8872(1)	7520(1)	9583(1)	31(1)
F(113)	9637(1)	7135(1)	9511(1)	41(1)
C(114)	8833(1)	8156(1)	9627(1)	34(1)

F(114)	9562(1)	8404(1)	9596(1)	45(1)
C(115)	8045(1)	8538(1)	9712(1)	34(1)
F(115)	7999(1)	9157(1)	9770(1)	47(1)
C(116)	7297(1)	8281(1)	9743(1)	30(1)
F(116)	6549(1)	8688(1)	9833(1)	43(1)
C(121)	5548(1)	7817(1)	9687(1)	20(1)
C(122)	5484(1)	8307(1)	9156(1)	23(1)
F(122)	6181(1)	8378(1)	8702(1)	36(1)
C(123)	4751(1)	8746(1)	9058(1)	26(1)
F(123)	4729(1)	9205(1)	8533(1)	42(1)
C(124)	4027(1)	8719(1)	9511(1)	29(1)
F(124)	3313(1)	9152(1)	9424(1)	42(1)
C(125)	4056(1)	8248(1)	10045(1)	34(1)
F(125)	3354(1)	8214(1)	10492(1)	60(1)
C(126)	4800(1)	7812(1)	10122(1)	29(1)
F(126)	4766(1)	7361(1)	10662(1)	49(1)
N(5)	8482(1)	6021(1)	8526(1)	16(1)
C(131)	9170(1)	6350(1)	8366(1)	21(1)
C(132)	9931(1)	6089(1)	8580(1)	23(1)
C(133)	9972(1)	5462(1)	8970(1)	21(1)
C(141)	10817(1)	5142(1)	9164(1)	28(1)
F(131)	11417(8)	5022(10)	8706(5)	58(2)
F(132)	10740(6)	4598(4)	9616(4)	30(2)
F(133)	11121(10)	5591(8)	9346(5)	45(2)

F(31B)	11375(9)	4925(7)	8716(6)	33(2)
F(32B)	10726(10)	4581(6)	9607(6)	39(3)
F(33B)	11206(10)	5501(9)	9375(6)	29(2)
C(134)	9255(1)	5128(1)	9158(1)	20(1)
C(135)	8507(1)	5424(1)	8932(1)	17(1)
C(136)	7708(1)	5107(1)	9097(1)	18(1)
C(137)	7595(1)	4519(1)	9541(1)	24(1)
C(138)	6832(1)	4256(1)	9652(1)	29(1)
C(142)	6695(2)	3607(1)	10115(1)	47(1)
F(134)	6483(6)	3179(3)	9866(4)	84(2)
F(135)	6082(6)	3645(6)	10571(4)	79(3)
F(136)	7418(3)	3286(2)	10310(3)	54(1)
F(34B)	6776(10)	3118(5)	9889(6)	89(3)
F(35B)	5903(7)	3681(9)	10447(6)	80(3)
F(36B)	7193(10)	3511(8)	10520(6)	97(4)
C(139)	6191(1)	4583(1)	9328(1)	30(1)
C(140)	6339(1)	5169(1)	8897(1)	24(1)
N(6)	7083(1)	5427(1)	8778(1)	17(1)
O(1S)	3570(20)	9085(9)	868(12)	171(8)
C(11S)	3416(10)	9731(9)	667(8)	66(4)
C(12S)	3730(17)	10080(11)	1077(9)	86(6)
O(2S)	3915(14)	9845(11)	827(10)	162(8)
C(21S)	4557(15)	10209(13)	354(11)	103(6)
C(22S)	5050(18)	9749(16)	-37(12)	120(8)

O(3S)	4341(11)	9795(9)	266(8)	85(4)
C(31S)	4127(16)	9213(14)	603(11)	81(5)
C(32S)	3500(20)	9279(14)	1189(12)	112(8)

Table 3. Bond lengths [Å] and angles [°] for D19108.

N(7)-P(1)	1.5762(14)
N(7)-P(2)	1.5819(14)
P(1)-C(51B)	1.763(11)
P(1)-C(161)	1.7931(19)
P(1)-C(171)	1.7932(18)
P(1)-C(151)	1.819(5)
C(151)-C(156)	1.384(5)
C(151)-C(152)	1.405(5)
C(152)-C(153)	1.391(5)
C(152)-H(152)	0.9500
C(153)-C(154)	1.378(7)
C(153)-H(153)	0.9500
C(154)-C(155)	1.396(7)
C(154)-H(154)	0.9500
C(155)-C(156)	1.391(5)
C(155)-H(155)	0.9500
C(156)-H(156)	0.9500
C(51B)-C(56B)	1.377(11)
C(51B)-C(52B)	1.383(11)
C(52B)-C(53B)	1.385(9)
C(52B)-H(52B)	0.9500
C(53B)-C(54B)	1.370(11)

C(53B)-H(53B)	0.9500
C(54B)-C(55B)	1.425(11)
C(54B)-H(54B)	0.9500
C(55B)-C(56B)	1.398(10)
C(55B)-H(55B)	0.9500
C(56B)-H(56B)	0.9500
C(161)-C(166)	1.383(3)
C(161)-C(162)	1.394(3)
C(162)-C(163)	1.379(3)
C(162)-H(162)	0.9500
C(163)-C(164)	1.373(3)
C(163)-H(163)	0.9500
C(164)-C(165)	1.378(3)
C(164)-H(164)	0.9500
C(165)-C(166)	1.391(3)
C(165)-H(165)	0.9500
C(166)-H(166)	0.9500
C(171)-C(176)	1.387(2)
C(171)-C(172)	1.389(3)
C(172)-C(173)	1.384(3)
C(172)-H(172)	0.9500
C(173)-C(174)	1.376(4)
C(173)-H(173)	0.9500
C(174)-C(175)	1.377(3)

C(174)-H(174)	0.9500
C(175)-C(176)	1.386(2)
C(175)-H(175)	0.9500
C(176)-H(176)	0.9500
P(2)-C(201)	1.7936(16)
P(2)-C(191)	1.7960(16)
P(2)-C(181)	1.7975(17)
C(181)-C(182)	1.392(2)
C(181)-C(186)	1.395(2)
C(182)-C(183)	1.386(2)
C(182)-H(182)	0.9500
C(183)-C(184)	1.378(3)
C(183)-H(183)	0.9500
C(184)-C(185)	1.385(3)
C(184)-H(184)	0.9500
C(185)-C(186)	1.384(2)
C(185)-H(185)	0.9500
C(186)-H(186)	0.9500
C(191)-C(196)	1.395(2)
C(191)-C(192)	1.395(2)
C(192)-C(193)	1.387(2)
C(192)-H(192)	0.9500
C(193)-C(194)	1.380(3)
C(193)-H(193)	0.9500

C(194)-C(195)	1.386(3)
C(194)-H(194)	0.9500
C(195)-C(196)	1.388(2)
C(195)-H(195)	0.9500
C(196)-H(196)	0.9500
C(201)-C(206)	1.392(2)
C(201)-C(202)	1.392(2)
C(202)-C(203)	1.388(2)
C(202)-H(202)	0.9500
C(203)-C(204)	1.385(3)
C(203)-H(203)	0.9500
C(204)-C(205)	1.380(3)
C(204)-H(204)	0.9500
C(205)-C(206)	1.391(2)
C(205)-H(205)	0.9500
C(206)-H(206)	0.9500
N(8)-P(4)	1.5745(17)
N(8)-P(3)	1.5754(17)
P(3)-C(221)	1.7919(18)
P(3)-C(231)	1.795(2)
P(3)-C(211)	1.7964(18)
C(211)-C(216)	1.384(3)
C(211)-C(212)	1.387(3)
C(212)-C(213)	1.391(3)

C(212)-H(212)	0.9500
C(213)-C(214)	1.379(4)
C(213)-H(213)	0.9500
C(214)-C(215)	1.369(4)
C(214)-H(214)	0.9500
C(215)-C(216)	1.389(3)
C(215)-H(215)	0.9500
C(216)-H(216)	0.9500
C(221)-C(222)	1.389(3)
C(221)-C(226)	1.391(2)
C(222)-C(223)	1.391(3)
C(222)-H(222)	0.9500
C(223)-C(224)	1.380(3)
C(223)-H(223)	0.9500
C(224)-C(225)	1.384(3)
C(224)-H(224)	0.9500
C(225)-C(226)	1.382(3)
C(225)-H(225)	0.9500
C(226)-H(226)	0.9500
C(231)-C(232)	1.392(3)
C(231)-C(236)	1.395(3)
C(232)-C(233)	1.392(3)
C(232)-H(232)	0.9500
C(233)-C(234)	1.381(4)

C(233)-H(233)	0.9500
C(234)-C(235)	1.375(4)
C(234)-H(234)	0.9500
C(235)-C(236)	1.397(3)
C(235)-H(235)	0.9500
C(236)-H(236)	0.9500
P(4)-C(251)	1.799(2)
P(4)-C(261)	1.7992(18)
P(4)-C(241)	1.8007(17)
C(241)-C(242)	1.390(3)
C(241)-C(246)	1.395(3)
C(242)-C(243)	1.389(3)
C(242)-H(242)	0.9500
C(243)-C(244)	1.374(3)
C(243)-H(243)	0.9500
C(244)-C(245)	1.381(3)
C(244)-H(244)	0.9500
C(245)-C(246)	1.388(3)
C(245)-H(245)	0.9500
C(246)-H(246)	0.9500
C(251)-C(252)	1.386(3)
C(251)-C(256)	1.394(3)
C(252)-C(253)	1.389(3)
C(252)-H(252)	0.9500

C(253)-C(254)	1.386(4)
C(253)-H(253)	0.9500
C(254)-C(255)	1.358(4)
C(254)-H(254)	0.9500
C(255)-C(256)	1.395(3)
C(255)-H(255)	0.9500
C(256)-H(256)	0.9500
C(261)-C(262)	1.395(2)
C(261)-C(266)	1.395(2)
C(262)-C(263)	1.382(3)
C(262)-H(262)	0.9500
C(263)-C(264)	1.381(3)
C(263)-H(263)	0.9500
C(264)-C(265)	1.383(3)
C(264)-H(264)	0.9500
C(265)-C(266)	1.386(3)
C(265)-H(265)	0.9500
C(266)-H(266)	0.9500
Ru(1)-C(3)	1.9640(16)
Ru(1)-C(2)	1.9687(16)
Ru(1)-C(4)	2.0137(16)
Ru(1)-C(1)	2.0167(16)
Ru(1)-N(6)	2.1043(14)
Ru(1)-N(5)	2.1052(14)

C(1)-N(1)	1.1494(19)
N(1)-B(1)	1.550(2)
B(1)-C(31)	1.634(2)
B(1)-C(11)	1.643(2)
B(1)-C(21)	1.643(2)
C(11)-C(12)	1.387(2)
C(11)-C(16)	1.387(2)
C(12)-F(12)	1.3546(19)
C(12)-C(13)	1.377(2)
C(13)-F(13)	1.346(2)
C(13)-C(14)	1.374(3)
C(14)-F(14)	1.3406(19)
C(14)-C(15)	1.373(3)
C(15)-F(15)	1.3411(19)
C(15)-C(16)	1.384(2)
C(16)-F(16)	1.3459(19)
C(21)-C(26)	1.386(2)
C(21)-C(22)	1.390(2)
C(22)-F(22)	1.347(2)
C(22)-C(23)	1.380(2)
C(23)-F(23)	1.343(2)
C(23)-C(24)	1.375(3)
C(24)-F(24)	1.339(2)
C(24)-C(25)	1.367(3)

C(25)-F(25)	1.344(2)
C(25)-C(26)	1.389(3)
C(26)-F(26)	1.342(2)
C(31)-C(32)	1.383(2)
C(31)-C(36)	1.387(2)
C(32)-F(32)	1.3508(19)
C(32)-C(33)	1.381(2)
C(33)-F(33)	1.344(2)
C(33)-C(34)	1.371(3)
C(34)-F(34)	1.343(2)
C(34)-C(35)	1.374(3)
C(35)-F(35)	1.342(2)
C(35)-C(36)	1.378(2)
C(36)-F(36)	1.3531(19)
C(2)-N(2)	1.155(2)
N(2)-B(2)	1.554(2)
B(2)-C(51)	1.636(2)
B(2)-C(61)	1.639(2)
B(2)-C(41)	1.640(2)
C(41)-C(46)	1.389(2)
C(41)-C(42)	1.389(2)
C(42)-F(42)	1.3511(18)
C(42)-C(43)	1.380(2)
C(43)-F(43)	1.3442(18)

C(43)-C(44)	1.374(2)
C(44)-F(44)	1.3416(17)
C(44)-C(45)	1.373(2)
C(45)-F(45)	1.3463(18)
C(45)-C(46)	1.385(2)
C(46)-F(46)	1.3475(18)
C(51)-C(52)	1.384(2)
C(51)-C(56)	1.388(2)
C(52)-F(52)	1.353(2)
C(52)-C(53)	1.383(2)
C(53)-F(53)	1.344(2)
C(53)-C(54)	1.369(3)
C(54)-F(54)	1.341(2)
C(54)-C(55)	1.359(3)
C(55)-F(55)	1.342(2)
C(55)-C(56)	1.381(3)
C(56)-F(56)	1.348(2)
C(61)-C(66)	1.383(2)
C(61)-C(62)	1.393(2)
C(62)-F(62)	1.349(2)
C(62)-C(63)	1.375(2)
C(63)-F(63)	1.347(2)
C(63)-C(64)	1.375(3)
C(64)-F(64)	1.348(2)

C(64)-C(65)	1.372(3)
C(65)-F(65)	1.344(2)
C(65)-C(66)	1.384(2)
C(66)-F(66)	1.3536(19)
C(3)-N(3)	1.1553(19)
N(3)-B(3)	1.551(2)
B(3)-C(91)	1.634(2)
B(3)-C(71)	1.638(3)
B(3)-C(71A)	1.644(12)
B(3)-C(81)	1.652(2)
C(71)-C(76)	1.380(3)
C(71)-C(72)	1.395(3)
C(72)-F(72)	1.349(3)
C(72)-C(73)	1.380(3)
C(73)-F(73)	1.349(3)
C(73)-C(74)	1.369(4)
C(74)-F(74)	1.343(3)
C(74)-C(75)	1.367(4)
C(75)-F(75)	1.343(3)
C(75)-C(76)	1.388(4)
C(76)-F(76)	1.350(3)
C(71A)-C(72A)	1.375(12)
C(71A)-C(76A)	1.381(11)
C(72A)-F(72A)	1.334(11)

C(72A)-C(73A)	1.399(11)
C(73A)-F(73A)	1.327(11)
C(73A)-C(74A)	1.342(11)
C(74A)-C(75A)	1.351(11)
C(74A)-F(74A)	1.353(11)
C(75A)-F(75A)	1.353(11)
C(75A)-C(76A)	1.391(11)
C(76A)-F(76A)	1.338(11)
C(81)-C(82)	1.389(2)
C(81)-C(86)	1.389(2)
C(82)-F(82)	1.3501(19)
C(82)-C(83)	1.385(2)
C(83)-F(83)	1.3454(19)
C(83)-C(84)	1.372(2)
C(84)-F(84)	1.3402(18)
C(84)-C(85)	1.376(2)
C(85)-F(85)	1.3430(19)
C(85)-C(86)	1.384(2)
C(86)-F(86)	1.3542(18)
C(91)-C(92)	1.385(2)
C(91)-C(96)	1.385(2)
C(92)-F(92)	1.3453(19)
C(92)-C(93)	1.389(2)
C(93)-F(93)	1.3465(19)

C(93)-C(94)	1.366(2)
C(94)-F(94)	1.3410(17)
C(94)-C(95)	1.374(2)
C(95)-F(95)	1.3447(19)
C(95)-C(96)	1.378(2)
C(96)-F(96)	1.3464(18)
C(4)-N(4)	1.150(2)
N(4)-B(4)	1.556(2)
B(4)-C(01B)	1.612(10)
B(4)-C(121)	1.625(2)
B(4)-C(111)	1.652(2)
B(4)-C(101)	1.656(5)
C(101)-C(102)	1.383(5)
C(101)-C(106)	1.393(6)
C(102)-F(102)	1.346(4)
C(102)-C(103)	1.382(5)
C(103)-F(103)	1.348(4)
C(103)-C(104)	1.376(6)
C(104)-F(104)	1.339(5)
C(104)-C(105)	1.360(6)
C(105)-F(105)	1.350(5)
C(105)-C(106)	1.395(6)
C(106)-F(106)	1.357(5)
C(01B)-C(06B)	1.360(11)

C(01B)-C(02B)	1.405(10)
C(02B)-F(02B)	1.338(8)
C(02B)-C(03B)	1.402(8)
C(03B)-F(03B)	1.340(7)
C(03B)-C(04B)	1.344(9)
C(04B)-F(04B)	1.348(9)
C(04B)-C(05B)	1.354(9)
C(05B)-F(05B)	1.336(10)
C(05B)-C(06B)	1.355(10)
C(06B)-F(06B)	1.336(9)
C(111)-C(116)	1.385(3)
C(111)-C(112)	1.390(3)
C(112)-F(112)	1.356(2)
C(112)-C(113)	1.378(3)
C(113)-F(113)	1.343(2)
C(113)-C(114)	1.372(3)
C(114)-F(114)	1.347(2)
C(114)-C(115)	1.372(3)
C(115)-F(115)	1.345(2)
C(115)-C(116)	1.388(3)
C(116)-F(116)	1.350(2)
C(121)-C(126)	1.383(2)
C(121)-C(122)	1.390(2)
C(122)-F(122)	1.3520(19)

C(122)-C(123)	1.375(2)
C(123)-F(123)	1.3401(19)
C(123)-C(124)	1.381(2)
C(124)-F(124)	1.340(2)
C(124)-C(125)	1.369(3)
C(125)-F(125)	1.348(2)
C(125)-C(126)	1.378(3)
C(126)-F(126)	1.351(2)
N(5)-C(131)	1.338(2)
N(5)-C(135)	1.3511(19)
C(131)-C(132)	1.384(2)
C(131)-H(131)	0.9500
C(132)-C(133)	1.382(2)
C(132)-H(132)	0.9500
C(133)-C(134)	1.381(2)
C(133)-C(141)	1.505(2)
C(141)-F(131)	1.318(7)
C(141)-F(33B)	1.325(9)
C(141)-F(132)	1.329(7)
C(141)-F(32B)	1.345(10)
C(141)-F(31B)	1.346(8)
C(141)-F(133)	1.355(8)
C(134)-C(135)	1.391(2)
C(134)-H(134)	0.9500

C(135)-C(136)	1.477(2)
C(136)-N(6)	1.3534(19)
C(136)-C(137)	1.390(2)
C(137)-C(138)	1.379(2)
C(137)-H(137)	0.9500
C(138)-C(139)	1.383(3)
C(138)-C(142)	1.507(2)
C(142)-F(34B)	1.270(9)
C(142)-F(135)	1.287(7)
C(142)-F(36B)	1.331(7)
C(142)-F(35B)	1.335(10)
C(142)-F(136)	1.336(4)
C(142)-F(134)	1.342(6)
C(139)-C(140)	1.380(2)
C(139)-H(139)	0.9500
C(140)-N(6)	1.344(2)
C(140)-H(140)	0.9500
O(1S)-C(11S)	1.311(17)
O(1S)-H(1S)	0.8400
C(11S)-C(12S)	1.585(16)
C(11S)-H(11A)	0.9900
C(11S)-H(11B)	0.9900
C(12S)-H(12A)	0.9800
C(12S)-H(12B)	0.9800

C(12S)-H(12C)	0.9800
O(2S)-C(21S)	1.472(18)
O(2S)-H(2S)	0.8400
C(21S)-C(22S)	1.520(17)
C(21S)-H(21A)	0.9900
C(21S)-H(21B)	0.9900
C(22S)-H(22A)	0.9800
C(22S)-H(22B)	0.9800
C(22S)-H(22C)	0.9800
O(3S)-C(31S)	1.32(3)
O(3S)-H(3S)	0.8400
C(31S)-C(32S)	1.536(17)
C(31S)-H(31A)	0.9900
C(31S)-H(31B)	0.9900
C(32S)-H(32A)	0.9800
C(32S)-H(32B)	0.9800
C(32S)-H(32C)	0.9800

P(1)-N(7)-P(2)	140.07(9)
N(7)-P(1)-C(51B)	117.5(4)
N(7)-P(1)-C(161)	114.94(8)
C(51B)-P(1)-C(161)	106.7(3)
N(7)-P(1)-C(171)	106.50(8)
C(51B)-P(1)-C(171)	102.7(3)

C(161)-P(1)-C(171)	107.36(8)
N(7)-P(1)-C(151)	111.45(16)
C(161)-P(1)-C(151)	107.53(16)
C(171)-P(1)-C(151)	108.86(16)
C(156)-C(151)-C(152)	119.3(4)
C(156)-C(151)-P(1)	120.3(3)
C(152)-C(151)-P(1)	120.4(3)
C(153)-C(152)-C(151)	119.6(4)
C(153)-C(152)-H(152)	120.2
C(151)-C(152)-H(152)	120.2
C(154)-C(153)-C(152)	120.7(4)
C(154)-C(153)-H(153)	119.7
C(152)-C(153)-H(153)	119.7
C(153)-C(154)-C(155)	119.8(5)
C(153)-C(154)-H(154)	120.1
C(155)-C(154)-H(154)	120.1
C(156)-C(155)-C(154)	119.5(4)
C(156)-C(155)-H(155)	120.3
C(154)-C(155)-H(155)	120.3
C(151)-C(156)-C(155)	120.7(4)
C(151)-C(156)-H(156)	119.6
C(155)-C(156)-H(156)	119.6
C(56B)-C(51B)-C(52B)	121.7(10)
C(56B)-C(51B)-P(1)	117.5(8)

C(52B)-C(51B)-P(1)	120.8(8)
C(51B)-C(52B)-C(53B)	119.1(8)
C(51B)-C(52B)-H(52B)	120.4
C(53B)-C(52B)-H(52B)	120.4
C(54B)-C(53B)-C(52B)	119.5(8)
C(54B)-C(53B)-H(53B)	120.3
C(52B)-C(53B)-H(53B)	120.3
C(53B)-C(54B)-C(55B)	122.0(10)
C(53B)-C(54B)-H(54B)	119.0
C(55B)-C(54B)-H(54B)	119.0
C(56B)-C(55B)-C(54B)	116.0(9)
C(56B)-C(55B)-H(55B)	122.0
C(54B)-C(55B)-H(55B)	122.0
C(51B)-C(56B)-C(55B)	120.5(9)
C(51B)-C(56B)-H(56B)	119.8
C(55B)-C(56B)-H(56B)	119.8
C(166)-C(161)-C(162)	120.03(17)
C(166)-C(161)-P(1)	120.38(13)
C(162)-C(161)-P(1)	119.44(15)
C(163)-C(162)-C(161)	119.5(2)
C(163)-C(162)-H(162)	120.2
C(161)-C(162)-H(162)	120.2
C(164)-C(163)-C(162)	120.30(19)
C(164)-C(163)-H(163)	119.8

C(162)-C(163)-H(163)	119.8
C(163)-C(164)-C(165)	120.70(19)
C(163)-C(164)-H(164)	119.6
C(165)-C(164)-H(164)	119.6
C(164)-C(165)-C(166)	119.6(2)
C(164)-C(165)-H(165)	120.2
C(166)-C(165)-H(165)	120.2
C(161)-C(166)-C(165)	119.82(19)
C(161)-C(166)-H(166)	120.1
C(165)-C(166)-H(166)	120.1
C(176)-C(171)-C(172)	119.92(17)
C(176)-C(171)-P(1)	119.60(13)
C(172)-C(171)-P(1)	120.43(16)
C(173)-C(172)-C(171)	119.6(2)
C(173)-C(172)-H(172)	120.2
C(171)-C(172)-H(172)	120.2
C(174)-C(173)-C(172)	120.2(2)
C(174)-C(173)-H(173)	119.9
C(172)-C(173)-H(173)	119.9
C(173)-C(174)-C(175)	120.48(19)
C(173)-C(174)-H(174)	119.8
C(175)-C(174)-H(174)	119.8
C(174)-C(175)-C(176)	119.78(19)
C(174)-C(175)-H(175)	120.1

C(176)-C(175)-H(175)	120.1
C(175)-C(176)-C(171)	119.99(17)
C(175)-C(176)-H(176)	120.0
C(171)-C(176)-H(176)	120.0
N(7)-P(2)-C(201)	115.59(7)
N(7)-P(2)-C(191)	109.14(8)
C(201)-P(2)-C(191)	108.21(7)
N(7)-P(2)-C(181)	109.29(7)
C(201)-P(2)-C(181)	106.93(7)
C(191)-P(2)-C(181)	107.38(7)
C(182)-C(181)-C(186)	119.55(14)
C(182)-C(181)-P(2)	120.57(12)
C(186)-C(181)-P(2)	119.86(11)
C(183)-C(182)-C(181)	119.82(16)
C(183)-C(182)-H(182)	120.1
C(181)-C(182)-H(182)	120.1
C(184)-C(183)-C(182)	120.34(16)
C(184)-C(183)-H(183)	119.8
C(182)-C(183)-H(183)	119.8
C(183)-C(184)-C(185)	120.28(16)
C(183)-C(184)-H(184)	119.9
C(185)-C(184)-H(184)	119.9
C(186)-C(185)-C(184)	119.89(16)
C(186)-C(185)-H(185)	120.1

C(184)-C(185)-H(185)	120.1
C(185)-C(186)-C(181)	120.12(15)
C(185)-C(186)-H(186)	119.9
C(181)-C(186)-H(186)	119.9
C(196)-C(191)-C(192)	119.89(14)
C(196)-C(191)-P(2)	121.64(12)
C(192)-C(191)-P(2)	118.41(12)
C(193)-C(192)-C(191)	119.80(16)
C(193)-C(192)-H(192)	120.1
C(191)-C(192)-H(192)	120.1
C(194)-C(193)-C(192)	120.10(16)
C(194)-C(193)-H(193)	119.9
C(192)-C(193)-H(193)	119.9
C(193)-C(194)-C(195)	120.51(16)
C(193)-C(194)-H(194)	119.7
C(195)-C(194)-H(194)	119.7
C(194)-C(195)-C(196)	119.95(17)
C(194)-C(195)-H(195)	120.0
C(196)-C(195)-H(195)	120.0
C(195)-C(196)-C(191)	119.74(16)
C(195)-C(196)-H(196)	120.1
C(191)-C(196)-H(196)	120.1
C(206)-C(201)-C(202)	119.74(14)
C(206)-C(201)-P(2)	120.25(12)

C(202)-C(201)-P(2)	119.90(13)
C(203)-C(202)-C(201)	119.76(17)
C(203)-C(202)-H(202)	120.1
C(201)-C(202)-H(202)	120.1
C(204)-C(203)-C(202)	120.32(17)
C(204)-C(203)-H(203)	119.8
C(202)-C(203)-H(203)	119.8
C(205)-C(204)-C(203)	120.07(16)
C(205)-C(204)-H(204)	120.0
C(203)-C(204)-H(204)	120.0
C(204)-C(205)-C(206)	120.14(17)
C(204)-C(205)-H(205)	119.9
C(206)-C(205)-H(205)	119.9
C(205)-C(206)-C(201)	119.95(16)
C(205)-C(206)-H(206)	120.0
C(201)-C(206)-H(206)	120.0
P(4)-N(8)-P(3)	142.43(10)
N(8)-P(3)-C(221)	113.61(8)
N(8)-P(3)-C(231)	106.67(9)
C(221)-P(3)-C(231)	107.66(9)
N(8)-P(3)-C(211)	113.00(9)
C(221)-P(3)-C(211)	107.92(8)
C(231)-P(3)-C(211)	107.71(8)
C(216)-C(211)-C(212)	119.73(17)

C(216)-C(211)-P(3)	120.89(14)
C(212)-C(211)-P(3)	119.38(14)
C(211)-C(212)-C(213)	119.9(2)
C(211)-C(212)-H(212)	120.1
C(213)-C(212)-H(212)	120.1
C(214)-C(213)-C(212)	119.9(2)
C(214)-C(213)-H(213)	120.0
C(212)-C(213)-H(213)	120.0
C(215)-C(214)-C(213)	120.28(18)
C(215)-C(214)-H(214)	119.9
C(213)-C(214)-H(214)	119.9
C(214)-C(215)-C(216)	120.3(2)
C(214)-C(215)-H(215)	119.8
C(216)-C(215)-H(215)	119.8
C(211)-C(216)-C(215)	119.9(2)
C(211)-C(216)-H(216)	120.1
C(215)-C(216)-H(216)	120.1
C(222)-C(221)-C(226)	119.77(17)
C(222)-C(221)-P(3)	123.18(14)
C(226)-C(221)-P(3)	117.06(13)
C(221)-C(222)-C(223)	119.89(18)
C(221)-C(222)-H(222)	120.1
C(223)-C(222)-H(222)	120.1
C(224)-C(223)-C(222)	119.9(2)

C(224)-C(223)-H(223)	120.0
C(222)-C(223)-H(223)	120.0
C(223)-C(224)-C(225)	120.25(18)
C(223)-C(224)-H(224)	119.9
C(225)-C(224)-H(224)	119.9
C(226)-C(225)-C(224)	120.14(17)
C(226)-C(225)-H(225)	119.9
C(224)-C(225)-H(225)	119.9
C(225)-C(226)-C(221)	119.95(17)
C(225)-C(226)-H(226)	120.0
C(221)-C(226)-H(226)	120.0
C(232)-C(231)-C(236)	120.26(18)
C(232)-C(231)-P(3)	120.65(14)
C(236)-C(231)-P(3)	119.05(16)
C(233)-C(232)-C(231)	119.7(2)
C(233)-C(232)-H(232)	120.1
C(231)-C(232)-H(232)	120.1
C(234)-C(233)-C(232)	119.9(2)
C(234)-C(233)-H(233)	120.1
C(232)-C(233)-H(233)	120.1
C(235)-C(234)-C(233)	120.8(2)
C(235)-C(234)-H(234)	119.6
C(233)-C(234)-H(234)	119.6
C(234)-C(235)-C(236)	120.2(2)

C(234)-C(235)-H(235)	119.9
C(236)-C(235)-H(235)	119.9
C(231)-C(236)-C(235)	119.2(2)
C(231)-C(236)-H(236)	120.4
C(235)-C(236)-H(236)	120.4
N(8)-P(4)-C(251)	110.02(9)
N(8)-P(4)-C(261)	116.07(8)
C(251)-P(4)-C(261)	106.42(8)
N(8)-P(4)-C(241)	107.25(8)
C(251)-P(4)-C(241)	110.30(9)
C(261)-P(4)-C(241)	106.70(8)
C(242)-C(241)-C(246)	119.73(16)
C(242)-C(241)-P(4)	118.90(13)
C(246)-C(241)-P(4)	121.37(14)
C(243)-C(242)-C(241)	120.00(18)
C(243)-C(242)-H(242)	120.0
C(241)-C(242)-H(242)	120.0
C(244)-C(243)-C(242)	120.16(19)
C(244)-C(243)-H(243)	119.9
C(242)-C(243)-H(243)	119.9
C(243)-C(244)-C(245)	120.19(17)
C(243)-C(244)-H(244)	119.9
C(245)-C(244)-H(244)	119.9
C(244)-C(245)-C(246)	120.48(18)

C(244)-C(245)-H(245)	119.8
C(246)-C(245)-H(245)	119.8
C(245)-C(246)-C(241)	119.43(18)
C(245)-C(246)-H(246)	120.3
C(241)-C(246)-H(246)	120.3
C(252)-C(251)-C(256)	119.86(19)
C(252)-C(251)-P(4)	121.13(15)
C(256)-C(251)-P(4)	118.91(17)
C(251)-C(252)-C(253)	119.9(2)
C(251)-C(252)-H(252)	120.0
C(253)-C(252)-H(252)	120.0
C(254)-C(253)-C(252)	119.6(2)
C(254)-C(253)-H(253)	120.2
C(252)-C(253)-H(253)	120.2
C(255)-C(254)-C(253)	121.0(2)
C(255)-C(254)-H(254)	119.5
C(253)-C(254)-H(254)	119.5
C(254)-C(255)-C(256)	120.2(2)
C(254)-C(255)-H(255)	119.9
C(256)-C(255)-H(255)	119.9
C(251)-C(256)-C(255)	119.5(2)
C(251)-C(256)-H(256)	120.3
C(255)-C(256)-H(256)	120.3
C(262)-C(261)-C(266)	119.35(16)

C(262)-C(261)-P(4)	121.52(13)
C(266)-C(261)-P(4)	119.02(13)
C(263)-C(262)-C(261)	119.86(17)
C(263)-C(262)-H(262)	120.1
C(261)-C(262)-H(262)	120.1
C(264)-C(263)-C(262)	120.53(18)
C(264)-C(263)-H(263)	119.7
C(262)-C(263)-H(263)	119.7
C(263)-C(264)-C(265)	120.09(18)
C(263)-C(264)-H(264)	120.0
C(265)-C(264)-H(264)	120.0
C(264)-C(265)-C(266)	119.93(17)
C(264)-C(265)-H(265)	120.0
C(266)-C(265)-H(265)	120.0
C(265)-C(266)-C(261)	120.21(17)
C(265)-C(266)-H(266)	119.9
C(261)-C(266)-H(266)	119.9
C(3)-Ru(1)-C(2)	89.82(6)
C(3)-Ru(1)-C(4)	90.89(6)
C(2)-Ru(1)-C(4)	95.16(6)
C(3)-Ru(1)-C(1)	91.81(6)
C(2)-Ru(1)-C(1)	91.23(6)
C(4)-Ru(1)-C(1)	173.07(6)
C(3)-Ru(1)-N(6)	173.07(5)

C(2)-Ru(1)-N(6)	97.09(6)
C(4)-Ru(1)-N(6)	87.97(6)
C(1)-Ru(1)-N(6)	88.57(6)
C(3)-Ru(1)-N(5)	95.39(6)
C(2)-Ru(1)-N(5)	173.98(5)
C(4)-Ru(1)-N(5)	87.79(6)
C(1)-Ru(1)-N(5)	85.60(6)
N(6)-Ru(1)-N(5)	77.74(5)
N(1)-C(1)-Ru(1)	170.03(13)
C(1)-N(1)-B(1)	178.37(15)
N(1)-B(1)-C(31)	102.99(12)
N(1)-B(1)-C(11)	106.78(12)
C(31)-B(1)-C(11)	114.19(13)
N(1)-B(1)-C(21)	109.46(13)
C(31)-B(1)-C(21)	116.03(13)
C(11)-B(1)-C(21)	106.93(12)
C(12)-C(11)-C(16)	113.69(14)
C(12)-C(11)-B(1)	120.88(14)
C(16)-C(11)-B(1)	125.36(14)
F(12)-C(12)-C(13)	115.56(14)
F(12)-C(12)-C(11)	119.88(14)
C(13)-C(12)-C(11)	124.55(15)
F(13)-C(13)-C(14)	119.89(15)
F(13)-C(13)-C(12)	121.08(16)

C(14)-C(13)-C(12)	119.02(15)
F(14)-C(14)-C(15)	120.79(16)
F(14)-C(14)-C(13)	119.86(16)
C(15)-C(14)-C(13)	119.34(15)
F(15)-C(15)-C(14)	119.71(15)
F(15)-C(15)-C(16)	120.67(15)
C(14)-C(15)-C(16)	119.59(15)
F(16)-C(16)-C(15)	115.76(14)
F(16)-C(16)-C(11)	120.55(14)
C(15)-C(16)-C(11)	123.68(15)
C(26)-C(21)-C(22)	113.12(15)
C(26)-C(21)-B(1)	126.92(14)
C(22)-C(21)-B(1)	119.87(14)
F(22)-C(22)-C(23)	115.97(15)
F(22)-C(22)-C(21)	119.40(15)
C(23)-C(22)-C(21)	124.62(17)
F(23)-C(23)-C(24)	120.04(17)
F(23)-C(23)-C(22)	120.39(19)
C(24)-C(23)-C(22)	119.58(17)
F(24)-C(24)-C(25)	120.98(19)
F(24)-C(24)-C(23)	120.39(19)
C(25)-C(24)-C(23)	118.63(16)
F(25)-C(25)-C(24)	120.01(17)
F(25)-C(25)-C(26)	119.97(18)

C(24)-C(25)-C(26)	120.02(17)
F(26)-C(26)-C(21)	121.21(15)
F(26)-C(26)-C(25)	114.77(16)
C(21)-C(26)-C(25)	124.01(16)
C(32)-C(31)-C(36)	113.95(14)
C(32)-C(31)-B(1)	125.82(14)
C(36)-C(31)-B(1)	119.75(13)
F(32)-C(32)-C(33)	115.56(14)
F(32)-C(32)-C(31)	120.42(14)
C(33)-C(32)-C(31)	124.02(15)
F(33)-C(33)-C(34)	119.99(16)
F(33)-C(33)-C(32)	120.75(16)
C(34)-C(33)-C(32)	119.26(16)
F(34)-C(34)-C(33)	119.91(17)
F(34)-C(34)-C(35)	120.60(17)
C(33)-C(34)-C(35)	119.49(16)
F(35)-C(35)-C(34)	119.82(16)
F(35)-C(35)-C(36)	120.95(16)
C(34)-C(35)-C(36)	119.24(16)
F(36)-C(36)-C(35)	116.39(15)
F(36)-C(36)-C(31)	119.59(14)
C(35)-C(36)-C(31)	124.01(15)
N(2)-C(2)-Ru(1)	176.87(13)
C(2)-N(2)-B(2)	171.18(14)

N(2)-B(2)-C(51)	108.03(12)
N(2)-B(2)-C(61)	104.28(12)
C(51)-B(2)-C(61)	109.69(12)
N(2)-B(2)-C(41)	107.00(12)
C(51)-B(2)-C(41)	112.71(12)
C(61)-B(2)-C(41)	114.55(12)
C(46)-C(41)-C(42)	113.96(13)
C(46)-C(41)-B(2)	125.04(13)
C(42)-C(41)-B(2)	121.00(13)
F(42)-C(42)-C(43)	116.20(14)
F(42)-C(42)-C(41)	119.79(13)
C(43)-C(42)-C(41)	124.00(14)
F(43)-C(43)-C(44)	119.42(14)
F(43)-C(43)-C(42)	120.99(15)
C(44)-C(43)-C(42)	119.60(14)
F(44)-C(44)-C(45)	120.26(15)
F(44)-C(44)-C(43)	120.71(15)
C(45)-C(44)-C(43)	119.03(14)
F(45)-C(45)-C(44)	119.66(13)
F(45)-C(45)-C(46)	120.56(14)
C(44)-C(45)-C(46)	119.77(14)
F(46)-C(46)-C(45)	115.10(13)
F(46)-C(46)-C(41)	121.27(13)
C(45)-C(46)-C(41)	123.62(14)

C(52)-C(51)-C(56)	113.64(15)
C(52)-C(51)-B(2)	122.03(14)
C(56)-C(51)-B(2)	124.32(14)
F(52)-C(52)-C(53)	116.23(16)
F(52)-C(52)-C(51)	119.84(14)
C(53)-C(52)-C(51)	123.88(17)
F(53)-C(53)-C(54)	120.45(17)
F(53)-C(53)-C(52)	120.03(19)
C(54)-C(53)-C(52)	119.50(18)
F(54)-C(54)-C(55)	120.4(2)
F(54)-C(54)-C(53)	120.2(2)
C(55)-C(54)-C(53)	119.38(17)
F(55)-C(55)-C(54)	119.72(18)
F(55)-C(55)-C(56)	120.6(2)
C(54)-C(55)-C(56)	119.64(18)
F(56)-C(56)-C(55)	114.93(16)
F(56)-C(56)-C(51)	121.15(15)
C(55)-C(56)-C(51)	123.93(18)
C(66)-C(61)-C(62)	114.07(14)
C(66)-C(61)-B(2)	126.81(13)
C(62)-C(61)-B(2)	119.05(14)
F(62)-C(62)-C(63)	115.98(15)
F(62)-C(62)-C(61)	119.90(14)
C(63)-C(62)-C(61)	124.10(17)

F(63)-C(63)-C(64)	120.14(16)
F(63)-C(63)-C(62)	120.59(18)
C(64)-C(63)-C(62)	119.27(17)
F(64)-C(64)-C(65)	120.4(2)
F(64)-C(64)-C(63)	120.30(19)
C(65)-C(64)-C(63)	119.33(16)
F(65)-C(65)-C(64)	120.30(16)
F(65)-C(65)-C(66)	120.03(17)
C(64)-C(65)-C(66)	119.67(18)
F(66)-C(66)-C(61)	121.12(14)
F(66)-C(66)-C(65)	115.31(15)
C(61)-C(66)-C(65)	123.56(16)
N(3)-C(3)-Ru(1)	175.87(13)
C(3)-N(3)-B(3)	175.27(14)
N(3)-B(3)-C(91)	104.58(12)
N(3)-B(3)-C(71)	105.47(15)
C(91)-B(3)-C(71)	115.06(15)
N(3)-B(3)-C(71A)	114.3(4)
C(91)-B(3)-C(71A)	109.1(4)
N(3)-B(3)-C(81)	107.77(12)
C(91)-B(3)-C(81)	114.15(12)
C(71)-B(3)-C(81)	109.10(14)
C(71A)-B(3)-C(81)	107.1(3)
C(76)-C(71)-C(72)	113.7(2)

C(76)-C(71)-B(3)	125.9(2)
C(72)-C(71)-B(3)	120.0(2)
F(72)-C(72)-C(73)	116.1(2)
F(72)-C(72)-C(71)	120.2(2)
C(73)-C(72)-C(71)	123.6(3)
F(73)-C(73)-C(74)	119.7(2)
F(73)-C(73)-C(72)	120.5(3)
C(74)-C(73)-C(72)	119.8(2)
F(74)-C(74)-C(75)	120.5(3)
F(74)-C(74)-C(73)	120.1(3)
C(75)-C(74)-C(73)	119.3(2)
F(75)-C(75)-C(74)	120.9(3)
F(75)-C(75)-C(76)	119.9(3)
C(74)-C(75)-C(76)	119.2(2)
F(76)-C(76)-C(71)	120.3(2)
F(76)-C(76)-C(75)	115.4(2)
C(71)-C(76)-C(75)	124.3(3)
C(72A)-C(71A)-C(76A)	114.7(10)
C(72A)-C(71A)-B(3)	121.9(9)
C(76A)-C(71A)-B(3)	123.3(9)
F(72A)-C(72A)-C(71A)	120.0(11)
F(72A)-C(72A)-C(73A)	115.3(10)
C(71A)-C(72A)-C(73A)	124.6(10)
F(73A)-C(73A)-C(74A)	123.0(10)

F(73A)-C(73A)-C(72A)	120.0(10)
C(74A)-C(73A)-C(72A)	117.0(9)
C(73A)-C(74A)-C(75A)	121.8(9)
C(73A)-C(74A)-F(74A)	119.2(10)
C(75A)-C(74A)-F(74A)	119.0(10)
C(74A)-C(75A)-F(75A)	121.8(9)
C(74A)-C(75A)-C(76A)	119.8(9)
F(75A)-C(75A)-C(76A)	118.4(9)
F(76A)-C(76A)-C(71A)	120.6(9)
F(76A)-C(76A)-C(75A)	117.2(9)
C(71A)-C(76A)-C(75A)	121.9(10)
C(82)-C(81)-C(86)	113.42(14)
C(82)-C(81)-B(3)	124.96(13)
C(86)-C(81)-B(3)	121.61(13)
F(82)-C(82)-C(83)	114.76(13)
F(82)-C(82)-C(81)	121.16(14)
C(83)-C(82)-C(81)	124.08(15)
F(83)-C(83)-C(84)	120.11(14)
F(83)-C(83)-C(82)	120.05(15)
C(84)-C(83)-C(82)	119.84(14)
F(84)-C(84)-C(83)	120.94(15)
F(84)-C(84)-C(85)	120.31(16)
C(83)-C(84)-C(85)	118.75(14)
F(85)-C(85)-C(84)	119.69(14)

F(85)-C(85)-C(86)	120.65(14)
C(84)-C(85)-C(86)	119.65(15)
F(86)-C(86)-C(85)	115.79(14)
F(86)-C(86)-C(81)	120.00(13)
C(85)-C(86)-C(81)	124.19(14)
C(92)-C(91)-C(96)	113.74(13)
C(92)-C(91)-B(3)	127.37(13)
C(96)-C(91)-B(3)	118.83(13)
F(92)-C(92)-C(91)	120.79(14)
F(92)-C(92)-C(93)	115.95(14)
C(91)-C(92)-C(93)	123.26(15)
F(93)-C(93)-C(94)	119.36(14)
F(93)-C(93)-C(92)	120.43(15)
C(94)-C(93)-C(92)	120.21(15)
F(94)-C(94)-C(93)	120.54(15)
F(94)-C(94)-C(95)	120.51(15)
C(93)-C(94)-C(95)	118.95(14)
F(95)-C(95)-C(94)	120.36(13)
F(95)-C(95)-C(96)	120.49(14)
C(94)-C(95)-C(96)	119.14(14)
F(96)-C(96)-C(95)	116.13(13)
F(96)-C(96)-C(91)	119.18(13)
C(95)-C(96)-C(91)	124.68(14)
N(4)-C(4)-Ru(1)	169.58(13)

C(4)-N(4)-B(4)	174.77(15)
N(4)-B(4)-C(01B)	102.8(4)
N(4)-B(4)-C(121)	105.41(13)
C(01B)-B(4)-C(121)	120.6(2)
N(4)-B(4)-C(111)	104.52(12)
C(01B)-B(4)-C(111)	107.0(3)
C(121)-B(4)-C(111)	114.61(14)
N(4)-B(4)-C(101)	110.2(2)
C(121)-B(4)-C(101)	115.49(17)
C(111)-B(4)-C(101)	106.10(19)
C(102)-C(101)-C(106)	113.2(4)
C(102)-C(101)-B(4)	121.0(4)
C(106)-C(101)-B(4)	125.5(4)
F(102)-C(102)-C(103)	116.8(3)
F(102)-C(102)-C(101)	119.2(3)
C(103)-C(102)-C(101)	124.0(4)
F(103)-C(103)-C(104)	119.8(3)
F(103)-C(103)-C(102)	120.3(4)
C(104)-C(103)-C(102)	119.9(3)
F(104)-C(104)-C(105)	120.2(4)
F(104)-C(104)-C(103)	120.6(4)
C(105)-C(104)-C(103)	119.1(4)
F(105)-C(105)-C(104)	120.9(4)
F(105)-C(105)-C(106)	119.8(5)

C(104)-C(105)-C(106)	119.3(4)
F(106)-C(106)-C(101)	121.4(5)
F(106)-C(106)-C(105)	114.4(4)
C(101)-C(106)-C(105)	124.2(5)
C(06B)-C(01B)-C(02B)	113.4(8)
C(06B)-C(01B)-B(4)	126.2(8)
C(02B)-C(01B)-B(4)	120.4(7)
F(02B)-C(02B)-C(03B)	116.3(6)
F(02B)-C(02B)-C(01B)	120.8(7)
C(03B)-C(02B)-C(01B)	122.9(7)
F(03B)-C(03B)-C(04B)	121.5(7)
F(03B)-C(03B)-C(02B)	119.5(7)
C(04B)-C(03B)-C(02B)	119.0(6)
C(03B)-C(04B)-F(04B)	118.7(8)
C(03B)-C(04B)-C(05B)	119.1(8)
F(04B)-C(04B)-C(05B)	122.1(8)
F(05B)-C(05B)-C(04B)	118.9(8)
F(05B)-C(05B)-C(06B)	119.9(8)
C(04B)-C(05B)-C(06B)	121.1(9)
F(06B)-C(06B)-C(05B)	117.5(8)
F(06B)-C(06B)-C(01B)	118.4(8)
C(05B)-C(06B)-C(01B)	124.0(9)
C(116)-C(111)-C(112)	114.04(16)
C(116)-C(111)-B(4)	126.00(16)

C(112)-C(111)-B(4)	119.89(15)
F(112)-C(112)-C(113)	115.80(16)
F(112)-C(112)-C(111)	119.80(15)
C(113)-C(112)-C(111)	124.39(18)
F(113)-C(113)-C(114)	120.41(17)
F(113)-C(113)-C(112)	120.65(18)
C(114)-C(113)-C(112)	118.94(18)
F(114)-C(114)-C(115)	119.94(19)
F(114)-C(114)-C(113)	120.46(19)
C(115)-C(114)-C(113)	119.60(17)
F(115)-C(115)-C(114)	120.01(17)
F(115)-C(115)-C(116)	120.36(19)
C(114)-C(115)-C(116)	119.62(18)
F(116)-C(116)-C(111)	120.92(16)
F(116)-C(116)-C(115)	115.69(17)
C(111)-C(116)-C(115)	123.39(18)
C(126)-C(121)-C(122)	113.71(15)
C(126)-C(121)-B(4)	126.08(14)
C(122)-C(121)-B(4)	120.16(14)
F(122)-C(122)-C(123)	116.36(14)
F(122)-C(122)-C(121)	119.46(15)
C(123)-C(122)-C(121)	124.16(15)
F(123)-C(123)-C(122)	121.33(15)
F(123)-C(123)-C(124)	119.25(16)

C(122)-C(123)-C(124)	119.42(15)
F(124)-C(124)-C(125)	121.22(16)
F(124)-C(124)-C(123)	119.99(16)
C(125)-C(124)-C(123)	118.78(16)
F(125)-C(125)-C(124)	119.53(17)
F(125)-C(125)-C(126)	120.54(17)
C(124)-C(125)-C(126)	119.93(16)
F(126)-C(126)-C(125)	115.69(15)
F(126)-C(126)-C(121)	120.33(16)
C(125)-C(126)-C(121)	123.98(16)
C(131)-N(5)-C(135)	119.33(13)
C(131)-N(5)-Ru(1)	125.08(10)
C(135)-N(5)-Ru(1)	115.28(10)
N(5)-C(131)-C(132)	122.61(15)
N(5)-C(131)-H(131)	118.7
C(132)-C(131)-H(131)	118.7
C(133)-C(132)-C(131)	117.97(15)
C(133)-C(132)-H(132)	121.0
C(131)-C(132)-H(132)	121.0
C(134)-C(133)-C(132)	120.04(14)
C(134)-C(133)-C(141)	120.95(15)
C(132)-C(133)-C(141)	118.97(15)
F(131)-C(141)-F(132)	111.0(9)
F(33B)-C(141)-F(32B)	104.5(9)

F(33B)-C(141)-F(31B)	109.4(8)
F(32B)-C(141)-F(31B)	102.6(9)
F(131)-C(141)-F(133)	104.4(9)
F(132)-C(141)-F(133)	108.5(7)
F(131)-C(141)-C(133)	111.7(6)
F(33B)-C(141)-C(133)	116.7(9)
F(132)-C(141)-C(133)	113.1(5)
F(32B)-C(141)-C(133)	111.9(7)
F(31B)-C(141)-C(133)	110.7(7)
F(133)-C(141)-C(133)	107.7(8)
C(133)-C(134)-C(135)	118.96(14)
C(133)-C(134)-H(134)	120.5
C(135)-C(134)-H(134)	120.5
N(5)-C(135)-C(134)	120.94(14)
N(5)-C(135)-C(136)	115.63(13)
C(134)-C(135)-C(136)	123.39(14)
N(6)-C(136)-C(137)	121.34(14)
N(6)-C(136)-C(135)	115.23(13)
C(137)-C(136)-C(135)	123.43(14)
C(138)-C(137)-C(136)	119.03(15)
C(138)-C(137)-H(137)	120.5
C(136)-C(137)-H(137)	120.5
C(137)-C(138)-C(139)	119.70(15)
C(137)-C(138)-C(142)	120.70(16)

C(139)-C(138)-C(142)	119.59(17)
F(34B)-C(142)-F(36B)	113.8(7)
F(34B)-C(142)-F(35B)	109.6(10)
F(36B)-C(142)-F(35B)	101.9(8)
F(135)-C(142)-F(136)	109.4(5)
F(135)-C(142)-F(134)	105.3(7)
F(136)-C(142)-F(134)	102.9(4)
F(34B)-C(142)-C(138)	113.8(6)
F(135)-C(142)-C(138)	115.1(5)
F(36B)-C(142)-C(138)	109.2(4)
F(35B)-C(142)-C(138)	107.8(7)
F(136)-C(142)-C(138)	113.0(3)
F(134)-C(142)-C(138)	110.3(4)
C(140)-C(139)-C(138)	118.56(16)
C(140)-C(139)-H(139)	120.7
C(138)-C(139)-H(139)	120.7
N(6)-C(140)-C(139)	122.45(15)
N(6)-C(140)-H(140)	118.8
C(139)-C(140)-H(140)	118.8
C(140)-N(6)-C(136)	118.91(13)
C(140)-N(6)-Ru(1)	125.46(10)
C(136)-N(6)-Ru(1)	115.64(10)
C(11S)-O(1S)-H(1S)	109.5
O(1S)-C(11S)-C(12S)	109.5(16)

O(1S)-C(11S)-H(11A)	109.8
C(12S)-C(11S)-H(11A)	109.8
O(1S)-C(11S)-H(11B)	109.8
C(12S)-C(11S)-H(11B)	109.8
H(11A)-C(11S)-H(11B)	108.2
C(11S)-C(12S)-H(12A)	109.5
C(11S)-C(12S)-H(12B)	109.5
H(12A)-C(12S)-H(12B)	109.5
C(11S)-C(12S)-H(12C)	109.5
H(12A)-C(12S)-H(12C)	109.5
H(12B)-C(12S)-H(12C)	109.5
C(21S)-O(2S)-H(2S)	109.5
O(2S)-C(21S)-C(22S)	108.2(16)
O(2S)-C(21S)-H(21A)	110.1
C(22S)-C(21S)-H(21A)	110.1
O(2S)-C(21S)-H(21B)	110.1
C(22S)-C(21S)-H(21B)	110.1
H(21A)-C(21S)-H(21B)	108.4
C(21S)-C(22S)-H(22A)	109.5
C(21S)-C(22S)-H(22B)	109.5
H(22A)-C(22S)-H(22B)	109.5
C(21S)-C(22S)-H(22C)	109.5
H(22A)-C(22S)-H(22C)	109.5
H(22B)-C(22S)-H(22C)	109.5

C(31S)-O(3S)-H(3S)	109.5
O(3S)-C(31S)-C(32S)	111.4(19)
O(3S)-C(31S)-H(31A)	109.4
C(32S)-C(31S)-H(31A)	109.4
O(3S)-C(31S)-H(31B)	109.4
C(32S)-C(31S)-H(31B)	109.4
H(31A)-C(31S)-H(31B)	108.0
C(31S)-C(32S)-H(32A)	109.5
C(31S)-C(32S)-H(32B)	109.5
H(32A)-C(32S)-H(32B)	109.5
C(31S)-C(32S)-H(32C)	109.5
H(32A)-C(32S)-H(32C)	109.5
H(32B)-C(32S)-H(32C)	109.5

Symmetry transformations used to generate equivalent atoms:

Table 4. Anisotropic displacement parameters ($Å^2 x\ 10^3$) for D19108. The anisotropic displacement factor exponent takes the form: $-2\pi^2[\ h^2\ a^{*2}U^{11} + ... + 2\ h\ k\ a^*\ b^*\ U^{12}\ ]$

	U^{11}	U^{22}	U^{33}	U^{23}	U^{13}	U^{12}
N(7)	21(1)	19(1)	22(1)	-7(1)	2(1)	-8(1)
P(1)	22(1)	24(1)	21(1)	-6(1)	0(1)	-10(1)
C(151)	18(2)	33(2)	40(2)	-5(2)	-1(2)	-13(1)
C(152)	28(2)	46(2)	70(3)	9(2)	-6(2)	-17(2)
C(153)	26(2)	73(3)	106(4)	15(3)	-9(2)	-25(2)
C(154)	30(2)	68(3)	116(4)	2(3)	-23(2)	-8(2)
C(155)	33(2)	71(3)	46(2)	-1(2)	-13(2)	-13(2)
C(156)	24(2)	43(2)	28(2)	-6(1)	-4(1)	-10(1)
C(51B)	39(5)	44(5)	31(5)	3(4)	-13(4)	-16(3)
C(52B)	32(3)	44(4)	57(5)	4(3)	-18(3)	-19(3)
C(53B)	28(3)	51(4)	66(5)	3(4)	-14(3)	-20(3)
C(54B)	28(4)	65(6)	106(6)	1(6)	-39(4)	-17(4)
C(55B)	34(4)	40(4)	105(7)	-13(5)	-30(5)	3(3)
C(56B)	34(4)	30(3)	78(6)	-11(4)	-19(5)	-12(3)
C(161)	28(1)	26(1)	22(1)	-7(1)	3(1)	-15(1)
C(162)	34(1)	44(1)	31(1)	-9(1)	10(1)	-10(1)
C(163)	42(1)	56(1)	31(1)	-18(1)	15(1)	-21(1)
C(164)	50(1)	61(1)	21(1)	-13(1)	3(1)	-36(1)
C(165)	53(1)	51(1)	26(1)	-8(1)	-12(1)	-12(1)

C(166)	40(1)	38(1)	24(1)	-11(1)	-4(1)	-5(1)
C(171)	38(1)	23(1)	22(1)	-7(1)	-6(1)	-11(1)
C(172)	109(2)	37(1)	36(1)	-18(1)	16(1)	-41(1)
C(173)	142(3)	32(1)	47(1)	-19(1)	9(2)	-39(2)
C(174)	83(2)	28(1)	39(1)	-18(1)	-17(1)	0(1)
C(175)	36(1)	32(1)	30(1)	-12(1)	-13(1)	6(1)
C(176)	25(1)	24(1)	28(1)	-6(1)	-9(1)	-1(1)
P(2)	13(1)	17(1)	15(1)	-5(1)	0(1)	-3(1)
C(181)	15(1)	20(1)	14(1)	-6(1)	-1(1)	-2(1)
C(182)	22(1)	20(1)	26(1)	-7(1)	-7(1)	-1(1)
C(183)	26(1)	30(1)	38(1)	-13(1)	-16(1)	6(1)
C(184)	20(1)	40(1)	31(1)	-13(1)	-10(1)	-4(1)
C(185)	26(1)	28(1)	30(1)	-6(1)	-8(1)	-10(1)
C(186)	22(1)	20(1)	26(1)	-4(1)	-7(1)	-4(1)
C(191)	13(1)	24(1)	17(1)	-4(1)	-1(1)	-4(1)
C(192)	19(1)	30(1)	21(1)	-9(1)	-2(1)	-3(1)
C(193)	22(1)	44(1)	16(1)	-9(1)	-2(1)	-5(1)
C(194)	21(1)	42(1)	19(1)	4(1)	-4(1)	-6(1)
C(195)	24(1)	25(1)	28(1)	1(1)	-6(1)	-4(1)
C(196)	20(1)	23(1)	21(1)	-4(1)	-4(1)	-4(1)
C(201)	16(1)	21(1)	17(1)	-6(1)	2(1)	-3(1)
C(202)	19(1)	36(1)	22(1)	-3(1)	0(1)	2(1)
C(203)	22(1)	42(1)	32(1)	-6(1)	6(1)	6(1)
C(204)	30(1)	36(1)	27(1)	-12(1)	12(1)	-5(1)

C(205)	32(1)	44(1)	20(1)	-14(1)	2(1)	-10(1)
C(206)	21(1)	36(1)	21(1)	-10(1)	-2(1)	-4(1)
N(8)	20(1)	37(1)	27(1)	-3(1)	-5(1)	5(1)
P(3)	12(1)	35(1)	21(1)	-5(1)	-3(1)	-2(1)
C(211)	15(1)	24(1)	39(1)	-7(1)	-8(1)	-1(1)
C(212)	28(1)	57(1)	56(1)	-29(1)	-21(1)	9(1)
C(213)	41(1)	43(1)	79(2)	-24(1)	-40(1)	6(1)
C(214)	20(1)	23(1)	86(2)	4(1)	-23(1)	-3(1)
C(215)	15(1)	41(1)	59(1)	13(1)	-4(1)	0(1)
C(216)	16(1)	24(1)	39(1)	5(1)	-3(1)	-1(1)
C(221)	18(1)	38(1)	18(1)	-7(1)	-1(1)	-6(1)
C(222)	22(1)	66(2)	34(1)	11(1)	-11(1)	-10(1)
C(223)	32(1)	69(2)	38(1)	19(1)	-12(1)	-14(1)
C(224)	30(1)	52(1)	27(1)	1(1)	-2(1)	-15(1)
C(225)	22(1)	40(1)	32(1)	-11(1)	-2(1)	-8(1)
C(226)	20(1)	32(1)	28(1)	-9(1)	-6(1)	-3(1)
C(231)	13(1)	53(1)	21(1)	-7(1)	0(1)	-9(1)
C(232)	18(1)	57(1)	25(1)	-14(1)	0(1)	-6(1)
C(233)	24(1)	77(2)	32(1)	-25(1)	2(1)	-12(1)
C(234)	30(1)	101(2)	23(1)	-19(1)	4(1)	-24(1)
C(235)	30(1)	88(2)	22(1)	4(1)	-1(1)	-25(1)
C(236)	23(1)	64(1)	26(1)	-1(1)	-1(1)	-17(1)
P(4)	15(1)	27(1)	26(1)	0(1)	-6(1)	-1(1)
C(241)	17(1)	27(1)	31(1)	-4(1)	-8(1)	-1(1)

C(242)	21(1)	52(1)	24(1)	-1(1)	-4(1)	6(1)
C(243)	26(1)	57(1)	28(1)	1(1)	-10(1)	5(1)
C(244)	21(1)	33(1)	49(1)	-5(1)	-14(1)	3(1)
C(245)	25(1)	42(1)	57(1)	-29(1)	-16(1)	9(1)
C(246)	25(1)	41(1)	43(1)	-21(1)	-15(1)	4(1)
C(251)	22(1)	29(1)	35(1)	10(1)	-14(1)	-6(1)
C(252)	33(1)	31(1)	48(1)	3(1)	-17(1)	-7(1)
C(253)	52(1)	30(1)	60(1)	7(1)	-30(1)	-13(1)
C(254)	39(1)	42(1)	63(2)	24(1)	-31(1)	-19(1)
C(255)	27(1)	50(1)	58(1)	17(1)	-15(1)	-14(1)
C(256)	25(1)	43(1)	45(1)	9(1)	-10(1)	-7(1)
C(261)	19(1)	24(1)	24(1)	-4(1)	-5(1)	-2(1)
C(262)	24(1)	29(1)	33(1)	2(1)	-12(1)	-9(1)
C(263)	35(1)	40(1)	32(1)	2(1)	-17(1)	-14(1)
C(264)	37(1)	42(1)	27(1)	1(1)	-8(1)	-15(1)
C(265)	29(1)	48(1)	29(1)	-5(1)	-4(1)	-19(1)
C(266)	24(1)	40(1)	26(1)	-9(1)	-5(1)	-11(1)
Ru(1)	10(1)	12(1)	16(1)	-3(1)	-4(1)	-2(1)
C(1)	12(1)	16(1)	20(1)	-1(1)	-6(1)	-4(1)
N(1)	15(1)	16(1)	21(1)	-4(1)	-4(1)	-2(1)
B(1)	15(1)	16(1)	20(1)	-6(1)	-3(1)	1(1)
C(11)	16(1)	17(1)	21(1)	-6(1)	-5(1)	2(1)
C(12)	22(1)	19(1)	24(1)	-7(1)	-7(1)	3(1)
F(12)	41(1)	24(1)	23(1)	-9(1)	-12(1)	2(1)

C(13)	26(1)	25(1)	22(1)	-1(1)	-7(1)	3(1)
F(13)	46(1)	32(1)	21(1)	1(1)	-8(1)	2(1)
C(14)	26(1)	16(1)	33(1)	3(1)	-8(1)	-1(1)
F(14)	49(1)	19(1)	38(1)	6(1)	-12(1)	-5(1)
C(15)	25(1)	17(1)	33(1)	-8(1)	-10(1)	0(1)
F(15)	49(1)	18(1)	42(1)	-10(1)	-15(1)	-4(1)
C(16)	20(1)	19(1)	22(1)	-6(1)	-6(1)	0(1)
F(16)	38(1)	21(1)	22(1)	-8(1)	-9(1)	-3(1)
C(21)	16(1)	23(1)	19(1)	-4(1)	-4(1)	-2(1)
C(22)	19(1)	31(1)	26(1)	-9(1)	-5(1)	1(1)
F(22)	25(1)	40(1)	48(1)	-28(1)	-4(1)	5(1)
C(23)	18(1)	46(1)	30(1)	-7(1)	-5(1)	6(1)
F(23)	22(1)	70(1)	69(1)	-29(1)	-9(1)	18(1)
C(24)	16(1)	58(1)	27(1)	-2(1)	-7(1)	-9(1)
F(24)	18(1)	90(1)	50(1)	-10(1)	-13(1)	-12(1)
C(25)	26(1)	44(1)	26(1)	-6(1)	-4(1)	-19(1)
F(25)	39(1)	63(1)	52(1)	-18(1)	-6(1)	-31(1)
C(26)	21(1)	28(1)	28(1)	-8(1)	-1(1)	-7(1)
F(26)	28(1)	33(1)	66(1)	-27(1)	-1(1)	-10(1)
C(31)	17(1)	15(1)	21(1)	-5(1)	-5(1)	1(1)
C(32)	18(1)	22(1)	24(1)	-4(1)	-6(1)	-2(1)
F(32)	18(1)	50(1)	25(1)	-1(1)	-3(1)	-12(1)
C(33)	30(1)	26(1)	22(1)	-1(1)	-4(1)	-4(1)
F(33)	41(1)	50(1)	22(1)	6(1)	-6(1)	-15(1)

C(34)	31(1)	34(1)	27(1)	-2(1)	-16(1)	4(1)
F(34)	44(1)	62(1)	34(1)	3(1)	-25(1)	4(1)
C(35)	17(1)	40(1)	34(1)	-10(1)	-11(1)	3(1)
F(35)	19(1)	82(1)	44(1)	-16(1)	-15(1)	1(1)
C(36)	17(1)	25(1)	24(1)	-7(1)	-3(1)	0(1)
F(36)	18(1)	45(1)	28(1)	-8(1)	-2(1)	-9(1)
C(2)	14(1)	14(1)	16(1)	-5(1)	0(1)	-2(1)
N(2)	13(1)	18(1)	19(1)	-6(1)	-2(1)	-2(1)
B(2)	11(1)	19(1)	18(1)	-6(1)	-4(1)	-2(1)
C(41)	13(1)	16(1)	15(1)	-3(1)	-4(1)	-2(1)
C(42)	15(1)	19(1)	22(1)	-6(1)	-5(1)	-2(1)
F(42)	19(1)	29(1)	41(1)	-18(1)	-5(1)	-7(1)
C(43)	24(1)	21(1)	20(1)	-10(1)	-8(1)	3(1)
F(43)	32(1)	34(1)	36(1)	-25(1)	-9(1)	3(1)
C(44)	17(1)	25(1)	17(1)	-5(1)	-2(1)	6(1)
F(44)	20(1)	38(1)	25(1)	-12(1)	1(1)	7(1)
C(45)	11(1)	26(1)	21(1)	-3(1)	-3(1)	-3(1)
F(45)	12(1)	46(1)	42(1)	-17(1)	1(1)	-8(1)
C(46)	14(1)	18(1)	19(1)	-5(1)	-5(1)	-2(1)
F(46)	15(1)	31(1)	32(1)	-16(1)	-5(1)	-5(1)
C(51)	10(1)	23(1)	27(1)	-12(1)	-2(1)	-2(1)
C(52)	17(1)	22(1)	36(1)	-11(1)	-8(1)	-1(1)
F(52)	42(1)	26(1)	34(1)	0(1)	-13(1)	-12(1)
C(53)	28(1)	19(1)	63(1)	-14(1)	-15(1)	2(1)

F(53)	64(1)	18(1)	90(1)	-8(1)	-36(1)	0(1)
C(54)	32(1)	31(1)	71(2)	-34(1)	-16(1)	2(1)
F(54)	72(1)	39(1)	109(1)	-50(1)	-38(1)	5(1)
C(55)	32(1)	45(1)	46(1)	-29(1)	-14(1)	-3(1)
F(55)	74(1)	69(1)	58(1)	-39(1)	-30(1)	-12(1)
C(56)	22(1)	31(1)	33(1)	-15(1)	-8(1)	-5(1)
F(56)	59(1)	42(1)	35(1)	-7(1)	-27(1)	-16(1)
C(61)	16(1)	24(1)	16(1)	-8(1)	-3(1)	-7(1)
C(62)	19(1)	32(1)	20(1)	-11(1)	-1(1)	-9(1)
F(62)	19(1)	36(1)	34(1)	-17(1)	2(1)	-2(1)
C(63)	27(1)	52(1)	19(1)	-14(1)	3(1)	-19(1)
F(63)	32(1)	77(1)	28(1)	-22(1)	14(1)	-24(1)
C(64)	44(1)	51(1)	14(1)	0(1)	-2(1)	-27(1)
F(64)	67(1)	70(1)	19(1)	7(1)	1(1)	-36(1)
C(65)	40(1)	33(1)	21(1)	3(1)	-14(1)	-13(1)
F(65)	59(1)	38(1)	35(1)	15(1)	-21(1)	-10(1)
C(66)	20(1)	28(1)	18(1)	-5(1)	-7(1)	-7(1)
F(66)	21(1)	24(1)	27(1)	-2(1)	-9(1)	0(1)
C(3)	11(1)	16(1)	19(1)	-7(1)	-6(1)	1(1)
N(3)	14(1)	16(1)	22(1)	-4(1)	-6(1)	-1(1)
B(3)	13(1)	15(1)	18(1)	-4(1)	-4(1)	-3(1)
C(71)	13(1)	21(1)	18(1)	-6(1)	-2(1)	-9(1)
C(72)	18(1)	25(1)	28(1)	-12(1)	-1(1)	-6(1)
F(72)	26(1)	21(1)	40(1)	-8(1)	0(1)	4(1)

C(73)	17(1)	47(2)	41(2)	-29(1)	2(1)	-8(1)
F(73)	28(1)	59(1)	68(2)	-50(1)	4(1)	-2(1)
C(74)	20(1)	70(2)	28(1)	-29(2)	0(1)	-12(1)
F(74)	31(1)	125(2)	34(1)	-50(1)	3(1)	-16(1)
C(75)	20(1)	59(2)	20(1)	-8(1)	-6(1)	-13(1)
F(75)	30(1)	92(2)	18(1)	-1(1)	-7(1)	-13(1)
C(76)	15(1)	31(1)	23(1)	-7(1)	-4(1)	-6(1)
F(76)	30(1)	33(1)	22(1)	3(1)	-5(1)	3(1)
C(71A)	18(5)	30(5)	27(4)	-12(4)	1(4)	-5(4)
C(72A)	31(5)	29(5)	27(4)	-4(4)	0(4)	-13(4)
F(72A)	42(6)	31(5)	37(6)	-11(4)	7(4)	1(4)
C(73A)	27(5)	45(5)	29(4)	-23(4)	4(4)	-10(4)
F(73A)	66(7)	59(6)	66(7)	-48(5)	24(5)	-18(5)
C(74A)	21(5)	61(5)	24(4)	-17(4)	3(4)	-19(4)
F(74A)	66(7)	111(9)	27(4)	-34(5)	15(4)	-56(6)
C(75A)	16(4)	53(5)	22(4)	-8(4)	1(3)	-19(4)
F(75A)	41(4)	84(7)	17(3)	12(4)	-5(3)	-15(5)
C(76A)	17(4)	37(5)	14(3)	-4(4)	-2(3)	-12(5)
F(76A)	43(5)	36(5)	23(4)	5(3)	2(3)	10(4)
C(81)	14(1)	13(1)	21(1)	-4(1)	-4(1)	-1(1)
C(82)	18(1)	19(1)	21(1)	-5(1)	-5(1)	-3(1)
F(82)	25(1)	38(1)	21(1)	-4(1)	-2(1)	-16(1)
C(83)	14(1)	21(1)	31(1)	-6(1)	-2(1)	-4(1)
F(83)	16(1)	42(1)	37(1)	-9(1)	2(1)	-14(1)

C(84)	14(1)	22(1)	38(1)	-6(1)	-13(1)	-2(1)
F(84)	20(1)	38(1)	49(1)	-3(1)	-20(1)	-9(1)
C(85)	23(1)	18(1)	26(1)	-2(1)	-12(1)	-3(1)
F(85)	34(1)	34(1)	27(1)	1(1)	-18(1)	-11(1)
C(86)	16(1)	14(1)	23(1)	-3(1)	-6(1)	-3(1)
F(86)	23(1)	29(1)	20(1)	-3(1)	-4(1)	-11(1)
C(91)	14(1)	16(1)	17(1)	-3(1)	-4(1)	-2(1)
C(92)	20(1)	21(1)	33(1)	-10(1)	-13(1)	0(1)
F(92)	27(1)	27(1)	82(1)	-29(1)	-31(1)	5(1)
C(93)	29(1)	20(1)	35(1)	-16(1)	-14(1)	5(1)
F(93)	42(1)	35(1)	81(1)	-40(1)	-34(1)	16(1)
C(94)	19(1)	23(1)	22(1)	-6(1)	-2(1)	6(1)
F(94)	23(1)	31(1)	36(1)	-13(1)	-3(1)	10(1)
C(95)	12(1)	23(1)	25(1)	-4(1)	-2(1)	-3(1)
F(95)	11(1)	32(1)	54(1)	-12(1)	-7(1)	-2(1)
C(96)	16(1)	17(1)	21(1)	-6(1)	-4(1)	-3(1)
F(96)	18(1)	25(1)	44(1)	-17(1)	-11(1)	-2(1)
C(4)	13(1)	18(1)	19(1)	-2(1)	-6(1)	-3(1)
N(4)	18(1)	23(1)	20(1)	-6(1)	-5(1)	-4(1)
B(4)	21(1)	27(1)	16(1)	-7(1)	-3(1)	-7(1)
C(101)	15(2)	26(2)	14(1)	-4(1)	1(1)	-4(1)
C(102)	30(2)	43(2)	19(1)	-6(1)	-4(1)	-16(2)
F(102)	86(2)	54(2)	21(1)	-13(1)	-1(1)	-40(2)
C(103)	32(2)	63(2)	20(2)	1(1)	-9(1)	-23(2)

F(103)	91(3)	106(3)	21(1)	8(1)	-25(1)	-64(2)
C(104)	31(2)	52(2)	24(2)	12(2)	-3(2)	-6(2)
F(104)	45(1)	74(2)	42(2)	29(1)	-6(1)	1(2)
C(105)	47(4)	30(2)	32(3)	2(2)	6(2)	-3(2)
F(105)	128(4)	28(1)	49(2)	0(1)	29(2)	-5(2)
C(106)	38(4)	36(2)	19(2)	-9(1)	4(2)	-8(2)
F(106)	117(4)	36(2)	23(1)	-9(1)	6(2)	-35(2)
C(01B)	30(4)	45(4)	21(3)	-10(3)	-11(3)	-14(3)
C(02B)	22(3)	44(4)	22(3)	-3(2)	-4(3)	-18(3)
F(02B)	83(5)	66(4)	19(2)	-4(2)	-11(3)	-46(4)
C(03B)	24(3)	61(4)	21(3)	5(3)	-14(2)	-13(3)
F(03B)	66(4)	103(5)	28(3)	19(3)	-29(3)	-50(4)
C(04B)	19(3)	48(4)	29(4)	10(3)	-6(3)	-6(3)
F(04B)	29(2)	65(4)	48(4)	33(3)	-2(3)	-7(3)
C(05B)	29(4)	41(3)	29(4)	-1(3)	1(3)	-13(3)
F(05B)	73(5)	34(3)	54(4)	5(2)	8(3)	-26(3)
C(06B)	22(4)	33(3)	20(4)	2(3)	-4(3)	-16(3)
F(06B)	56(4)	44(4)	23(2)	1(2)	-6(2)	-40(3)
C(111)	24(1)	35(1)	17(1)	-8(1)	-3(1)	-11(1)
C(112)	25(1)	37(1)	20(1)	-6(1)	-7(1)	-10(1)
F(112)	25(1)	36(1)	35(1)	-10(1)	-12(1)	-2(1)
C(113)	24(1)	49(1)	23(1)	-5(1)	-7(1)	-12(1)
F(113)	22(1)	61(1)	39(1)	-7(1)	-11(1)	-9(1)
C(114)	31(1)	54(1)	23(1)	-2(1)	-8(1)	-26(1)

F(114)	39(1)	66(1)	37(1)	-1(1)	-12(1)	-35(1)
C(115)	42(1)	40(1)	26(1)	-11(1)	-5(1)	-22(1)
F(115)	56(1)	50(1)	49(1)	-22(1)	-5(1)	-31(1)
C(116)	30(1)	40(1)	26(1)	-15(1)	-1(1)	-13(1)
F(116)	35(1)	45(1)	60(1)	-35(1)	1(1)	-12(1)
C(121)	22(1)	26(1)	16(1)	-8(1)	-2(1)	-8(1)
C(122)	24(1)	25(1)	18(1)	-6(1)	2(1)	-6(1)
F(122)	37(1)	31(1)	26(1)	-1(1)	10(1)	0(1)
C(123)	31(1)	26(1)	20(1)	-2(1)	-4(1)	-5(1)
F(123)	46(1)	37(1)	28(1)	8(1)	-1(1)	3(1)
C(124)	21(1)	35(1)	30(1)	-5(1)	-6(1)	-2(1)
F(124)	24(1)	49(1)	44(1)	-1(1)	-7(1)	3(1)
C(125)	19(1)	51(1)	26(1)	-5(1)	3(1)	-5(1)
F(125)	26(1)	84(1)	39(1)	9(1)	13(1)	7(1)
C(126)	25(1)	40(1)	16(1)	0(1)	-1(1)	-6(1)
F(126)	35(1)	69(1)	19(1)	12(1)	5(1)	4(1)
N(5)	14(1)	16(1)	20(1)	-4(1)	-6(1)	-2(1)
C(131)	17(1)	19(1)	28(1)	-3(1)	-8(1)	-3(1)
C(132)	15(1)	27(1)	29(1)	-5(1)	-9(1)	-5(1)
C(133)	17(1)	26(1)	23(1)	-8(1)	-10(1)	1(1)
C(141)	20(1)	36(1)	31(1)	-6(1)	-13(1)	0(1)
F(131)	24(2)	95(6)	38(3)	-7(3)	-6(2)	16(3)
F(132)	26(4)	31(3)	32(3)	-7(2)	-14(3)	9(3)
F(133)	35(3)	41(3)	63(3)	7(2)	-39(2)	-9(3)

F(31B)	20(3)	43(4)	37(3)	-18(2)	-13(2)	15(2)
F(32B)	36(6)	36(5)	48(5)	3(4)	-32(4)	-4(4)
F(33B)	22(2)	33(3)	40(3)	-8(3)	-25(3)	0(2)
C(134)	21(1)	19(1)	21(1)	-4(1)	-10(1)	1(1)
C(135)	16(1)	17(1)	19(1)	-6(1)	-6(1)	-1(1)
C(136)	17(1)	17(1)	20(1)	-4(1)	-6(1)	-3(1)
C(137)	27(1)	21(1)	23(1)	2(1)	-10(1)	-5(1)
C(138)	34(1)	22(1)	28(1)	5(1)	-10(1)	-12(1)
C(142)	47(1)	35(1)	51(1)	18(1)	-19(1)	-22(1)
F(134)	134(5)	33(3)	100(4)	23(2)	-74(4)	-46(3)
F(135)	82(4)	50(2)	60(3)	32(2)	18(3)	-9(3)
F(136)	52(2)	34(2)	64(3)	25(2)	-26(2)	-13(1)
F(34B)	112(7)	23(2)	102(6)	8(3)	14(5)	-13(4)
F(35B)	64(4)	70(5)	69(5)	42(4)	2(3)	-28(3)
F(36B)	101(6)	88(7)	86(6)	67(5)	-63(5)	-58(5)
C(139)	27(1)	29(1)	33(1)	2(1)	-8(1)	-16(1)
C(140)	20(1)	24(1)	28(1)	-1(1)	-7(1)	-8(1)
N(6)	16(1)	17(1)	19(1)	-3(1)	-5(1)	-4(1)
O(1S)	205(17)	124(9)	175(16)	-41(11)	-7(15)	-28(11)
C(11S)	33(6)	100(8)	82(9)	-55(7)	11(6)	-31(7)
C(12S)	104(13)	107(13)	59(10)	-18(9)	-8(9)	-57(11)
O(2S)	144(12)	113(11)	148(13)	23(10)	16(10)	36(10)
C(21S)	71(12)	116(13)	110(15)	-12(11)	-37(10)	15(11)
C(22S)	97(17)	138(19)	133(18)	-36(16)	-53(11)	8(18)

O(3S)	63(9)	102(9)	99(10)	-46(8)	9(7)	-31(8)
C(31S)	69(10)	98(10)	94(11)	-49(8)	-1(9)	-33(8)
C(32S)	108(14)	86(13)	131(14)	-52(11)	34(12)	-23(12)

Table 5. Hydrogen coordinates (x 10^4) and isotropic displacement parameters ($Å^2$x 10^{3}) for D19108.

	x	y	z	U(eq)
H(152)	6553	7946	2425	62
H(153)	5172	8199	2185	90
H(154)	4886	9065	1360	90
H(155)	6039	9569	673	61
H(156)	7397	9378	947	38
H(52B)	6935	7555	2063	53
H(53B)	5516	7740	1886	59
H(54B)	5019	8759	1302	78
H(55B)	5704	9712	1182	71
H(56B)	7177	9494	1290	55
H(162)	7044	8794	2845	46
H(163)	6972	8497	3885	52
H(164)	7997	7689	4312	49
H(165)	9111	7166	3711	51
H(166)	9195	7458	2663	40
H(172)	7981	7037	2148	71
H(173)	8639	6147	1736	87
H(174)	9755	6295	901	58

H(175)	10235	7327	473	39
H(176)	9606	8217	894	30
H(182)	10290	8688	1876	27
H(183)	11698	8694	1988	36
H(184)	12209	9693	1850	34
H(185)	11308	10696	1620	32
H(186)	9896	10698	1511	27
H(192)	8970	9603	384	27
H(193)	8842	10358	-544	33
H(194)	8582	11492	-618	35
H(195)	8423	11884	234	33
H(196)	8531	11135	1170	26
H(202)	7172	10409	1694	33
H(203)	6188	10744	2487	44
H(204)	6558	10509	3433	40
H(205)	7911	9943	3591	38
H(206)	8920	9634	2793	31
H(212)	5664	2816	5237	53
H(213)	4213	2985	5137	59
H(214)	3119	3159	5942	54
H(215)	3460	3154	6844	54
H(216)	4904	2978	6955	36
H(222)	6028	3951	5279	54
H(223)	6800	4759	4560	62

H(224)	8284	4699	4499	46
H(225)	8987	3874	5187	37
H(226)	8232	3054	5889	32
H(232)	6635	3801	6695	40
H(233)	6628	3860	7673	51
H(234)	6528	2911	8470	60
H(235)	6482	1895	8301	59
H(236)	6516	1818	7322	47
H(242)	8126	1241	6696	43
H(243)	9418	625	6953	48
H(244)	10417	152	6256	42
H(245)	10143	292	5299	46
H(246)	8849	898	5033	41
H(252)	7359	490	5188	46
H(253)	6305	-158	5226	57
H(254)	4904	52	5757	60
H(255)	4560	858	6279	59
H(256)	5615	1493	6273	49
H(262)	6552	1855	4620	35
H(263)	6847	2489	3628	43
H(264)	8056	3050	3285	43
H(265)	8954	3014	3946	42
H(266)	8680	2371	4939	35
H(131)	9136	6779	8096	25

H(132)	10410	6333	8461	28
H(134)	9273	4704	9436	24
H(137)	8036	4303	9766	29
H(139)	5661	4409	9401	36
H(140)	5897	5398	8676	29
H(1S)	3429	8901	641	257
H(11A)	2788	9865	676	79
H(11B)	3724	9872	245	79
H(12A)	3612	10563	927	129
H(12B)	3419	9943	1494	129
H(12C)	4353	9949	1064	129
H(2S)	3637	10091	1049	243
H(21A)	4961	10349	540	123
H(21B)	4263	10610	106	123
H(22A)	5482	9983	-355	180
H(22B)	5341	9355	213	180
H(22C)	4645	9615	-220	180
H(3S)	3893	10049	180	127
H(31A)	4656	8913	702	97
H(31B)	3854	9013	373	97
H(32A)	3351	8840	1429	167
H(32B)	3771	9471	1420	167
H(32C)	2970	9570	1092	167

Table 6. Torsion angles [°] for D19108.

P(2)-N(7)-P(1)-C(51B)	77.2(4)
P(2)-N(7)-P(1)-C(161)	-49.65(18)
P(2)-N(7)-P(1)-C(171)	-168.39(14)
P(2)-N(7)-P(1)-C(151)	73.0(2)
N(7)-P(1)-C(151)-C(156)	21.4(4)
C(161)-P(1)-C(151)-C(156)	148.2(4)
C(171)-P(1)-C(151)-C(156)	-95.8(4)
N(7)-P(1)-C(151)-C(152)	-160.7(4)
C(161)-P(1)-C(151)-C(152)	-33.9(4)
C(171)-P(1)-C(151)-C(152)	82.2(4)
C(156)-C(151)-C(152)-C(153)	0.8(7)
P(1)-C(151)-C(152)-C(153)	-177.2(4)
C(151)-C(152)-C(153)-C(154)	-1.5(9)
C(152)-C(153)-C(154)-C(155)	4.8(11)
C(153)-C(154)-C(155)-C(156)	-7.3(10)
C(152)-C(151)-C(156)-C(155)	-3.4(7)
P(1)-C(151)-C(156)-C(155)	174.6(4)
C(154)-C(155)-C(156)-C(151)	6.7(8)
N(7)-P(1)-C(51B)-C(56B)	-12.9(9)
C(161)-P(1)-C(51B)-C(56B)	117.8(8)
C(171)-P(1)-C(51B)-C(56B)	-129.4(8)
N(7)-P(1)-C(51B)-C(52B)	166.0(7)

C(161)-P(1)-C(51B)-C(52B)	-63.2(8)
C(171)-P(1)-C(51B)-C(52B)	49.6(8)
C(56B)-C(51B)-C(52B)-C(53B)	-1.3(13)
P(1)-C(51B)-C(52B)-C(53B)	179.8(8)
C(51B)-C(52B)-C(53B)-C(54B)	4.3(16)
C(52B)-C(53B)-C(54B)-C(55B)	-11(2)
C(53B)-C(54B)-C(55B)-C(56B)	13(2)
C(52B)-C(51B)-C(56B)-C(55B)	4.4(15)
P(1)-C(51B)-C(56B)-C(55B)	-176.6(9)
C(54B)-C(55B)-C(56B)-C(51B)	-10.0(18)
N(7)-P(1)-C(161)-C(166)	-87.05(16)
C(51B)-P(1)-C(161)-C(166)	140.8(4)
C(171)-P(1)-C(161)-C(166)	31.21(17)
C(151)-P(1)-C(161)-C(166)	148.2(2)
N(7)-P(1)-C(161)-C(162)	88.43(16)
C(51B)-P(1)-C(161)-C(162)	-43.7(4)
C(171)-P(1)-C(161)-C(162)	-153.31(15)
C(151)-P(1)-C(161)-C(162)	-36.3(2)
C(166)-C(161)-C(162)-C(163)	-0.8(3)
P(1)-C(161)-C(162)-C(163)	-176.31(16)
C(161)-C(162)-C(163)-C(164)	0.3(3)
C(162)-C(163)-C(164)-C(165)	0.1(3)
C(163)-C(164)-C(165)-C(166)	-0.1(3)
C(162)-C(161)-C(166)-C(165)	0.8(3)

P(1)-C(161)-C(166)-C(165)	176.28(16)
C(164)-C(165)-C(166)-C(161)	-0.4(3)
N(7)-P(1)-C(171)-C(176)	-9.90(17)
C(51B)-P(1)-C(171)-C(176)	114.2(4)
C(161)-P(1)-C(171)-C(176)	-133.49(14)
C(151)-P(1)-C(171)-C(176)	110.4(2)
N(7)-P(1)-C(171)-C(172)	172.67(19)
C(51B)-P(1)-C(171)-C(172)	-63.3(4)
C(161)-P(1)-C(171)-C(172)	49.1(2)
C(151)-P(1)-C(171)-C(172)	-67.0(3)
C(176)-C(171)-C(172)-C(173)	0.2(4)
P(1)-C(171)-C(172)-C(173)	177.7(2)
C(171)-C(172)-C(173)-C(174)	-0.7(5)
C(172)-C(173)-C(174)-C(175)	0.3(5)
C(173)-C(174)-C(175)-C(176)	0.5(4)
C(174)-C(175)-C(176)-C(171)	-0.9(3)
C(172)-C(171)-C(176)-C(175)	0.5(3)
P(1)-C(171)-C(176)-C(175)	-176.92(14)
P(1)-N(7)-P(2)-C(201)	-0.57(18)
P(1)-N(7)-P(2)-C(191)	-122.77(15)
P(1)-N(7)-P(2)-C(181)	120.07(15)
N(7)-P(2)-C(181)-C(182)	-11.82(14)
C(201)-P(2)-C(181)-C(182)	113.97(13)
C(191)-P(2)-C(181)-C(182)	-130.09(13)

N(7)-P(2)-C(181)-C(186)	166.50(12)
C(201)-P(2)-C(181)-C(186)	-67.70(14)
C(191)-P(2)-C(181)-C(186)	48.24(14)
C(186)-C(181)-C(182)-C(183)	-0.4(2)
P(2)-C(181)-C(182)-C(183)	177.94(13)
C(181)-C(182)-C(183)-C(184)	-0.3(3)
C(182)-C(183)-C(184)-C(185)	0.8(3)
C(183)-C(184)-C(185)-C(186)	-0.6(3)
C(184)-C(185)-C(186)-C(181)	-0.1(3)
C(182)-C(181)-C(186)-C(185)	0.6(2)
P(2)-C(181)-C(186)-C(185)	-177.79(13)
N(7)-P(2)-C(191)-C(196)	163.68(12)
C(201)-P(2)-C(191)-C(196)	37.13(15)
C(181)-P(2)-C(191)-C(196)	-77.96(14)
N(7)-P(2)-C(191)-C(192)	-18.97(14)
C(201)-P(2)-C(191)-C(192)	-145.52(12)
C(181)-P(2)-C(191)-C(192)	99.39(13)
C(196)-C(191)-C(192)-C(193)	-0.9(2)
P(2)-C(191)-C(192)-C(193)	-178.25(12)
C(191)-C(192)-C(193)-C(194)	0.9(2)
C(192)-C(193)-C(194)-C(195)	-0.5(3)
C(193)-C(194)-C(195)-C(196)	0.0(3)
C(194)-C(195)-C(196)-C(191)	0.0(2)
C(192)-C(191)-C(196)-C(195)	0.4(2)

P(2)-C(191)-C(196)-C(195)	177.73(12)
N(7)-P(2)-C(201)-C(206)	90.10(15)
C(191)-P(2)-C(201)-C(206)	-147.20(13)
C(181)-P(2)-C(201)-C(206)	-31.81(15)
N(7)-P(2)-C(201)-C(202)	-85.95(15)
C(191)-P(2)-C(201)-C(202)	36.75(16)
C(181)-P(2)-C(201)-C(202)	152.14(14)
C(206)-C(201)-C(202)-C(203)	0.7(3)
P(2)-C(201)-C(202)-C(203)	176.76(15)
C(201)-C(202)-C(203)-C(204)	-1.0(3)
C(202)-C(203)-C(204)-C(205)	0.2(3)
C(203)-C(204)-C(205)-C(206)	0.9(3)
C(204)-C(205)-C(206)-C(201)	-1.2(3)
C(202)-C(201)-C(206)-C(205)	0.4(3)
P(2)-C(201)-C(206)-C(205)	-175.69(14)
P(4)-N(8)-P(3)-C(221)	-52.2(2)
P(4)-N(8)-P(3)-C(231)	-170.62(16)
P(4)-N(8)-P(3)-C(211)	71.22(19)
N(8)-P(3)-C(211)-C(216)	115.23(15)
C(221)-P(3)-C(211)-C(216)	-118.30(15)
C(231)-P(3)-C(211)-C(216)	-2.33(17)
N(8)-P(3)-C(211)-C(212)	-64.02(18)
C(221)-P(3)-C(211)-C(212)	62.45(18)
C(231)-P(3)-C(211)-C(212)	178.43(17)

C(216)-C(211)-C(212)-C(213)	0.4(3)
P(3)-C(211)-C(212)-C(213)	179.70(18)
C(211)-C(212)-C(213)-C(214)	0.1(4)
C(212)-C(213)-C(214)-C(215)	-0.4(3)
C(213)-C(214)-C(215)-C(216)	0.1(3)
C(212)-C(211)-C(216)-C(215)	-0.7(3)
P(3)-C(211)-C(216)-C(215)	-179.96(15)
C(214)-C(215)-C(216)-C(211)	0.4(3)
N(8)-P(3)-C(221)-C(222)	126.38(18)
C(231)-P(3)-C(221)-C(222)	-115.74(18)
C(211)-P(3)-C(221)-C(222)	0.3(2)
N(8)-P(3)-C(221)-C(226)	-53.11(16)
C(231)-P(3)-C(221)-C(226)	64.77(16)
C(211)-P(3)-C(221)-C(226)	-179.22(14)
C(226)-C(221)-C(222)-C(223)	2.6(3)
P(3)-C(221)-C(222)-C(223)	-176.9(2)
C(221)-C(222)-C(223)-C(224)	-0.7(4)
C(222)-C(223)-C(224)-C(225)	-2.0(4)
C(223)-C(224)-C(225)-C(226)	2.8(3)
C(224)-C(225)-C(226)-C(221)	-0.9(3)
C(222)-C(221)-C(226)-C(225)	-1.8(3)
P(3)-C(221)-C(226)-C(225)	177.71(14)
N(8)-P(3)-C(231)-C(232)	149.52(14)
C(221)-P(3)-C(231)-C(232)	27.25(16)

C(211)-P(3)-C(231)-C(232)	-88.90(15)
N(8)-P(3)-C(231)-C(236)	-32.73(16)
C(221)-P(3)-C(231)-C(236)	-155.00(14)
C(211)-P(3)-C(231)-C(236)	88.85(15)
C(236)-C(231)-C(232)-C(233)	-0.2(3)
P(3)-C(231)-C(232)-C(233)	177.50(14)
C(231)-C(232)-C(233)-C(234)	-0.8(3)
C(232)-C(233)-C(234)-C(235)	1.1(3)
C(233)-C(234)-C(235)-C(236)	-0.5(3)
C(232)-C(231)-C(236)-C(235)	0.9(3)
P(3)-C(231)-C(236)-C(235)	-176.90(15)
C(234)-C(235)-C(236)-C(231)	-0.5(3)
P(3)-N(8)-P(4)-C(251)	-99.35(18)
P(3)-N(8)-P(4)-C(261)	21.5(2)
P(3)-N(8)-P(4)-C(241)	140.66(17)
N(8)-P(4)-C(241)-C(242)	18.58(18)
C(251)-P(4)-C(241)-C(242)	-101.23(17)
C(261)-P(4)-C(241)-C(242)	143.58(16)
N(8)-P(4)-C(241)-C(246)	-160.45(16)
C(251)-P(4)-C(241)-C(246)	79.74(18)
C(261)-P(4)-C(241)-C(246)	-35.45(18)
C(246)-C(241)-C(242)-C(243)	-0.8(3)
P(4)-C(241)-C(242)-C(243)	-179.84(17)
C(241)-C(242)-C(243)-C(244)	0.4(3)

C(242)-C(243)-C(244)-C(245)	0.2(3)
C(243)-C(244)-C(245)-C(246)	-0.5(3)
C(244)-C(245)-C(246)-C(241)	0.2(3)
C(242)-C(241)-C(246)-C(245)	0.5(3)
P(4)-C(241)-C(246)-C(245)	179.50(16)
N(8)-P(4)-C(251)-C(252)	-171.83(14)
C(261)-P(4)-C(251)-C(252)	61.66(16)
C(241)-P(4)-C(251)-C(252)	-53.71(17)
N(8)-P(4)-C(251)-C(256)	11.77(17)
C(261)-P(4)-C(251)-C(256)	-114.74(15)
C(241)-P(4)-C(251)-C(256)	129.89(15)
C(256)-C(251)-C(252)-C(253)	0.8(3)
P(4)-C(251)-C(252)-C(253)	-175.58(15)
C(251)-C(252)-C(253)-C(254)	0.9(3)
C(252)-C(253)-C(254)-C(255)	-1.6(3)
C(253)-C(254)-C(255)-C(256)	0.5(3)
C(252)-C(251)-C(256)-C(255)	-1.8(3)
P(4)-C(251)-C(256)-C(255)	174.64(15)
C(254)-C(255)-C(256)-C(251)	1.1(3)
N(8)-P(4)-C(261)-C(262)	-104.67(16)
C(251)-P(4)-C(261)-C(262)	18.12(17)
C(241)-P(4)-C(261)-C(262)	135.89(15)
N(8)-P(4)-C(261)-C(266)	71.38(16)
C(251)-P(4)-C(261)-C(266)	-165.84(14)

C(241)-P(4)-C(261)-C(266)	-48.07(16)
C(266)-C(261)-C(262)-C(263)	0.5(3)
P(4)-C(261)-C(262)-C(263)	176.54(15)
C(261)-C(262)-C(263)-C(264)	0.1(3)
C(262)-C(263)-C(264)-C(265)	-1.2(3)
C(263)-C(264)-C(265)-C(266)	1.6(3)
C(264)-C(265)-C(266)-C(261)	-1.0(3)
C(262)-C(261)-C(266)-C(265)	-0.1(3)
P(4)-C(261)-C(266)-C(265)	-176.21(15)
N(1)-B(1)-C(11)-C(12)	-42.59(18)
C(31)-B(1)-C(11)-C(12)	-155.72(14)
C(21)-B(1)-C(11)-C(12)	74.51(17)
N(1)-B(1)-C(11)-C(16)	140.78(15)
C(31)-B(1)-C(11)-C(16)	27.7(2)
C(21)-B(1)-C(11)-C(16)	-102.11(17)
C(16)-C(11)-C(12)-F(12)	175.29(13)
B(1)-C(11)-C(12)-F(12)	-1.7(2)
C(16)-C(11)-C(12)-C(13)	-3.3(2)
B(1)-C(11)-C(12)-C(13)	179.67(15)
F(12)-C(12)-C(13)-F(13)	6.2(2)
C(11)-C(12)-C(13)-F(13)	-175.16(15)
F(12)-C(12)-C(13)-C(14)	-174.32(15)
C(11)-C(12)-C(13)-C(14)	4.4(3)
F(13)-C(13)-C(14)-F(14)	-0.9(2)

C(12)-C(13)-C(14)-F(14)	179.56(15)
F(13)-C(13)-C(14)-C(15)	177.69(15)
C(12)-C(13)-C(14)-C(15)	-1.8(3)
F(14)-C(14)-C(15)-F(15)	-0.8(2)
C(13)-C(14)-C(15)-F(15)	-179.45(15)
F(14)-C(14)-C(15)-C(16)	177.33(15)
C(13)-C(14)-C(15)-C(16)	-1.3(3)
F(15)-C(15)-C(16)-F(16)	-0.1(2)
C(14)-C(15)-C(16)-F(16)	-178.25(15)
F(15)-C(15)-C(16)-C(11)	-179.59(15)
C(14)-C(15)-C(16)-C(11)	2.3(3)
C(12)-C(11)-C(16)-F(16)	-179.49(14)
B(1)-C(11)-C(16)-F(16)	-2.7(2)
C(12)-C(11)-C(16)-C(15)	0.0(2)
B(1)-C(11)-C(16)-C(15)	176.82(15)
N(1)-B(1)-C(21)-C(26)	-9.8(2)
C(31)-B(1)-C(21)-C(26)	106.22(18)
C(11)-B(1)-C(21)-C(26)	-125.07(17)
N(1)-B(1)-C(21)-C(22)	166.32(14)
C(31)-B(1)-C(21)-C(22)	-77.70(18)
C(11)-B(1)-C(21)-C(22)	51.01(19)
C(26)-C(21)-C(22)-F(22)	-177.99(15)
B(1)-C(21)-C(22)-F(22)	5.4(2)
C(26)-C(21)-C(22)-C(23)	1.0(3)

B(1)-C(21)-C(22)-C(23)	-175.60(16)
F(22)-C(22)-C(23)-F(23)	-1.2(3)
C(21)-C(22)-C(23)-F(23)	179.76(17)
F(22)-C(22)-C(23)-C(24)	178.75(16)
C(21)-C(22)-C(23)-C(24)	-0.3(3)
F(23)-C(23)-C(24)-F(24)	0.6(3)
C(22)-C(23)-C(24)-F(24)	-179.40(17)
F(23)-C(23)-C(24)-C(25)	-179.85(17)
C(22)-C(23)-C(24)-C(25)	0.2(3)
F(24)-C(24)-C(25)-F(25)	-1.5(3)
C(23)-C(24)-C(25)-F(25)	178.96(17)
F(24)-C(24)-C(25)-C(26)	178.68(17)
C(23)-C(24)-C(25)-C(26)	-0.9(3)
C(22)-C(21)-C(26)-F(26)	178.13(15)
B(1)-C(21)-C(26)-F(26)	-5.6(3)
C(22)-C(21)-C(26)-C(25)	-1.7(2)
B(1)-C(21)-C(26)-C(25)	174.55(16)
F(25)-C(25)-C(26)-F(26)	2.1(2)
C(24)-C(25)-C(26)-F(26)	-178.10(16)
F(25)-C(25)-C(26)-C(21)	-178.06(16)
C(24)-C(25)-C(26)-C(21)	1.8(3)
N(1)-B(1)-C(31)-C(32)	115.46(16)
C(11)-B(1)-C(31)-C(32)	-129.18(16)
C(21)-B(1)-C(31)-C(32)	-4.1(2)

N(1)-B(1)-C(31)-C(36)	-56.07(17)
C(11)-B(1)-C(31)-C(36)	59.29(18)
C(21)-B(1)-C(31)-C(36)	-175.63(14)
C(36)-C(31)-C(32)-F(32)	-178.91(14)
B(1)-C(31)-C(32)-F(32)	9.1(2)
C(36)-C(31)-C(32)-C(33)	1.6(2)
B(1)-C(31)-C(32)-C(33)	-170.33(15)
F(32)-C(32)-C(33)-F(33)	-0.2(2)
C(31)-C(32)-C(33)-F(33)	179.30(15)
F(32)-C(32)-C(33)-C(34)	-179.86(16)
C(31)-C(32)-C(33)-C(34)	-0.4(3)
F(33)-C(33)-C(34)-F(34)	0.1(3)
C(32)-C(33)-C(34)-F(34)	179.73(17)
F(33)-C(33)-C(34)-C(35)	179.55(17)
C(32)-C(33)-C(34)-C(35)	-0.8(3)
F(34)-C(34)-C(35)-F(35)	-0.1(3)
C(33)-C(34)-C(35)-F(35)	-179.54(17)
F(34)-C(34)-C(35)-C(36)	-179.98(17)
C(33)-C(34)-C(35)-C(36)	0.5(3)
F(35)-C(35)-C(36)-F(36)	-0.1(3)
C(34)-C(35)-C(36)-F(36)	179.76(16)
F(35)-C(35)-C(36)-C(31)	-179.04(16)
C(34)-C(35)-C(36)-C(31)	0.9(3)
C(32)-C(31)-C(36)-F(36)	179.26(14)

B(1)-C(31)-C(36)-F(36)	-8.2(2)
C(32)-C(31)-C(36)-C(35)	-1.9(2)
B(1)-C(31)-C(36)-C(35)	170.61(16)
N(2)-B(2)-C(41)-C(46)	-133.88(14)
C(51)-B(2)-C(41)-C(46)	-15.3(2)
C(61)-B(2)-C(41)-C(46)	111.07(16)
N(2)-B(2)-C(41)-C(42)	45.40(18)
C(51)-B(2)-C(41)-C(42)	164.01(13)
C(61)-B(2)-C(41)-C(42)	-69.65(18)
C(46)-C(41)-C(42)-F(42)	-177.38(13)
B(2)-C(41)-C(42)-F(42)	3.3(2)
C(46)-C(41)-C(42)-C(43)	1.2(2)
B(2)-C(41)-C(42)-C(43)	-178.14(14)
F(42)-C(42)-C(43)-F(43)	-2.5(2)
C(41)-C(42)-C(43)-F(43)	178.89(14)
F(42)-C(42)-C(43)-C(44)	177.70(14)
C(41)-C(42)-C(43)-C(44)	-0.9(2)
F(43)-C(43)-C(44)-F(44)	-0.1(2)
C(42)-C(43)-C(44)-F(44)	179.71(14)
F(43)-C(43)-C(44)-C(45)	-179.98(14)
C(42)-C(43)-C(44)-C(45)	-0.2(2)
F(44)-C(44)-C(45)-F(45)	1.4(2)
C(43)-C(44)-C(45)-F(45)	-178.73(14)
F(44)-C(44)-C(45)-C(46)	-179.02(14)

C(43)-C(44)-C(45)-C(46)	0.8(2)
F(45)-C(45)-C(46)-F(46)	0.2(2)
C(44)-C(45)-C(46)-F(46)	-179.35(13)
F(45)-C(45)-C(46)-C(41)	179.05(14)
C(44)-C(45)-C(46)-C(41)	-0.5(2)
C(42)-C(41)-C(46)-F(46)	178.28(13)
B(2)-C(41)-C(46)-F(46)	-2.4(2)
C(42)-C(41)-C(46)-C(45)	-0.5(2)
B(2)-C(41)-C(46)-C(45)	178.85(14)
N(2)-B(2)-C(51)-C(52)	41.81(18)
C(61)-B(2)-C(51)-C(52)	154.90(14)
C(41)-B(2)-C(51)-C(52)	-76.19(17)
N(2)-B(2)-C(51)-C(56)	-139.39(15)
C(61)-B(2)-C(51)-C(56)	-26.31(19)
C(41)-B(2)-C(51)-C(56)	102.60(17)
C(56)-C(51)-C(52)-F(52)	-176.18(14)
B(2)-C(51)-C(52)-F(52)	2.7(2)
C(56)-C(51)-C(52)-C(53)	1.0(2)
B(2)-C(51)-C(52)-C(53)	179.95(15)
F(52)-C(52)-C(53)-F(53)	-0.7(2)
C(51)-C(52)-C(53)-F(53)	-178.00(16)
F(52)-C(52)-C(53)-C(54)	177.77(17)
C(51)-C(52)-C(53)-C(54)	0.5(3)
F(53)-C(53)-C(54)-F(54)	-1.9(3)

C(52)-C(53)-C(54)-F(54)	179.60(17)
F(53)-C(53)-C(54)-C(55)	177.58(18)
C(52)-C(53)-C(54)-C(55)	-0.9(3)
F(54)-C(54)-C(55)-F(55)	-1.2(3)
C(53)-C(54)-C(55)-F(55)	179.26(18)
F(54)-C(54)-C(55)-C(56)	179.26(18)
C(53)-C(54)-C(55)-C(56)	-0.3(3)
F(55)-C(55)-C(56)-F(56)	2.8(3)
C(54)-C(55)-C(56)-F(56)	-177.65(17)
F(55)-C(55)-C(56)-C(51)	-177.57(17)
C(54)-C(55)-C(56)-C(51)	2.0(3)
C(52)-C(51)-C(56)-F(56)	177.33(15)
B(2)-C(51)-C(56)-F(56)	-1.6(2)
C(52)-C(51)-C(56)-C(55)	-2.2(2)
B(2)-C(51)-C(56)-C(55)	178.87(16)
N(2)-B(2)-C(61)-C(66)	-127.62(15)
C(51)-B(2)-C(61)-C(66)	116.89(16)
C(41)-B(2)-C(61)-C(66)	-11.0(2)
N(2)-B(2)-C(61)-C(62)	55.53(17)
C(51)-B(2)-C(61)-C(62)	-59.96(17)
C(41)-B(2)-C(61)-C(62)	172.15(13)
C(66)-C(61)-C(62)-F(62)	-178.62(14)
B(2)-C(61)-C(62)-F(62)	-1.4(2)
C(66)-C(61)-C(62)-C(63)	-0.2(2)

B(2)-C(61)-C(62)-C(63)	177.06(15)
F(62)-C(62)-C(63)-F(63)	-1.1(2)
C(61)-C(62)-C(63)-F(63)	-179.64(15)
F(62)-C(62)-C(63)-C(64)	178.47(16)
C(61)-C(62)-C(63)-C(64)	0.0(3)
F(63)-C(63)-C(64)-F(64)	-1.5(3)
C(62)-C(63)-C(64)-F(64)	178.91(16)
F(63)-C(63)-C(64)-C(65)	179.63(17)
C(62)-C(63)-C(64)-C(65)	0.0(3)
F(64)-C(64)-C(65)-F(65)	1.4(3)
C(63)-C(64)-C(65)-F(65)	-179.75(17)
F(64)-C(64)-C(65)-C(66)	-178.69(16)
C(63)-C(64)-C(65)-C(66)	0.2(3)
C(62)-C(61)-C(66)-F(66)	179.68(14)
B(2)-C(61)-C(66)-F(66)	2.7(2)
C(62)-C(61)-C(66)-C(65)	0.4(2)
B(2)-C(61)-C(66)-C(65)	-176.57(15)
F(65)-C(65)-C(66)-F(66)	0.2(2)
C(64)-C(65)-C(66)-F(66)	-179.74(16)
F(65)-C(65)-C(66)-C(61)	179.51(15)
C(64)-C(65)-C(66)-C(61)	-0.4(3)
N(3)-B(3)-C(71)-C(76)	137.9(2)
C(91)-B(3)-C(71)-C(76)	23.2(3)
C(81)-B(3)-C(71)-C(76)	-106.6(3)

N(3)-B(3)-C(71)-C(72)	-48.8(2)
C(91)-B(3)-C(71)-C(72)	-163.45(19)
C(81)-B(3)-C(71)-C(72)	66.8(2)
C(76)-C(71)-C(72)-F(72)	178.4(3)
B(3)-C(71)-C(72)-F(72)	4.2(3)
C(76)-C(71)-C(72)-C(73)	2.7(4)
B(3)-C(71)-C(72)-C(73)	-171.5(3)
F(72)-C(72)-C(73)-F(73)	2.8(4)
C(71)-C(72)-C(73)-F(73)	178.7(2)
F(72)-C(72)-C(73)-C(74)	-176.3(3)
C(71)-C(72)-C(73)-C(74)	-0.5(4)
F(73)-C(73)-C(74)-F(74)	-2.0(4)
C(72)-C(73)-C(74)-F(74)	177.1(3)
F(73)-C(73)-C(74)-C(75)	178.2(3)
C(72)-C(73)-C(74)-C(75)	-2.7(4)
F(74)-C(74)-C(75)-F(75)	1.9(4)
C(73)-C(74)-C(75)-F(75)	-178.3(3)
F(74)-C(74)-C(75)-C(76)	-176.5(3)
C(73)-C(74)-C(75)-C(76)	3.3(4)
C(72)-C(71)-C(76)-F(76)	-178.3(3)
B(3)-C(71)-C(76)-F(76)	-4.5(4)
C(72)-C(71)-C(76)-C(75)	-2.0(4)
B(3)-C(71)-C(76)-C(75)	171.7(3)
F(75)-C(75)-C(76)-F(76)	-2.9(4)

C(74)-C(75)-C(76)-F(76)	175.5(3)
F(75)-C(75)-C(76)-C(71)	-179.3(3)
C(74)-C(75)-C(76)-C(71)	-0.9(5)
N(3)-B(3)-C(71A)-C(72A)	-39.5(6)
C(91)-B(3)-C(71A)-C(72A)	-156.2(6)
C(81)-B(3)-C(71A)-C(72A)	79.7(6)
N(3)-B(3)-C(71A)-C(76A)	139.3(9)
C(91)-B(3)-C(71A)-C(76A)	22.7(10)
C(81)-B(3)-C(71A)-C(76A)	-101.4(9)
C(76A)-C(71A)-C(72A)-F(72A)	-178.8(13)
B(3)-C(71A)-C(72A)-F(72A)	0.1(13)
C(76A)-C(71A)-C(72A)-C(73A)	3.8(14)
B(3)-C(71A)-C(72A)-C(73A)	-177.2(11)
F(72A)-C(72A)-C(73A)-F(73A)	0(2)
C(71A)-C(72A)-C(73A)-F(73A)	177.4(11)
F(72A)-C(72A)-C(73A)-C(74A)	-178.3(13)
C(71A)-C(72A)-C(73A)-C(74A)	-0.8(19)
F(73A)-C(73A)-C(74A)-C(75A)	179.5(13)
C(72A)-C(73A)-C(74A)-C(75A)	-2(2)
F(73A)-C(73A)-C(74A)-F(74A)	0(2)
C(72A)-C(73A)-C(74A)-F(74A)	178.0(12)
C(73A)-C(74A)-C(75A)-F(75A)	-179.2(13)
F(74A)-C(74A)-C(75A)-F(75A)	0.5(19)
C(73A)-C(74A)-C(75A)-C(76A)	2(2)

F(74A)-C(74A)-C(75A)-C(76A)	-178.1(12)
C(72A)-C(71A)-C(76A)-F(76A)	-176.7(11)
B(3)-C(71A)-C(76A)-F(76A)	4.3(17)
C(72A)-C(71A)-C(76A)-C(75A)	-3.9(16)
B(3)-C(71A)-C(76A)-C(75A)	177.1(10)
C(74A)-C(75A)-C(76A)-F(76A)	174.2(13)
F(75A)-C(75A)-C(76A)-F(76A)	-4.5(19)
C(74A)-C(75A)-C(76A)-C(71A)	1(2)
F(75A)-C(75A)-C(76A)-C(71A)	-177.5(11)
N(3)-B(3)-C(81)-C(82)	138.19(14)
C(91)-B(3)-C(81)-C(82)	-106.13(16)
C(71)-B(3)-C(81)-C(82)	24.1(2)
C(71A)-B(3)-C(81)-C(82)	14.8(5)
N(3)-B(3)-C(81)-C(86)	-40.67(18)
C(91)-B(3)-C(81)-C(86)	75.01(17)
C(71)-B(3)-C(81)-C(86)	-154.72(17)
C(71A)-B(3)-C(81)-C(86)	-164.1(5)
C(86)-C(81)-C(82)-F(82)	-176.81(13)
B(3)-C(81)-C(82)-F(82)	4.2(2)
C(86)-C(81)-C(82)-C(83)	2.6(2)
B(3)-C(81)-C(82)-C(83)	-176.37(14)
F(82)-C(82)-C(83)-F(83)	-0.3(2)
C(81)-C(82)-C(83)-F(83)	-179.78(14)
F(82)-C(82)-C(83)-C(84)	178.67(14)

C(81)-C(82)-C(83)-C(84)	-0.8(2)
F(83)-C(83)-C(84)-F(84)	-1.2(2)
C(82)-C(83)-C(84)-F(84)	179.79(14)
F(83)-C(83)-C(84)-C(85)	178.06(14)
C(82)-C(83)-C(84)-C(85)	-1.0(2)
F(84)-C(84)-C(85)-F(85)	1.2(2)
C(83)-C(84)-C(85)-F(85)	-178.07(14)
F(84)-C(84)-C(85)-C(86)	179.89(14)
C(83)-C(84)-C(85)-C(86)	0.6(2)
F(85)-C(85)-C(86)-F(86)	1.8(2)
C(84)-C(85)-C(86)-F(86)	-176.94(14)
F(85)-C(85)-C(86)-C(81)	-179.86(14)
C(84)-C(85)-C(86)-C(81)	1.5(2)
C(82)-C(81)-C(86)-F(86)	175.40(13)
B(3)-C(81)-C(86)-F(86)	-5.6(2)
C(82)-C(81)-C(86)-C(85)	-2.9(2)
B(3)-C(81)-C(86)-C(85)	176.06(14)
N(3)-B(3)-C(91)-C(92)	121.94(16)
C(71)-B(3)-C(91)-C(92)	-122.85(19)
C(71A)-B(3)-C(91)-C(92)	-115.4(3)
C(81)-B(3)-C(91)-C(92)	4.4(2)
N(3)-B(3)-C(91)-C(96)	-54.84(17)
C(71)-B(3)-C(91)-C(96)	60.4(2)
C(71A)-B(3)-C(91)-C(96)	67.8(3)

C(81)-B(3)-C(91)-C(96)	-172.36(13)
C(96)-C(91)-C(92)-F(92)	179.80(15)
B(3)-C(91)-C(92)-F(92)	2.9(3)
C(96)-C(91)-C(92)-C(93)	0.3(2)
B(3)-C(91)-C(92)-C(93)	-176.61(16)
F(92)-C(92)-C(93)-F(93)	0.6(3)
C(91)-C(92)-C(93)-F(93)	-179.87(16)
F(92)-C(92)-C(93)-C(94)	-178.80(16)
C(91)-C(92)-C(93)-C(94)	0.7(3)
F(93)-C(93)-C(94)-F(94)	-1.1(3)
C(92)-C(93)-C(94)-F(94)	178.30(15)
F(93)-C(93)-C(94)-C(95)	178.94(16)
C(92)-C(93)-C(94)-C(95)	-1.6(3)
F(94)-C(94)-C(95)-F(95)	2.6(2)
C(93)-C(94)-C(95)-F(95)	-177.45(15)
F(94)-C(94)-C(95)-C(96)	-178.42(14)
C(93)-C(94)-C(95)-C(96)	1.5(2)
F(95)-C(95)-C(96)-F(96)	-0.1(2)
C(94)-C(95)-C(96)-F(96)	-179.07(14)
F(95)-C(95)-C(96)-C(91)	178.48(14)
C(94)-C(95)-C(96)-C(91)	-0.5(2)
C(92)-C(91)-C(96)-F(96)	178.12(14)
B(3)-C(91)-C(96)-F(96)	-4.7(2)
C(92)-C(91)-C(96)-C(95)	-0.4(2)

B(3)-C(91)-C(96)-C(95)	176.79(14)
N(4)-B(4)-C(101)-C(102)	161.1(3)
C(121)-B(4)-C(101)-C(102)	-79.7(3)
C(111)-B(4)-C(101)-C(102)	48.5(3)
N(4)-B(4)-C(101)-C(106)	-13.6(5)
C(121)-B(4)-C(101)-C(106)	105.7(5)
C(111)-B(4)-C(101)-C(106)	-126.2(5)
C(106)-C(101)-C(102)-F(102)	-176.2(5)
B(4)-C(101)-C(102)-F(102)	8.5(5)
C(106)-C(101)-C(102)-C(103)	5.9(6)
B(4)-C(101)-C(102)-C(103)	-169.3(3)
F(102)-C(102)-C(103)-F(103)	0.7(5)
C(101)-C(102)-C(103)-F(103)	178.5(3)
F(102)-C(102)-C(103)-C(104)	179.8(4)
C(101)-C(102)-C(103)-C(104)	-2.3(6)
F(103)-C(103)-C(104)-F(104)	-2.7(7)
C(102)-C(103)-C(104)-F(104)	178.2(4)
F(103)-C(103)-C(104)-C(105)	177.6(5)
C(102)-C(103)-C(104)-C(105)	-1.5(7)
F(104)-C(104)-C(105)-F(105)	2.0(9)
C(103)-C(104)-C(105)-F(105)	-178.3(5)
F(104)-C(104)-C(105)-C(106)	-178.5(6)
C(103)-C(104)-C(105)-C(106)	1.2(9)
C(102)-C(101)-C(106)-F(106)	173.7(6)

B(4)-C(101)-C(106)-F(106)	-11.3(9)
C(102)-C(101)-C(106)-C(105)	-6.3(9)
B(4)-C(101)-C(106)-C(105)	168.7(6)
F(105)-C(105)-C(106)-F(106)	2.5(10)
C(104)-C(105)-C(106)-F(106)	-176.9(6)
F(105)-C(105)-C(106)-C(101)	-177.5(6)
C(104)-C(105)-C(106)-C(101)	3.0(11)
N(4)-B(4)-C(01B)-C(06B)	-33.9(10)
C(121)-B(4)-C(01B)-C(06B)	82.9(11)
C(111)-B(4)-C(01B)-C(06B)	-143.7(10)
N(4)-B(4)-C(01B)-C(02B)	146.1(4)
C(121)-B(4)-C(01B)-C(02B)	-97.0(5)
C(111)-B(4)-C(01B)-C(02B)	36.3(5)
C(06B)-C(01B)-C(02B)-F(02B)	-173.6(10)
B(4)-C(01B)-C(02B)-F(02B)	6.4(7)
C(06B)-C(01B)-C(02B)-C(03B)	5.7(11)
B(4)-C(01B)-C(02B)-C(03B)	-174.3(6)
F(02B)-C(02B)-C(03B)-F(03B)	-0.9(10)
C(01B)-C(02B)-C(03B)-F(03B)	179.7(6)
F(02B)-C(02B)-C(03B)-C(04B)	179.1(7)
C(01B)-C(02B)-C(03B)-C(04B)	-0.3(10)
F(03B)-C(03B)-C(04B)-F(04B)	-1.4(12)
C(02B)-C(03B)-C(04B)-F(04B)	178.6(7)
F(03B)-C(03B)-C(04B)-C(05B)	174.8(10)

C(02B)-C(03B)-C(04B)-C(05B)	-5.2(14)
C(03B)-C(04B)-C(05B)-F(05B)	-176.5(10)
F(04B)-C(04B)-C(05B)-F(05B)	-0.4(19)
C(03B)-C(04B)-C(05B)-C(06B)	5(2)
F(04B)-C(04B)-C(05B)-C(06B)	-178.9(12)
F(05B)-C(05B)-C(06B)-F(06B)	1(2)
C(04B)-C(05B)-C(06B)-F(06B)	179.0(14)
F(05B)-C(05B)-C(06B)-C(01B)	-177.4(14)
C(04B)-C(05B)-C(06B)-C(01B)	1(2)
C(02B)-C(01B)-C(06B)-F(06B)	176.0(11)
B(4)-C(01B)-C(06B)-F(06B)	-4.0(19)
C(02B)-C(01B)-C(06B)-C(05B)	-6.2(19)
B(4)-C(01B)-C(06B)-C(05B)	173.9(12)
N(4)-B(4)-C(111)-C(116)	130.42(17)
C(01B)-B(4)-C(111)-C(116)	-121.0(3)
C(121)-B(4)-C(111)-C(116)	15.6(2)
C(101)-B(4)-C(111)-C(116)	-113.1(2)
N(4)-B(4)-C(111)-C(112)	-53.04(19)
C(01B)-B(4)-C(111)-C(112)	55.6(3)
C(121)-B(4)-C(111)-C(112)	-167.90(14)
C(101)-B(4)-C(111)-C(112)	63.4(2)
C(116)-C(111)-C(112)-F(112)	176.89(15)
B(4)-C(111)-C(112)-F(112)	-0.1(2)
C(116)-C(111)-C(112)-C(113)	-1.8(2)

B(4)-C(111)-C(112)-C(113)	-178.77(15)
F(112)-C(112)-C(113)-F(113)	1.5(2)
C(111)-C(112)-C(113)-F(113)	-179.77(15)
F(112)-C(112)-C(113)-C(114)	-177.77(15)
C(111)-C(112)-C(113)-C(114)	1.0(3)
F(113)-C(113)-C(114)-F(114)	0.4(3)
C(112)-C(113)-C(114)-F(114)	179.61(16)
F(113)-C(113)-C(114)-C(115)	-178.72(16)
C(112)-C(113)-C(114)-C(115)	0.5(3)
F(114)-C(114)-C(115)-F(115)	-0.6(3)
C(113)-C(114)-C(115)-F(115)	178.47(16)
F(114)-C(114)-C(115)-C(116)	179.89(16)
C(113)-C(114)-C(115)-C(116)	-1.0(3)
C(112)-C(111)-C(116)-F(116)	-177.98(15)
B(4)-C(111)-C(116)-F(116)	-1.3(3)
C(112)-C(111)-C(116)-C(115)	1.3(3)
B(4)-C(111)-C(116)-C(115)	178.00(16)
F(115)-C(115)-C(116)-F(116)	-0.1(3)
C(114)-C(115)-C(116)-F(116)	179.36(16)
F(115)-C(115)-C(116)-C(111)	-179.42(16)
C(114)-C(115)-C(116)-C(111)	0.1(3)
N(4)-B(4)-C(121)-C(126)	126.36(17)
C(01B)-B(4)-C(121)-C(126)	10.8(5)
C(111)-B(4)-C(121)-C(126)	-119.29(18)

C(101)-B(4)-C(121)-C(126)	4.5(3)
N(4)-B(4)-C(121)-C(122)	-51.12(19)
C(01B)-B(4)-C(121)-C(122)	-166.6(4)
C(111)-B(4)-C(121)-C(122)	63.23(19)
C(101)-B(4)-C(121)-C(122)	-173.0(2)
C(126)-C(121)-C(122)-F(122)	177.83(15)
B(4)-C(121)-C(122)-F(122)	-4.4(2)
C(126)-C(121)-C(122)-C(123)	-0.7(3)
B(4)-C(121)-C(122)-C(123)	177.07(16)
F(122)-C(122)-C(123)-F(123)	1.9(3)
C(121)-C(122)-C(123)-F(123)	-179.51(16)
F(122)-C(122)-C(123)-C(124)	-177.39(16)
C(121)-C(122)-C(123)-C(124)	1.2(3)
F(123)-C(123)-C(124)-F(124)	-0.4(3)
C(122)-C(123)-C(124)-F(124)	178.95(17)
F(123)-C(123)-C(124)-C(125)	179.91(18)
C(122)-C(123)-C(124)-C(125)	-0.8(3)
F(124)-C(124)-C(125)-F(125)	0.4(3)
C(123)-C(124)-C(125)-F(125)	-179.85(19)
F(124)-C(124)-C(125)-C(126)	-179.75(19)
C(123)-C(124)-C(125)-C(126)	0.0(3)
F(125)-C(125)-C(126)-F(126)	0.4(3)
C(124)-C(125)-C(126)-F(126)	-179.38(19)
F(125)-C(125)-C(126)-C(121)	-179.67(19)

C(124)-C(125)-C(126)-C(121)	0.5(3)
C(122)-C(121)-C(126)-F(126)	179.74(17)
B(4)-C(121)-C(126)-F(126)	2.1(3)
C(122)-C(121)-C(126)-C(125)	-0.2(3)
B(4)-C(121)-C(126)-C(125)	-177.78(18)
C(135)-N(5)-C(131)-C(132)	3.1(2)
Ru(1)-N(5)-C(131)-C(132)	-170.14(12)
N(5)-C(131)-C(132)-C(133)	0.3(3)
C(131)-C(132)-C(133)-C(134)	-2.9(2)
C(131)-C(132)-C(133)-C(141)	174.53(15)
C(134)-C(133)-C(141)-F(131)	112.4(11)
C(132)-C(133)-C(141)-F(131)	-65.0(11)
C(134)-C(133)-C(141)-F(33B)	-131.7(7)
C(132)-C(133)-C(141)-F(33B)	50.9(7)
C(134)-C(133)-C(141)-F(132)	-13.7(5)
C(132)-C(133)-C(141)-F(132)	168.9(5)
C(134)-C(133)-C(141)-F(32B)	-11.4(7)
C(132)-C(133)-C(141)-F(32B)	171.2(7)
C(134)-C(133)-C(141)-F(31B)	102.3(7)
C(132)-C(133)-C(141)-F(31B)	-75.1(7)
C(134)-C(133)-C(141)-F(133)	-133.6(5)
C(132)-C(133)-C(141)-F(133)	49.0(6)
C(132)-C(133)-C(134)-C(135)	2.0(2)
C(141)-C(133)-C(134)-C(135)	-175.33(15)

C(131)-N(5)-C(135)-C(134)	-4.0(2)
Ru(1)-N(5)-C(135)-C(134)	169.91(11)
C(131)-N(5)-C(135)-C(136)	178.09(14)
Ru(1)-N(5)-C(135)-C(136)	-8.01(16)
C(133)-C(134)-C(135)-N(5)	1.4(2)
C(133)-C(134)-C(135)-C(136)	179.20(14)
N(5)-C(135)-C(136)-N(6)	5.92(19)
C(134)-C(135)-C(136)-N(6)	-171.94(14)
N(5)-C(135)-C(136)-C(137)	-174.72(15)
C(134)-C(135)-C(136)-C(137)	7.4(2)
N(6)-C(136)-C(137)-C(138)	0.8(2)
C(135)-C(136)-C(137)-C(138)	-178.56(16)
C(136)-C(137)-C(138)-C(139)	-1.0(3)
C(136)-C(137)-C(138)-C(142)	177.82(19)
C(137)-C(138)-C(142)-F(34B)	-103.2(9)
C(139)-C(138)-C(142)-F(34B)	75.6(9)
C(137)-C(138)-C(142)-F(135)	115.9(7)
C(139)-C(138)-C(142)-F(135)	-65.3(7)
C(137)-C(138)-C(142)-F(36B)	25.1(11)
C(139)-C(138)-C(142)-F(36B)	-156.1(11)
C(137)-C(138)-C(142)-F(35B)	135.0(9)
C(139)-C(138)-C(142)-F(35B)	-46.2(9)
C(137)-C(138)-C(142)-F(136)	-10.7(5)
C(139)-C(138)-C(142)-F(136)	168.1(4)

C(137)-C(138)-C(142)-F(134)	-125.2(5)
C(139)-C(138)-C(142)-F(134)	53.6(5)
C(137)-C(138)-C(139)-C(140)	0.3(3)
C(142)-C(138)-C(139)-C(140)	-178.52(19)
C(138)-C(139)-C(140)-N(6)	0.7(3)
C(139)-C(140)-N(6)-C(136)	-0.9(2)
C(139)-C(140)-N(6)-Ru(1)	179.59(14)
C(137)-C(136)-N(6)-C(140)	0.2(2)
C(135)-C(136)-N(6)-C(140)	179.55(14)
C(137)-C(136)-N(6)-Ru(1)	179.73(12)
C(135)-C(136)-N(6)-Ru(1)	-0.90(17)

Symmetry transformations used to generate equivalent atoms:

Table 7. Hydrogen bonds for D19108 [Å and °].

D-H...A	d(D-H)	d(H...A)	d(D...A)	<(DHA)
C(196)-H(196)...F(44)#1	0.95	2.57	3.252(2)	129.2
C(222)-H(222)...F(55)#2	0.95	2.62	3.217(3)	121.0
C(131)-H(131)...F(86)	0.95	2.60	3.398(2)	142.3
C(132)-H(132)...F(45)#3	0.95	2.53	3.473(2)	170.5
C(140)-H(140)...F(52)	0.95	2.45	3.288(2)	147.0
O(1S^a)-H(1S^a)...F(125)#4	0.84	1.63	2.38(2)	148.0
C(11S^a)-H(11A^a)...F(115)#1	0.99	2.32	3.073(18)	132.3
C(12S^a)-H(12A^a)...F(116)#1	0.98	2.06	2.90(2)	143.3
C(12S^a)-H(12B^a)...F(93)#1	0.98	2.28	3.20(2)	157.4
C(21S^b)-H(21B^b)...F(116)#1	0.99	1.80	2.65(2)	141.8
C(22S^b)-H(22B^b)...F(116)#4	0.98	2.33	2.99(3)	123.9
O(3S^c)-H(3S^c)...F(116)#1	0.84	2.63	3.231(19)	129.3
C(31S^c)-H(31B^c)...F(124)#4	0.99	2.50	3.38(3)	147.0
C(31S^c)-H(31B^c)...F(125)#4	0.99	1.93	2.75(2)	138.3

Symmetry transformations used to generate equivalent atoms:

#1 -x+1,-y+2,-z+1 #2 -x+1,-y+1,-z+1 #3 x+1,y,z

#4 x,y,z-1